CZECH UNIVERSITY OF LIFE SCIENCES PRAGUE

FACULTY OF ENGINEERING

AGRICULTURAL INFORMATION MANAGEMENT SYSTEM (AGIS): MAPPING SYSTEM OF SAGO POTENTIAL IN SOUTHERN PAPUA, INDONESIA

DEPARTMENT OF MECHANICAL ENGINEERING

DOCTORAL DISSERTATION

Author
Sri Murniani Angelina Letsoin

Supervisor
Prof. Ing. David Herak, Ph.D

Co-Supervisor
Ing. Cestmir Mizera, Ph.D

2023

DECLARATION

I hereby declare that I have done the doctoral dissertation entitled **Agricultural Information Management System (AGIS): Mapping System of Sago Potential in Southern Papua, Indonesia** independently. The doctoral dissertation is submitted in partial fulfillment of the requirements for the Engineering of Agricultural Technological Systems in the Faculty of Engineering. I also declare that the doctoral dissertation is arranged according to the guidelines established by the Faculty of Engineering and has not been submitted for any other purposes.

In Prague,

Date: 7 June 2023

Sri Murniani Angelina Letsoin

Signature:

ACKNOWLEDGEMENT

By God's grace, this arduous research journey has finally been completed. First of all, I would like to thank my supervisor, Prof. Ing David Herak, Ph.D., for his support, effort, and assistance throughout the study and research. I thank him for supporting me and allowing me to be involved in innovative project research.

This doctoral study would not have been accomplished without the scholarship provided by the Indonesia Endowment Fund for Education (Lembaga Pengelola Dana Pendidikan), Ministry of Finance of Indonesia, Republic of Indonesia (LPDP-RI). This dissertation research was also part of the IGA project of the Faculty of Engineering 2021 with grant number 31130/1312/3105 Smart sago palm detection using Internet of Things (IoT) and Unmanned Aerial Vehicle (UAV) imagery.

Throughout this long endeavor, I greatly appreciated the assistance, support, and sharing of expertise in remote sensing with doc. Mgr. Jitka Kumhalova, Ph.D. I appreciate the opportunity to work in the field and to process Radar data in computer laboratories. I also appreciate her assistance in setting up the drone with the PRO LAB team of the Faculty of Engineering.

I also appreciate the aid and support I have received from the head of my department, doc. Ing. Pavel Neuberger, Ph.D., who was always willing to help and support me during my study. I am grateful for offering hands and prompt responses during the study to Mgr. Zuzana Polakova, who has also greatly contributed as a proofreader of my dissertation writing. Sincere thanks also to doc. Ing. Abraham Kabutey, Ph.D., for his knowledge and continuous support. I appreciate all the encouragement. I wish to thank my co-supervisor, Ing. Cestmir Mizera, Ph.D. for his feedback during the PhD presentation.

I sincerely appreciate the effort of Ir. Ratna Chrismiari Purwestri, MSc, Dr.sc.agr for many fruitful thoughts and discussions related to publications and research, also her prayers and encouragement. This research journey would not have been obtained without her contribution. I would like to thank the local stakeholders of Merauke Regency and Mappi Regency, sago farmers, fellow lecturers, researchers, and stakeholders at Universitas Musamus Merauke, who have supported this research. I truly value the prayers and friendship of the Indonesian Christian Fellowship, Priest Billy, and family. To Mayrina Andriani, Alex Dimitriu, and other Indonesian friends. Thank you for the past years of togetherness and cheerfulness.

This educational journey of approximately four years would certainly not have been achieved without the support, prayers, and enthusiasm of my beloved parents, siblings, mother-in-law, and all family. Especially my beloved husband, Ebenezer Butarbutar, for his continuous attention, love, and patience during this time of journey.

ABSTRACT

Metroxylon Sagu Rottb, the scientific name of Sago Palm, is one of the primary native products in selected fieldwork, namely Papua, Indonesia. Sago's palm offers a prominent potential as raw material in low bioenergy, agro-industry, and traditional building construction. The current review studies related to sago's potential reveal the advantages of the palm not only in supporting food security but also in health aspects and bio-economy. According to the previous observation, some problems were faced by the community as well as stakeholders, i.e., (1) the lack of data about sago habitat or sago yield areas and (2) harvest time prediction employed thorough visual eye inspection. To address this, the research contribution was arranged into three experiments. (1) The first experiment was to acquire recent information from remote sensing data. This experiment was used to perceive the potential habitat of sago as well as current conditions during observer years from 1990 to 2019. The result of this experiment was considerably important to address the first problem mentioned. (2) The second experiment was to arrange a technique for detecting sago palms. This result essentially addressed the second problem of the study. (3) The third experiment was to adjust the parameter of the model to a good fit. As a result, eight potential habitats of sago were investigated, namely primary and secondary dryland, grassland, primary and secondary swamp, bush/shrub, swamp shrub, and swamp. Statistically significant changes were observed at primary dryland, grassland, and swamp with a p-value less than 0.05. The result of mean values demonstrated that 12 districts from 20 districts of Merauke Regency lost the natural habitat of sago palm, while a larger potential area in 6 districts. The sago palm detection based on Convolutional Neural Network (CNN) models in this study enabled good fit conditions with about 0.2 differentiation between training loss and validation loss, also less than 9% of differentiation between training accuracy and validation accuracy. The most considerable limitation identified was the lack of data on sago areas and sago yield areas in the regency. Consequently, the research effort of the first experiment could not compare periodically. Nevertheless, this research effort can be considered an unprecedented prior study. The study suggested (1) an additional network by using semantic segmentation and (2) integration with mobile applications and the Internet of Things (IoT) in future work.

Keywords: remote sensing data, transfer learning, CNN, sago, detection

TABLE OF CONTENT

LIST OF FIGURES

LIST OF TABLES

LIST OF APPENDIXES

1. INTRODUCTION

1.1 Background

The sago palm *(Metroxylon Sagu Rottb)* is one of the ecological tree species that may grow wildly in the forest, primarily in Southeast Asian countries and Papua New Guinea (PNG). Sago palm trees could potentially be found in various environments in Indonesia, particularly in South Papua. About 85% of the world's sago production is in Indonesia, of which 90% is located in Papua and West Papua (Ehara et al., 2018). A number of earlier studies (Amin et al., 1841; Awg-Adeni et al., n.d.; Jonatan et al., 2017; Karim et al., 2008) revealed the food and non-food industry features of sago. Using the bark, leaves, starch, and sago waste is possible. The bark can be used for traditional flooring, walls, or craft paper. Further, the leaves are used for roofing, and the waste is for animal feed or compost. Sago palms contain a lot of starch which is used as a food product in traditional cakes, as well as by the food and beverage industries, and also as a raw material for the agro-industry, biopesticides, and the bioethanol industry (Amin et al., 1841; Karim et al., 2008; Metaragakusuma et al., 2016; Mofu & Abbas, 2015). In the next chapter, the potential uses of sago in the food and non-food industry are presented.

In the study location, Merauke Regency, the easternmost city in Indonesia, sago palm trees typically grow in wild stands with a height of 7-15 meters. These trees associate with different types of ecosystems, such as peatland areas or swampy forests. During the harvesting season, which may be distinguished manually by the white flowers blossoming between the leaves on the tops of palm trees, sago plays an important role as a staple food in the area. Nevertheless, some previous studies highlighted the effect of land use changes, for example, the conversion of sago areas to other crops (Salosa, 2016; Sidiq et al., 2021) or the inefficient utilization of resources (Rasyid et al., 2020). Also the sago area has not been investigated yet in the statistical report of local stakeholders, besides grains crops, due to the manual inspection since 2016 (BPS, 2021).

Several studies were focused on investigating the sago palm's condition, for instance, by extracting satellite imageries combined with relevant methods, such as support vector machine (SVM), object-based image analysis (OBIA), and image processing (Hidayat et al., 2018). Nevertheless, the study pointed out that morphology and similarity with other palms could affect the classification result. Moreover, the maximum likelihood as a classifier in sago palm distribution from the satellite was studied in the Philippines (Santillan & Makinano-Santillan, 2016). The previously related works were not applicable to our fieldwork settings. One of the specific problems is the challenge of harvesting time prediction that is practically defined through the morphology of sago. However, as mentioned precedent, due to the wild stand sago, the height of the sago surrounded by swampy areas could influence the result. Another sago palm detection model uses the convolutional neural network (CNN) architecture, namely Alex Net, Xception, ResNet and CraunNet, to identify the maturity of sago acquired from Unmanned Aerial Vehicle (UAV) images (Wahed et al., 2022). This related study focused on the maturity identification of sago palms through their canopies. Conversely, our research dataset collected not only the sago canopy tree but also the physical appearance of sago, for instance, trunks, and flowers. Furthermore, other dataset was also provided, such as coconout, oil plam and non-sago. Detection by physical appearance and the sago canopy is used to differentiate sago palm from others, and also to recognize wild sago palm areas.

According to the statistics of National Leading Estate Crops Commodity 2019-2021, Ministry of Agriculture (Directorate General of Estate Crops, 2020), Indonesia has a potential sago land area of 5.5 million ha. However, its utilization has only reached 5%, i.e., 196.831 ha; 99.65% of it is in the form of smallholder plantations with a production of 359.838 tonnes. As described earlier, the potential uses of sago can support various sectors, including the circular economy. In this point, the integration with a smart farming environment to enhance the usefulness of sago in commercial sago plantations is possible to broaden the sago utilization and how the advantages that go with them can be vital to the robustness of the regional chain system (Sidiq et al., 2021). To address this, sago detection by combining with the Internet of Things (IoT) is useful for observing newly formed sago plants (Kho et al., 2022). However, as explained previously, the sago palm in the fieldwork was mostly a wild stand in the sago forest. It was located around rivers and swampy areas with limited network infrastructure. Nevertheless, the advancement of using IoT in sago palm detection is beneficial for monitoring sago environment, such as temperature, humidity or diseases particularly for young sago plant.

Although sago palm has multiple advantages, the existing condition of sago as well the impact of land conversion to the natural habitat of sago in this regency is still being questioned. An earlier study in Jayapura, a different region of Papua Province, investigated sago palm terrain based on its environment, such as climate, proximity from a river or lake, altitude, gradient derived from spatial satellite data integrated with field data, and other geographical information software (Dimara et al., 2021), which differed from our research. First, this research examines the impact of Land Use Land Cover (LULC) on the natural habitat of sago, as well as perceives the current condition of sago habitat in the regency. The LULC and the ancillary LULC data from Indonesia Land Cover classes and remote sensing data are presented in the next chapter. Next, sago detection is performed using deep learning, as proposed in this study.

1.2 Research Problem

Our study site has a shortage of documentation regarding sago palm areas. It might be due to human eye inspection, and the ecosystem of sago, which is typically surrounded by swampy areas, rivers or lakes. Since this palm lives with other vegetation, and the sago trees canopy overlaps and is unclearly defined, sago detection becomes rather challenging. As a consequence, the existing condition of the sago on this site has not been examined, still. The local community predicts the harvest time conventionally, specifically by employing a human eye inspection. The natural stand of the sago reaches 7-15 meters in height. Therefore, the human evaluation might be biased by the palms' height as well as their ecosystems, as mentioned previously, the proximity of a long river or lake. On the one hand, the conversion of land use from one purpose to another could contribute to the extinction of various native plants, including sago palm trees. A previous study used satellite data combined with machine learning methods and image processing in sago palm mapping as one of the approaches to detect the sago palm (Hidayat et al., 2018); however, the wild stand and the similarity of palm life to other vegetation are challenging. There is an urgent need to study sago palms with respect to sago detection using different approaches to address this problem.

1.3 Outline of the Doctoral Dissertation

The doctoral research substantially focused on how to detect the existence of sago palms in this area. Three experiments were arranged on detecting the potential habitat of wild sago palm by using remote sensing data, deep learning and transfer learning techniques. Each chapter is presented as follows:

Chapter 1 Describes the introduction to the research efforts and a brief view of current knowledge. General research objectives are stated and how they relate to the research problem.

Chapter 2 Provides a state-of-the-art research study related to the hypothesis. This includes the theory and methods used in the experiment. This chapter also evaluates how related work, and the findings can be distinguished from proposed study in arranging the experiments and the hypotheses.

Chapter 3 Describes the objectives of study, and sixth hypotheses were determined to strengthen the specific objectives.

Chapter 4 Presents the material and methods implemented through the study effort in Chapter 2 and Chapter 3. Experiments related to the objectives and hypothesis are performed. The first experiment gains remote sensing data, and the second experiment utilizes the UAV data, deep learning and transfer learning technique. This chapter also provides parameters and network layers used. Lastly, the analysis and evaluation techniques are also provided.

Chapter 5 Reports the result of the publication on investigating of the potential habitat of sago palm based on Land Use Land Cover changes. This chapter displays the land cover maps from 1990 to 2019, the estimation area, and their changes. Next, the results on recognizing the sago palm based on its physical appearance are also presented. This is followed by various evaluations for each model network.

Chapter 6 Contains a discussion of research findings based on these two experiments. This research effort includes the interpretation, discussion, and evaluation related to the hypothesis. The presented results are used to affirm or disprove hypotheses and obtained objective described in Chapter 3.

Chapter 7 Summarizes the research effort by concluding the study and pointing out the research contribution. Additionally, further study recommendation is presented. This research effort encompasses various amounts of data from different sources and datasets. Therefore, significant challenges related to the proposed hypotheses are also addressed in this chapter.

2. STATE OF THE ART

2.1 Sago Palm

Metroxylon Sagu is a genuine palm comprised of the family Palmae, and sub-family Calamoideae, specified in the order Arecales. It is generally grown in wild and swampy regions of Southeast Asia, for instance, Indonesia, Malaysia, and New Guinea. The palm reaches a natural height of up to 15 meters, reaching maturity at around 12-15 years. The main role of a carbohydrate provider is used in food processing industries, as a staple food, and for other potential uses. As a carbohydrate provider, the palm produces approximately 300-400 kg/tree of dry starch (Figure 1c). Sago yields are four times higher than those of other starchy foods, such as paddy *(Oryza sativa)*, corn *(Zea mays)*, and wheat (J.J. Lal, 2003; Lim et al., 2019).

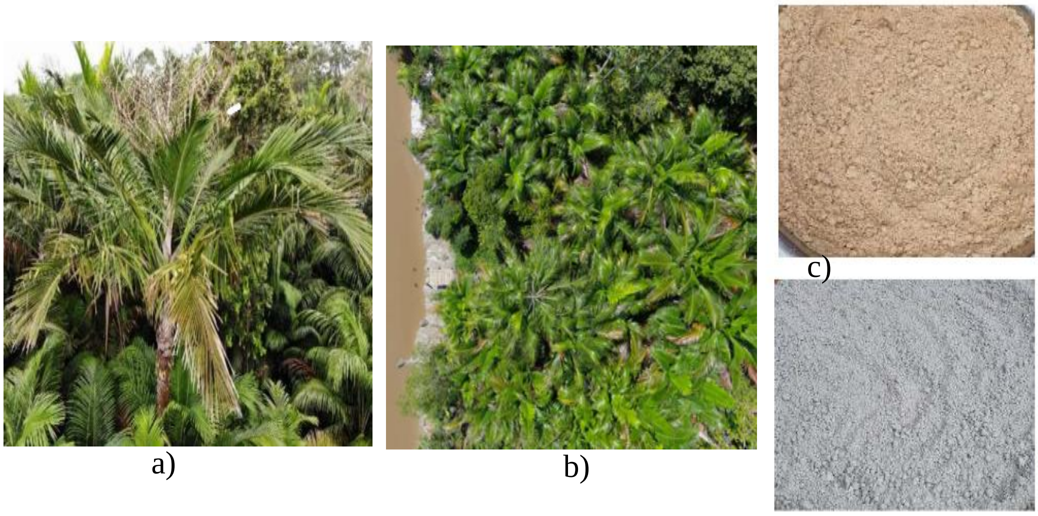

Figure 1. Sago palm in the fieldwork,
(a) sago palm (b) sago palm area (c) sago dry starch (Letsoin et al., 2022).

Sago starch can be used as a substitute for rice or other staple foods, which might decrease reliance on a single product from the perspective of food security. Regarding the sago plant, every part of the sago palm can be used to support various sectors, as shown in Figure 2, that will improve society's living standard or enhance the bioeconomy field. A classic roof can be made from the leaves. Sago leaf sheaths can be utilized as furniture, flooring, temporary walls, rope, and ceilings. Additionally, the trunk is part of the sago palm, where starch is primarily produced. The starch can be transformed and industrially developed into bio-thermoplastic, bio-cellulose, biopolymer, capsule coating, etc. (Singhal et al., 2008), in addition to being used as staple foods and snacks. The palm is becoming more important for the communities due to the significance of sago in the food industry as a source of carbohydrates and food ingredients, as well as its value-added commodities, such as in health aspects (Setiawan, Fetriyuna, Angelina, et al., 2022) and non-food sectors. Sago waste from *hampas* or pulp can provide low bioethanol (Amin et al., 1841; Jonatan et al., 2017).

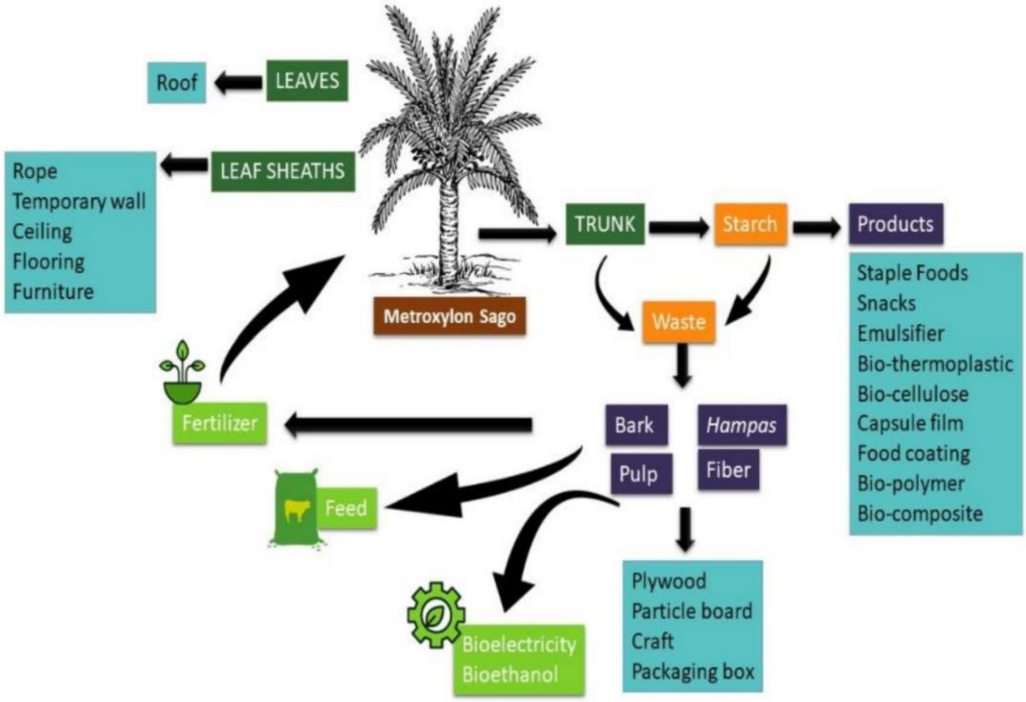

Figure 2. Potential uses of sago (Fetriyuna, 2022).

2.2 Land Cover Classes in Indonesia

The land cover class denotes the physical land class covered by swamp forests, mining areas, and other classes. On the other hand, land use refers to the purpose of land, such as recreation or wildlife habitat. Land cover and land use are frequently used interchangeably, but both can be employed to support a variety of purposes, including identification and change detection (Guo et al., 2020; Halmy et al., 2015). Land use land cover (LULC) is typically applied to examine the dynamic changes of one area, the types of changes estimated, the development of various activities such as the extension of settlement areas, the expansion of crops and agriculture areas, the degradation of forest area due to urban development or deforestation (Aliani et al., 2019; Cheng & Wang, 2019; Hamad et al., 2018; Tripathy & Kumar, 2019; Whittle et al., 2012). The supply of numerous necessary commodities, such as water bodies and forests, is impacted by LULC dynamic changes. Studies in LULC are crucial to learning about past and existing circumstances, forecasting other peculiarities and helping the stakeholders set up the strategic plans (Mathewos et al., 2022; Velastegui-Montoya et al., 2022).

The land cover classes in Indonesia refer to the Ministry of Environment and Forestry (MoEF), which includes the Standardization Agency of Indonesia, specifically the Indonesian National Standard or Standard Nasional Indonesia (SNI 8033:2014). They classified the land cover into twenty-three classes. The land cover classes and the description are presented in Table 1. These land cover classes are generated based on biophysical appearance sensed by remote sensing data, i.e., Landsat data 7 ETM+, Landsat 5 at 30-meter spatial resolution and other supporting satellite data, namely MODIS, Quick bird, Worldview, and SPOT 4/5.

Table 1. Land cover classes of Indonesia and the description.*

No.	Classes	Definition
1.	Primary dryland forest	Natural tropical forests grow in dryland habitats such as lowland, upland, and mountain forests, with no indications of human or logging occurrence.
2.	Secondary dryland forest	The natural tropical forest grows in non-wet habitats such as lowland, upland, and montane forests that show signs of logging activity such as patterns and spotting of logging (appearance of roads and patches of the logged-over forest).
3.	Primary mangrove forest	Wetland forests in coastal areas, such as plains, that are still influenced by tides, muddy and brackish water, and are dominated by mangrove and Nipa (Nipa frutescens) species, and are not or are only minimally influenced by human activities or logging.
4.	Secondary mangrove forest	Wetland forests on coastlines such as plains that are still influenced by tides, muddy and brackish water, and dominated by species of mangrove and Nipa (Nipa frutescens), and exhibit signs of commercial logging.
5.	Primary swamp forest	Natural tropical forest that grows in wet habitat in swamp form, such as brackish swamp, marshes, sago, and peat swamp, and is not or minimally influenced by human activities or logging.
6.	Secondary swamp forest	Natural tropical forest grows in swamp habitats such as brackish swamps, marshes, sago swamps, and peat swamps that show signs of logging activity such as patterns and patches (appearance of logging roads and logging patches.
7.	Plantation forest	The structural composition of forest vegetation in large areas is dominated by homogeneous tree species planted for specific purposes. Planted forest, which includes reforestation areas, industrial plantation forest, and community plantation forest.
8.	Estate cropland	Estates that have been planted, typically with intercrops or other agricultural tree commodities.
9.	Pure dry agriculture	All land uses associated with agriculture on dry/non-wet land, such as moor, mixed gardens, and agriculture fields.
10	Mixed dry agriculture	All agricultural land covers dry/non-wet land that are mixed with shrubs, bushes, and logs in the forest. This cover type is frequently the result of shifting cultivation and rotation.

11	Dry shrub	Immensely deteriorated log over areas in non-wet habitats that are undergoing succession but have not yet reached a stable forest ecosystem, with natural scattered trees or shrubs.
12	Paddy field	Agriculture areas in wet habitats, particularly paddy, with typical dyke patterns. Rainfed, seasonal, and irrigated paddy fields are examples of this cover type.
13	Wet shrub	Strongly degraded log over areas in wet habitats that are undergoing succession but have not yet reached a stable forest ecosystem, with naturally scattered trees or shrubs.
14	Savanna and grasses	Grassy areas with scattered natural trees and shrubs. This is typical of the natural ecosystem and appearance in Sulawesi Tenggara, Nusa Tenggara Timur, and the southern part of Papua. This type of cover could be found in either wet or dry habitats.
15	Open swamp	Observation of an open swamp with little vegetation.
16	Open water	Observation of open water, such as the ocean, rivers, lakes, and ponds.
17	Fishpond	Aquaculture activities such as fish ponds, shrimp ponds, and salt ponds can be found in these areas.
18	Port and harbor	Discovery of a port or harbor large enough to be delineated as a separate object.
19	Transmigration areas	Unique settlement areas with a mix of houses, agroforestry, and/or gardens in the surrounding area.
20	Settlement areas	Settlement areas with typical appearances involve rural, urban, industrial, and other urban areas.
21	Mining areas	Extraction areas are characterized by open mining activities such as expansive mining and mining waste ground.
22	Bare ground	Areas with no vegetation cover, such as open exposure areas, craters, sandbanks, sediments, and post-fire areas that have not yet shown regrowth.
23	Clouds and no-data	Cloud sightings and cloud shadows larger than 4 cm^2 at 100.000 scales are displayed.

* (Letsoin et al., 2020).

The LC classes displayed in Table 1 are categorized into 6 group classes. The first group is forestland consisting of primary dryland forest, secondary dryland forest, primary mangrove forest, secondary mangrove forest, primary swamp forest, secondary swamp forest and plantation forest. The second group is called cropland; it relates to crops and agriculture classes, namely estate cropland, pure dry agriculture, mixed dry agriculture, paddy field, and transmigration. The third group is grassland, which covers savanna, grasses, and also dry shrub. The fourth group is wetlands, including wet shrubs, swamp or swamp shrubs. The fifth group involves the settlement area and the transmigration area. Thus, other typical land categories cover, for example, ports and harbors, bare ground, fish ponds, and mining areas.

2.3 Remote Sensing Data

Remote sensing is a technique to detect and acquire the physical features of an area or object. The measurement process is done through various distant platforms, such as airborne, spaceborne, or ground-based. The ground-based platform consists of a handled and vehicle mounted type. Airborne and spaceborne platforms include unmanned aerial vehicles (UAV), piloted airplanes and satellites. Remote sensing system involves satellite sensors, for instance, hyperspectral, multispectral, thermal, infrared, and near infra-red, which supports radiometric, spectral, spatial and temporal properties of objects (Berger et al., 2022; Shafique et al., 2022). Radiometric data involves the amount of information perceived by the satellite sensor. Spectral data is information obtained from different sensor bands and visual wavelengths, then spatial data focuses on geographical location, while temporal data relates to different time acquisition. Table 2 shows the feature of the existing remote sensing (Chen et al., 2022; Y. Huang et al., 2018).

Table 2. The feature of satellite data.

Category	Sensor	Data availability	Height on orbit (km)	Orbital swath (km)	Spatial resolution (m)	Temporal resolution	Bands	Spectral range (nm)	Signal-to-noise ratio	Acquisition method
Coarse resolution	AVHRR	1978~	833–870	2,800	1,100	0.5	5	550–12,500	/	free
	MODIS	1999~	705	2,330	250–1,000	0.5	36	400–14,400	/	free
	MERIS	2002–2012	790 ± 10	1,150	300	3	22	465–2,135	/	free
	GOCI	2010~	35,837	2,500	500	1/24	8	402–885	545–945	free
	Sentinel-3	2016~	814.5	1,270	300	2	21	400–1,020	50–168	free
Medium resolution	Landsat 1–3	1972–1983	907–915	185	78	18	4	500–1,100	<40	free
	Landsat-4/5	1982–2012	705	185	30–120	16	7	450–12,500	17–72	free
	Landsat-7	1999~	705	185	15–60	16	8	450–12,500	13–78	free
	Landsat-8	2013~	705	185	15–100	16	11	430–12,510	145–355	free
	Landsat-9	2021~	705	185	15–100	16	11	435–12,500	162–442	free
	SPOT 1–4	1986~2013	822	60	10–20	26	4–5	500–1,750	119–219	charge
	Hyperion	2000–2017	705	7.7	30	200	242	400–2,500	<50	free
	Sentinel-2	2015~	786	290	10–60	5	13	420–2,300	50–174	free
High resolution	IKONOS	1999–2015	681	11.3	0.82–4	1.5–3	5	445–900	67–143	charge
	Quick Bird	2001–2014	450–482	16.8–18	0.61–2.88	1–6	5	450–900	25–32	charge
	Worldview 1–4	2007~	496	17.6	0.31–3.7	1.7–5.9	4–28	450–800	0.45–22	charge
	SPOT 5	2002–2015	822	60	2.5–20	26	5	480-1,750	/	charge
	SPOT 6/7	2012~	694	60	1.5–6	26	5	500–890	/	charge
	ZY-3	2012~	506	50	2.1–5.8	3–5	7	500–890	>25	charge
	GF-1/2/6	2013~	631–645	45–90	0.8–16	1–5	5–13	450–900	34–294	free
	Zhuhai-1	2017~	500	150	0.44–10	1–32	32	400–1,000	>300	free

Remote sensing has long been broadly used in various applications of change detection, precision agriculture, food crops, image classification, land cover land use classification, and yield estimation (García-Pardo et al., 2022; Jafarbiglu & Pourreza, 2022; Mehmood et al., 2022; Vallentin et al., 2022). Remote sensing abilities integrate with other approaches today, such as in-situ and climate data. Also, image processing methods significantly influence the measurement results (Figure 3). One significant drawback of the remote sensing system is atmospheric behavior, such as clouds. Nevertheless, several previous studies pointed out other algorithms to eliminate the noise, such as random forest, deep learning or the use of radar data, and other approaches (Z. Li, Shen, et al., 2022; Meraner et al., 2020; Tůma et al., 2022; Yao et al., 2022).

Figure 3. Remote sensing system integrated with others approaches (Awais et al., 2023; Zheng et al., 2022).

2.4 Artificial Intelligence

Artificial Intelligence (AI) has been defined variously, for instance, as the subdivision of computer science that focuses on the development of intelligent machines whose analytical and functional systems are related to human intelligence (Shivaprakash et al., 2022) or on the development of theories and algorithms to perform specific purposes or tasks that adopt or mimic the intelligence of human mechanisms (Artasanchez & Joshi, 2020; B. Zhang et al., 2023). As the science and engineering of creating intelligent technologies, AI has several branches, such as natural language processing, expert system, vision, speech, planning, robotics and machine learning. Machine learning is categorized into several subdivided fields: supervised, unsupervised, reinforcement learning, deep learning and transfer learning (Lamba et al., 2019; Reuters, 2016). This research study is concerned with deep learning and transfer learning purposes.

2.5 Deep Learning

Deep learning is a subfield of machine learning that is essentially based on neural network layers of learning and processing used to obtain higher-level inferences or features from data (Chollet, 2018; Letsoin, Purwestri, Rahmawan, et al., 2022). Deep learning mimics the structure of the human brain to analyze information; then, in deep learning form, the structure is known as an artificial neural network (ANN). Therefore, deep learning models are often indicated as the broadening of Artificial Neural Networks (ANNs) or called deep neural networks. The neural networks in both CNN and ANN are formed of learnable components namely weights and biases. The primary distinction is that ANN depends on the direct connections between layers while CNN introduces convolution operation for feature extraction. The convolution operation is presented in section 2.7.

In image classification tasks, the network learns to detect various features of an image using several or hundreds of hidden layers. Each hidden layer represents its tasks. For example, in Figure 4, the first hidden layer learns to detect points. In the next layers, it can identify more shapes and combine the previous knowledge to provide more information, such as the image of a cube or not a cube (Vasilev et al., 2019). The final layer provides the inference of the task. For instance, a well-trained deep neural network can classify an object on a picture with probability.

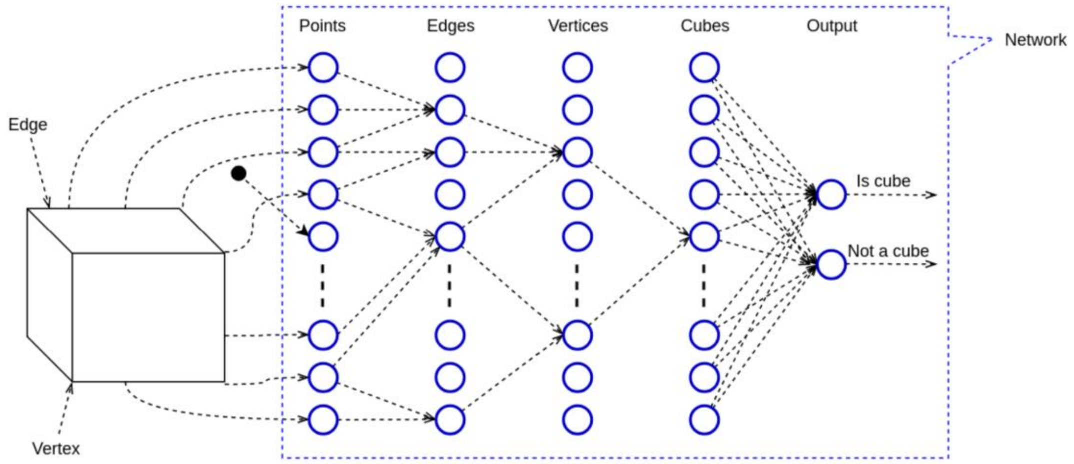

Figure 4. A multilayered abstraction in featured data extraction

A dataset is required for training and learning to obtain the inference; it could be images, numbers, texts, videos and other forms of data. Therefore, datasets can consist of several to hundreds of features to make the system learn specific tasks. A feature is one column of the data in the input set. For example, the input feature in face identification includes the nose, lips, eyes, etc. Then the label is relevant to the output or final class, such as man or woman.

Deep learning methods in object detection are generally divided into three categories (Zheng et al., 2021). (1) Convolutional Neural Network (CNN) that deforms learned features according to the input data and applies 2D convolutional layers, which are well-designed to process 2D data, for example, images. (2) Segmentation, a deep learning method that associates a label or category with every pixel in an image, and (3) object detection method refers to using deep learning to provide a specific location of an object in an image. According to a study review by (Yasir et al., 2023), the most prevalent deep learning method developed to cope with remote sensing image processing is CNN.

2.6 Transfer Learning

Transfer learning (TL) is another type of machine learning that emphasizes learning prevalent information from one base domain and applying it to another related domain (Letsoin, Purwestri, Rahmawan, et al., 2022; Zhuang et al., 2021). TL is used to refine the target domain by using the knowledge, for instance, optimal hyperparameters in the base model (Ashouri & Hashemi, 2022; L. Han et al., 2022). The idea of transfer learning was triggered by excessive data labelling, deep learning training, and also intensive resources such as processing time and hardware systems (Allworth et al., 2021; L. Zhang et al., 2022). Therefore, this technique is preferable specifically when there is a limited labelled dataset, less computational processing, or shorter training time (Baumann et al., 2022; Hao et al., 2021; M.-L. Huang et al., 2022). TL can be investigated as a process of refining the target prediction function $f_t(.)$ based on D^s and T^s, with $D^s \neq D^T$ or $T^s \neq T^T$ through knowledge transfer (Figure 5).

The form of knowledge transfer is categorized into four groups. Namely (1) instance-based transfer learning, an instance weighting strategy primarily used to develop instance-based learning, also appropriate for circumstances in which the source domain feature data cannot be repurposed. (2) Model-based transfer learning, the transferable knowledge is deeply integrated into a pretrained source deep model whose structure and parameters are useful for learning an effective target model. Model based techniques seek to determine the DL model components that can best contribute to improving the model learning process for the target domain. Further, (3) parameter-based transfer learning, the knowledge is carried at the parameter level, whereas the parameter in the source domain models have been improved to coincide with the target model. Furthermore, (4) feature-based transfer learning alters the original features to produce a new feature representation. Asymmetric techniques change the source feature in a way that makes them match the target feature. Conversely, symmetric techniques seek out the common feature spaces into which both source and target characteristics can be mapped.

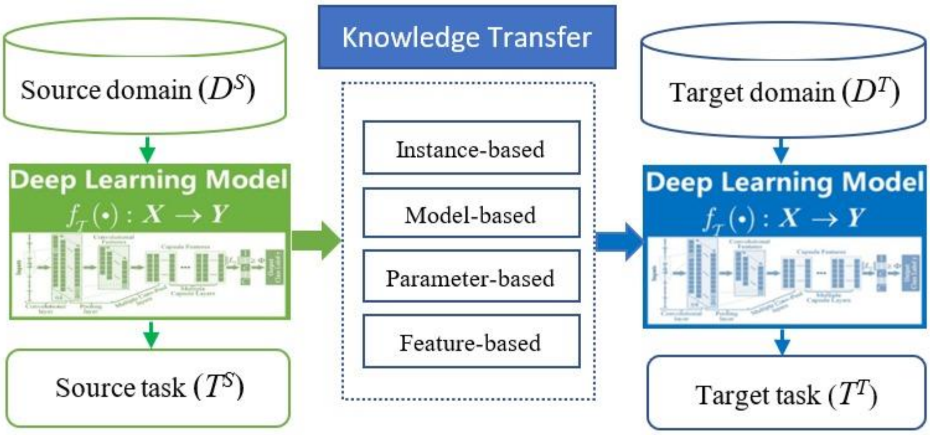

Figure 5. The concept of transfer learning with modification (W. Li et al., 2022; Z. Li, Kristofferson, et al., 2022)

The two components of a domain are a feature space X and a marginal distribution of probabilities $P(X)$, where $X = \{x_{1,}x_{2\ldots,}x_{n-1,}x_n\}$, n represents number of feature vectors in X. Similar to D, T contains two components, i.e., label space Y and a predictive function. Pairs of feature vectors and labels are used to train the predictive function $f(.)$, accordingly, a domain $D = \{X, P(X)\}$ and a task $T = \{Y, f(.)\}$. Henceforth, the source domain can be described as $D^s = \{X, P_s(X)\}$ with an associated source task $T^s = \{Y, f_s(\hat{A})\}$, equally the $D^T = \{X, P_t(X)\}$ with a related source task $T^T = \{Y, f_t(\hat{A})\}$. TL also can be divided into two categories namely heterogeneous specifically when $X_S \neq X_T$, vice versa, it is called homogenous when $X_S = X_T$.

2.7 Convolutional Neural Network (CNN)

A CNN, also known as a ConvNet, is a feed-forward neural network that is generally used to analyze visual images. In CNN, each image is represented in the form of arrays of pixel values. A CNN has many kinds of layers, generally consisting of a convolution layer, ReLU layer, pooling layer, flatten layer and fully connected layer (Kneusel, R. T., 2021). Convolutions operate in the structure of 3D tensors, namely *feature maps*, with two spatial axes, i.e., height, width and depth axis, or so-called channel axis (Figure 6). This layer contains various filters, also known as the kernel, with a trainable weight size of *f x f*. A convolution work is described by *sliding* the kernel window *f x f* with a specific *stride* over the input image and computing the dot product to detect the patterns.

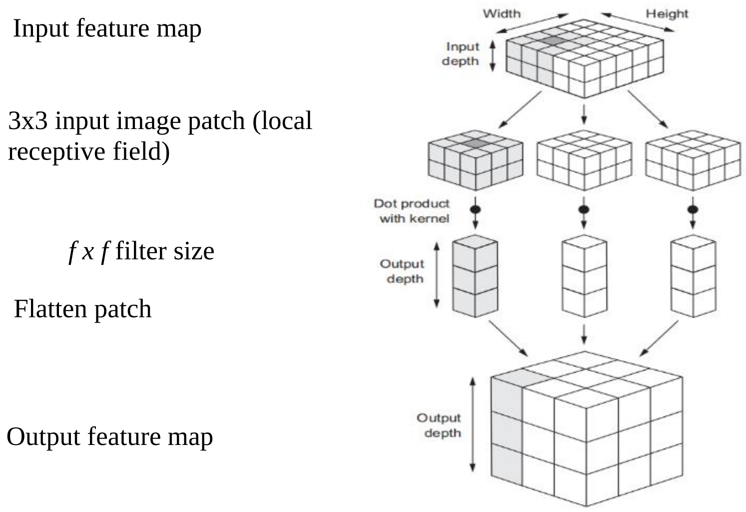

Figure 6. The convolution process with modification (Chollet, 2018).

However, after the convolution operation, the original image size could get smaller. Therefore, in order to preserve the size of the original image, the *padding* technique is an alternative. Figure 7 shows an input size of 5x5, with *zero padding*, *stride* 1, and *kernel* or *filter* size of 3x3. Then, the convolved feature as an output size of 5 x 5 is obtained.

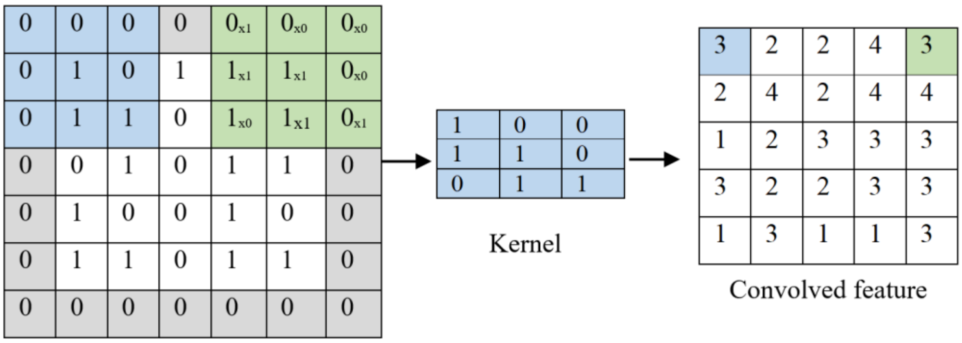

Figure 7. Padding technique with stride with modification (Kneusel, R. T., 2021).

After the padding technique, the input image 5x5 now *(N)* becomes 7x7, and then the rotated kernel *(F)* size of 3x3 moves one pixel *(stride=1)*. The output can be calculated as *(N-F)/stride + 1*. In this case, the output is (7-3) / 1 + 1 = 5; hence the convolved output size is 5x5. Without the padding technique, the convolved output is 3x3. Activation layers are used to enable non-linear mapping, which enhances feature maps' capabilities. Basically, linear multiplied categorization problems are remarkably rare. However, linear processes such as convolution and pooling diminish the capacity of non-linear data to learn. Feature map activations obtained from convolutional layers can be successfully transferred into non-linear domains by using activation layers, increasing the capacity of models to learn (Ornek & Ceylan, 2022).

Rectified Linear Unit (ReLU) is one of the activation functions that perform the element-wise operation; for example, it adjusts all negative pixels to zero. Otherwise, it returns the value as a rectified feature map. The relationship in this layer can be formulated as follows (Kneusel, R. T., 2021):

$$ReLU(x) = \max(0, x) \tag{1}$$

The pooling layer is an operation of down-sampling to downsize the dimensions of the rectified feature map. The pooling layer also uses filters and strides to identify various features such as corners, edges, leaves, etc. Since the pooling layer is used to reduce the number of parameters to train, the number of computation requirements is also declined. There are two kinds of pooling layers, i.e., average pooling and max pooling. Max pooling is most commonly used as pooling layer for selecting the largest value in each filter region. Two factors make the pooling layer of paramount importance to CNN. First, without diminution, the computation would crash when convolutional layers capture duplicate information. Second, the duplicate features would degrade the redundant information's ability to describe features. As a result, implementing a pooling layer is necessary for reducing the dimensions of features.

As shown in Figure 6 previously, the flattened patch is used to convert all the resultant dimensional arrays from pooled feature map to a single linear vector. Thus, the flattened matrix results act as an input to the fully connected layer to classify the object. The ConvNet often becomes smaller in dimension but larger in channel or depth as data passes through the network. The first layers, such as Convolution, activation, for example, ReLU, then pooling, are generally used to extract the feature, while the next layer, for instance fully connected layer, is to do the recognition task. Nevertheless, SoftMax designates probability to each class of output (Figure 8). The fully connected layers are often positioned near the output layers. In the image classification task, this layer acts as a classifier as well as the final output layers.

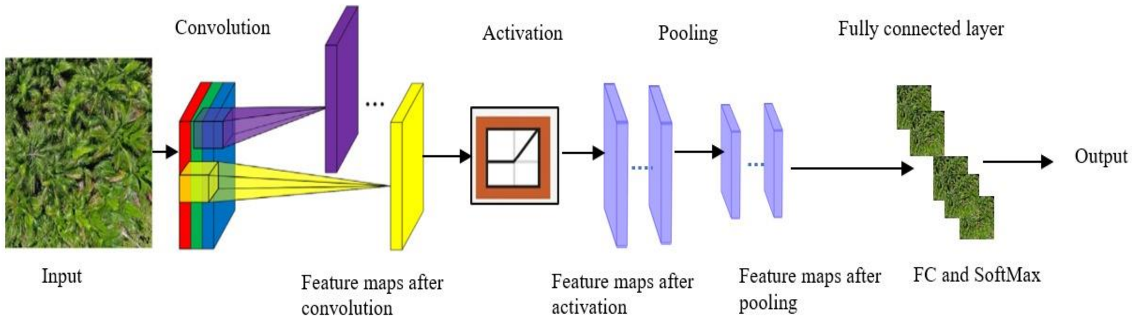

Figure 8. Illustration workflow of CNN architecture with modification (Ferchichi et al., 2022)

Fully connected layers provide an extensive number of characteristics due to their full connectivity; however, containing numerous parameters might also lead to overfitting. In this case, fully connected layers are typically replaced with global pooling. A SoftMax layer is used to determine class probability; this layer could be substituted with the regression layer in a regression task. The classic classifiers, the most common machine learning approaches that mostly rely on manually created features, including ANN, decision tree or Support Vector Machine (SVM), are susceptible to overfitting or underfitting issues. Compared to deep CNN models, existing pre-trained networks like AlexNet, VGGNet, GoogLeNet, etc., are preferred since they can learn high level features without requiring manual involvement (Orchi et al., 2023).

Deep CNN models as mentioned previously can use as the backbone network in another different purposes, such as Masked Region-based CNN (Mask R-CNN), as displayed in Figure 9. Figure 9 illustrates the Mask R-CNN model, the images are introduced into the backbone network for selecting and processing in order to produce feature maps. The background and foreground are then separated using the RPN network. Thus, specified into the ROI alignment then enters into the head network to create boxes, classes, and masks.

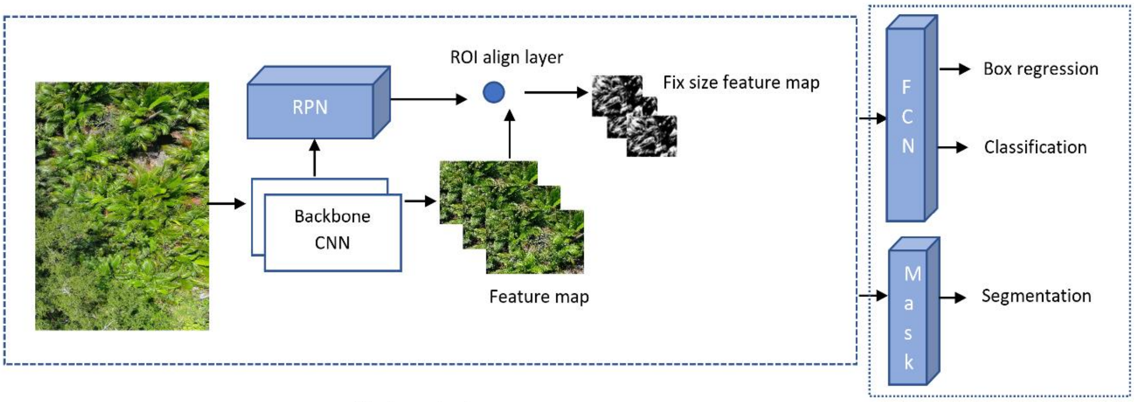

Figure 9. Mask R-CNN model with modification
(B. Han et al., 2022; Xu et al., 2022)

The Mask R-CNN network operates in two stages. In the first stage, the backbone networks, such as the CNN model, derive a feature map from the input image. Then the feature maps output from the backbone network is delivered to the Region Proposal Network (RPN), to generate Regions of Interest (ROIs). ROI maps are the outputs from the RPN mapped to the shared maps to produce the corresponding target features (He et al., 2018). To achieve higher accuracy in pixel computing, this model uses an ROI alignment layer instead of pooling (ROI pooling). The distorted alignment is corrected through ROI alignment by removing the quantization which usually occurred using ROI pooling. In the next stage, object classification, the output from the previous stage is delivered to the fully connected and fully convolutional network (FCN) for target classification and instance segmentation. This step commences with bounding boxes, classification and segmentation mask (Hu et al., 2022; Lu et al., 2021).

2.8 Model Evaluation

Evaluating a model is essential in order to examine the model performance by the metrics. Metric refers to a designated number that interprets the performance of a model. Several evaluation metrics are used in the classification task, such as confusion matrix, cross-validation, or plotting the receiver operating characteristic (ROC) curve (Kneusel, R. T., 2021).

The formula in Table 3 can be derived from a tabular visualization called a confusion matrix. Each cell in the confusion matrix indicates an evaluation parameter, namely True Positive (TP), True Negative (TN), False Positive (FP), and False Negative (FN).

Table 3. The classification metrics (Kneusel, R. T., 2021; Letsoin, Purwestri, Rahmawan, et al., 2022)

Metric	**Formula**	**Criteria**
F1-score	$\frac{2 \times (Recall \times Precision)}{Recall + Precision}$	Denotes a high value, which validates the model.
Precision	$\frac{TP}{TP + FP}$	Examines the ability of the model to the predict positive label.
Sensitivity (Recall)	$\frac{TP}{TP + FN}$	Defines the ability of the model to detect instances of certain classes well.
Specificity	$\frac{TN}{FP + TN}$	Defines the true negatives that are correctly identified by the model.
Accuracy	$\frac{TP + TN}{TP + FP + TN + FN}$	Examines the accuracy in identifying the images to the classes.

TP represents a positive sample predicted correctly, and FP represents a negative sample predicted incorrectly. While FN indicates a positive sample predicted incorrectly, TN indicates a negative sample predicted correctly. For example, if the testing image is sago flowers, the actual image being sago flowers, then:

1. TP, the number of actual images that display sago flowers (true) are classified as sago flowers (predicted).
2. FP, the number of actual images that do not display sago flowers (not true) are classified as sago flowers (predicted).
3. FN, the number of actual images that display sago flowers (true) are classified as a different class (predicted).
4. TN, the number of actual images that do not display sago flowers (not true) are classified as a different class (predicted).

The ROC represents the relationship between sensitivity or TP rate and specificity (1-PF rate). A good classifier can be indicated by the ROC curve and it is nearer to the top left corner or far away from the reference curve (Grigorev, 2021; Kneusel, R. T., 2021).

2.9 Related Work

Table 4 presents a list of related works on sago palm detection by applying remote sensing technology. These include the findings, approaches, aims, dataset and evaluation model. This table is used to differentiate the previous result from the proposed research.

Table 4. Related works in sago palm detection.

Findings	**Aims**	**Approaches**	**Dataset**	**Evaluation model**	**Authors**
The detection of maturity was found to be 85.7% accurate.	To detect sago trees and determine their maturity.	Proposed model based on CNN-deep learning networks, namely Alexnet, Xception, ResNet in Matlab software.	The self-made dataset from UAV consisting of harvestable sago, non-harvestable sago, background (other objects such as rivers, cars, etc.) of the sago palm canopy in Malaysia. Dataset contained 189 test images and 756 training images.	Fivefold validation	Wahed, Z., Joseph, A., Zen, H., & Kipli, K. (2022). Sago Palm Detection and its Maturity Identification Based on Improved Convolution Neural Network. *Pertanika Journal of Science & Technology*, *30*(2).
The overall accuracy of sago palm classification reached 85%.	To carry out sago palm classification according to eight most important attributes consisting of three spectral features, three arithmetic and two	Support Vector Machine (SVM) as a classifier; Vegetation index and image processing. Object-Based Image Analysis was also applied.	Satellite datasets, particularly VHR images (Pleiades 1A) and GIS software, namely PCI geomatics and e-cognition. Other LULC data generated	McNemar test	Hidayat, S., Matsuoka, M., Baja, S., & Rampisela, D. A. (2018). Object-based image analysis for sago palm classification: The most important features from high-resolution satellite imagery. *Remote Sensing*, *10*(8), 1319.

	textural features.		from the Global positioning system (GPS). Sago areas in Luwu, Indonesia.		
Prospective sago palm locations in the Philippines were discovered.	To accurately assess the availability of sago palms in the Philippines.	A GIS software, namely ENVI 5, with maximum likelihood classifier (MLC) and ground data to process the images. Before that, ArcGIS software was used to make the polygon shapes.	Landsat 7 ETM+, world view-2 images, also supported by GPS.	Visual interpretation from ground surveys and by support of world view-2 images.	Jojene, R. Santillan & Meriam Makinano-Santillan Recent Distribution of Sago Palms in the Philippines. In BANWA Monograph Series 1 Mapping Sago: Anthropological, Biophysical and Economic Aspects; Paluga, M.J.D., Ed.; University of the Philippines: Mindanao, Philippines, 2016; p. 186. ISBN1 6219560701. ISBN2 9786219560702
The sago habitat using spatial data in Jayapura were investigated.	To identify the sago environment based on elevation, slope, soil, climate, and distance from river and lake in Jayapura, Indonesia.	A supervised classification and ArcGIS software. Fieldwork survey also involved measurement of temperature, humidity and sunlight intensity.	Spatial dataset including soil type, elevation, slope, rivers, rain precipitation, watershed area, province boundary also from satellite data such as Quickbird, Landsat 8 and shuttle radar topography mission.	Not defined specifically.	DIMARA, P. A., PURWANTO, R. H., & SUNARTA, S. (2021). The spatial distribution of sago palm landscape Sentani watershed in Jayapura District, Papua Province, Indonesia. *Biodiversitas Journal of Biological Diversity*, *22*(9).

3. OBJECTIVES AND HYPOTHESIS

3.1 Objectives

This research concerns how to detect the sago palm in the fieldwork by using remote sensing data, deep learning and transfer learning techniques. The specific objectives include the following:

1. To investigate the potential habitat of sago based on Land Use Land Cover (LULC) changes.
2. To differentiate the visible morphology of sago., i.e., leaves, trunks and flowers.
3. To distinguish the area of sago from other vegetation.
4. To design a sago palm detection model.
5. To evaluate the performance of the developed sago palm detection model.

In addition, potential uses in health aspects, bioenergy, as well as macro and micro nutrients of sago in Southern Papua were also reviewed.

3.2 Hypothesis

The hypotheses were designed to obtain the specific objects and to affirm or disprove these statements:

1. **Hypothesis 1: The potential habitat of sago can be evaluated through the Land Use Land Cover (LULC) changes and supported by stakeholders' data.**

   Several previous studies noticed the LULC as one of the approaches to examine the dynamic changes in one area. It is important to gain information on historical and present conditions, to predict other phenomena, and also assist the relevant stakeholders in arranging strategic plans (Guo et al., 2020; Halmy et al., 2015). This will be analyzed by utilizing remote sensing technology, specifically satellite data supported by stakeholders' data such as Land cover classes of Indonesia.

2. **Hypothesis 2: The expansion of crops and agriculture areas, the settlement sector and also the degradation of forested areas based on LULC data could contribute to the changes in the sago's ecosystem in the fieldwork.**

   This hypothesis is principally supported by the first hypothesis, that LULC dynamic changes affect the availability of several essential commodities including water bodies, the extension of settlement areas, and the expansion of crops and agriculture areas. Furthermore, the degradation of forest areas is due to urban development or deforestation (Aliani et al., 2019; Cheng & Wang, 2019; Hamad et al., 2018; Tripathy & Kumar, 2019). The statistical analysis with a p-value of less than 0.05 is applied in order to detect the changes in crops and agriculture areas, the settlement and forested areas.

3. **Hypothesis 3: Transfer learning techniques are able to differentiate the physical appearance of sago compared to others vegetation with small datasets.** The transfer learning based on deep Convolutional Neural Network (CNN) model will be recreated for a new task and trained with several different parameters. The optimized parameter is determined based on best practices from earlier studies (Mathewos et al., 2022; Whittle et al., 2012). The deep learning CNN model, based on AlexNet, Squeeze Net and ResNet-50 will be implemented with a small dataset of about 200 to 500 images. The physical appearance is described by visual morphology, for instance, leaves, flowers or trunk.

4. **Hypothesis 4: CNN deep learning networks are able to detect and predict sago palms captured by a UAV and ground photographs.** This hypothesis is inspired by the third hypothesis. Transfer learning (TL) is essentially a technique driven by transferring knowledge from one base domain to another relevant domain (Velastegui-Montoya et al., 2022). TL is used to refine the target domain using knowledge, such as the optimal parameter in the base model (Ashouri & Hashemi, 2022; L. Han et al., 2022). Then, the new task in the target model is expected to achieve better performance or obtain a different task in the same domain. Chapter 5 describes the existing CNN deep learning network in sago detection. Our own data set was obtained from UAV and ground photographs, while the new target task defined by the classification and the confidences of a model to distinguish the image.

5. **Hypothesis 5: In designing the sago palm detection, parameters and network structure must be considered.**

   Another motivation in the sago detection study is the morphology challenge due to the wild stand. Therefore, experiments with different networks and hyperparameters are performed. Hyperparameter refers to a parameter established before the learning process begins. These adjustable settings have a direct impact on how successfully a model trains. Two various sets of hyperparameters are implemented in the network structure. Chapter 5 presents the results and compare their impact in the training and testing stage.

6. **Hypothesis 6: The evaluation of the model is essential to ensure that the model performs in accordance with the expected outcomes.**

   This hypothesis (Hypothesis 6) is derived from the fourth and fifth Hypothesis. To visualize the performance of the model, the ROC curves are used as well as a tabular matrix, i.e., confusion matrix. The metric evaluation is described based on confusion matrix through the value of F1-score, precision, sensitivity, specificity, and accuracy, which is preferably to be close to 1 or 100% if defined as a percentage. A good classifier visualized by the ROC curve, is near the top left corner or far from the reference line (Grigorev, 2021; Kneusel, R. T., 2021).

4. MATERIALS AND METHODS

4.1 Materials

Two different types of a dataset were provided during the data preparation step in these two experiments. The first, from satellite data (Landsat data). The characteristics of the satellite data used are shown in Table 5. The data were collected with a resolution of 30m, 705 km of altitude and 50% of cloud cover by downloading it in the United States Geological Survey (USGS). To support the processing, Land cover maps for several years, i.e., 1990, 1996, 2003, 2006, 2011, 2014, 2017, and land cover classes of Indonesia were collected from the Ministry of Environment and Forestry (MoEF) of Indonesia.

Table 5. Satellite data performed in this study.

Property	Landsat 5	Landsat 7	Landsat 8
Spatial resolution	30m for visible and I.R.,	30m for visible and InfraRed (I.R.).,	30m for visible and I.R.
	120m for thermal	15m for Panchromatic (Pan) and 60m for thermal	15m for (Pan) and 100m for thermal
Spectral resolution	7 bands (visible, I.R., and thermal band)	8 bands (visible, I.R., Pan, and thermal band)	11 bands (visible, I.R., Pan, and thermal band)
Radiometric resolution	8 bit	8 bit	16 bit
Temporal resolution	16 days	16 days	16 days
Details of spectral resolutions (ɥm)	Band 1: (blue) 0.450-0.515	Band 1: (blue) 0.450-0.515	Band 1: (blue) 0.43-0.45
	Band 2: (green) 0.525-0.605	Band 2: (green) 0.525-0.605	Band 2: (blue-green) 0.45-0.51
	Band 3: (red) 0.63-0.69	Band 3: (red) 0.63-0.69	Band 3 (green) 0.53-0.59
	Band 4: Near Infra-Red (N.I.R.) 0.76-0.90	Band 4: (N.I.R.) 0.76-0.90	Band 4: (red) 0.64-0.67
	Band 5: Short-Wave Infra-Red (SWIR-1) 1.55-1.75	Band 5: (SWIR-1) 1.55-1.75	Band 5: (N.I.R.) 0.85-0.88
	Band 6: (thermal) 10.4-12.5	Band 6: (thermal) 10.4-12.5	Band 6: (SWIR-1) 1.57-1.65
	Band 7: (SWIR-2) 2.09-2.35	Band 7: (SWIR-2) 2.09-2.35	Band 7: (SWIR-2) 2.11-2.29

	Band 8: (Pan) 0.52-0.92	Band 8: (Pan) 0.50-0.68
		Band 9: (Cirrus) 1.36-1.38
		Band 10: (Thermal I.R.) 10.60-11.19
		Band 11: (Thermal I.R.) 11.50-12.51

In addition, auxiliary data were also gathered in the study field, such as the provincial boundary spatial data, forest type, and area of forest by function. The geographical location of the fieldwork is depicted in Figure 10. The regency consists of twenty regions namely Ulilin, Muting, Kaptel, Ngguti, Ilwayab, Tabonji, Waan, Kimaam, Tubang, Okaba, Malind, Kurik, Elikobel, Jagebob, Tanah Miring, Semangga, Sota Naukenjerai, Merauke and Animha; also recognized as the most paddy producer over Papua Province. Integrated with favorable temperature and humidity for particular crops and forest, this regency provides potential habitat of sago.

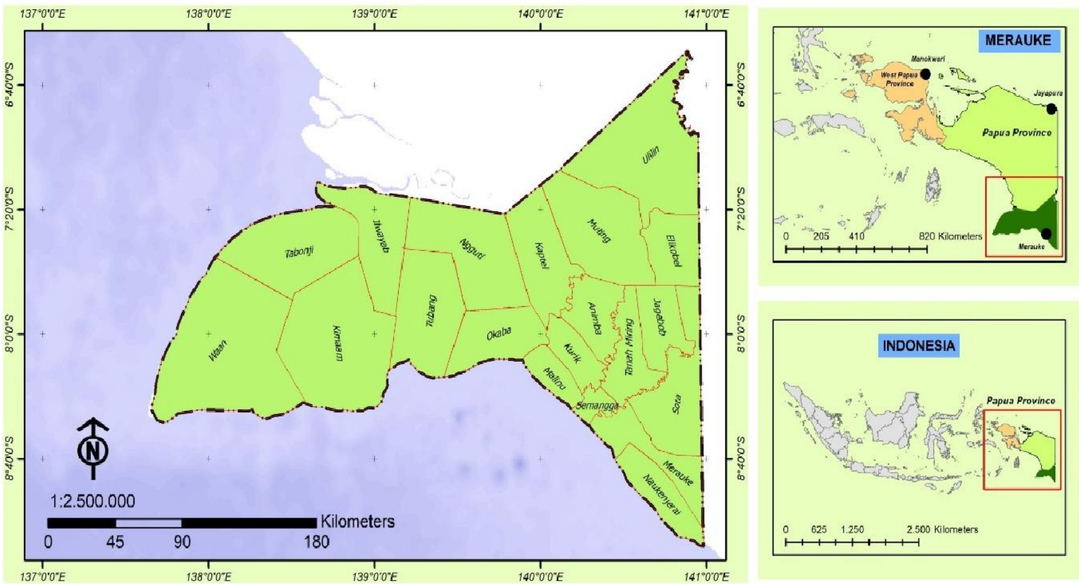

Figure 10. Study location (Letsoin et al., 2020).

The second dataset was used in the second experiment. The images were captured from the ground photograph and a UAV with a certain parameter. The UAV was integrated with the mission flight planner, and it flew over a sago area of 74.600 m^2 in Merauke Regency of Papua Province, Indonesia, collecting a total of 661 images. A double grid with 70% and 80% of front overlap, 70% and 60% of side overlap and 60.3 m of altitude was used to fly the Autel drone from 9:00 to 11:30 a.m. (Figure 11).

Afterwards, all the images were transferred to computer storage for the preprocessing stage. In this stage, all data were divided into three types, namely data for testing, training and validation. Image segmentation as well as a cropping process were required to designate the region of interest (ROI). Hence, the dataset also involved varied sizes of images, blurred and yellowish with varying angles.

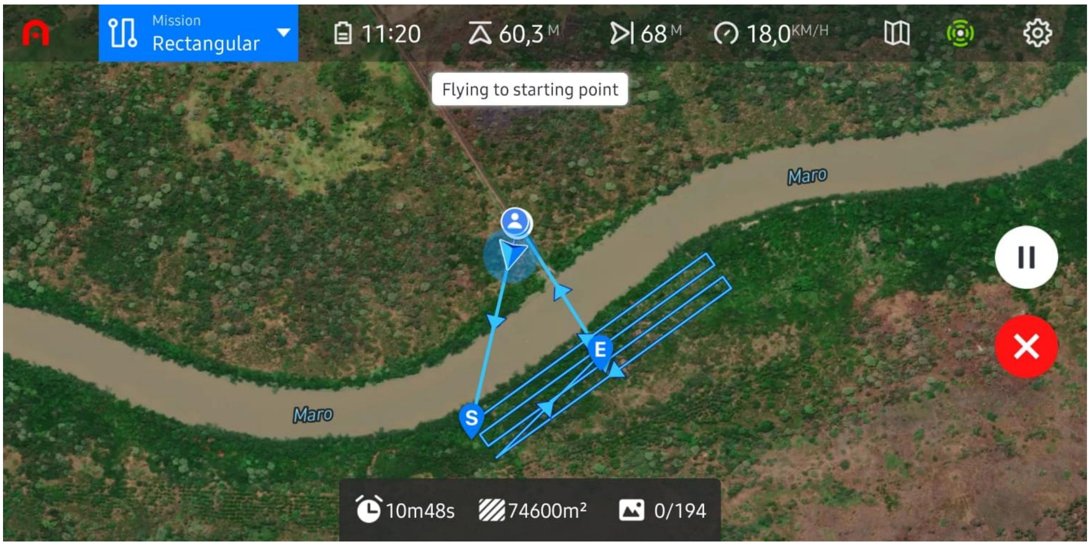

Figure 11. Mission flight Planner (Letsoin, Purwestri, & Herák, 2022).

Datasets can be found using self-created datasets, such as from those obtained using a UAV or taking photographs. Today, publicly open labelled datasets, for instance, ImageNet, CIFAR-10, Open Images, etc., are available. Each dataset provides a variety of images. For example, ImageNet supports the recognition of birds, vehicles, furniture, etc. CIFAR-10 and CIFAR-100 dataset consists of 60000 32x32 color images in 10 classes, with 6000 images in each class. Some classes in the dataset include airplane, bird, cat, deer, horse, ship, truck, etc. Open Images is recognized as the dataset containing object location and object segmentation masks that are currently available. In this study, we constructed self-made dataset using aerial and ground photographs that were labelled in accordance with the purposes and hypotheses of the study.

4.2 Methods

The methodology was developed to obtain the objectives and hypotheses of the dissertation work, as explained in section 3. Two different workflows were tested in this study. Firstly, the satellite data were processed using the GIS software and supervised classification. Secondly, a sago palm detection system from UAV and ground photograph images was developed by performing AI approaches, namely deep learning and transfer learning. In general, there are six procedures, namely (1) data preparation, (2) data preprocessing, (3) detection and classification modelling, (4) data training, (5) testing and validating, and (6) result analysis.

In the first experiment, satellite data such as Landsat TM, ETM+ and Landsat OLI were downloaded according to the study location (fieldwork) as a part of data preparation. Furthermore, image processing, as well as image correction, were developed. Data training, testing and validating stages were based on field surveys and visual interpretation based on existing data from the MoEF of Indonesia and the LC classes of Indonesia. Lastly, the rate of land cover changes was calculated. Moreover, the results were analyzed statistically with SPSS and an ANOVA with a *p*-value less than 0.05.

In the second experiment, data preparation was done through fieldwork activity consisting of a field survey using a UAV and ground photographs at the area of the sago palms. Thus, data preprocessing, modelling, data training and testing were accomplished by software laboratory experiments. The detection and classification modelling depends on the methods used. For instance, transfer learning is based on a CNN network. In this experiment, transfer learning based on the CNN model was applied, for instance, AlexNet, SqueezeNet and ResNet50, as shown in Figure 12. The target label consisted of nine classes and their probability.

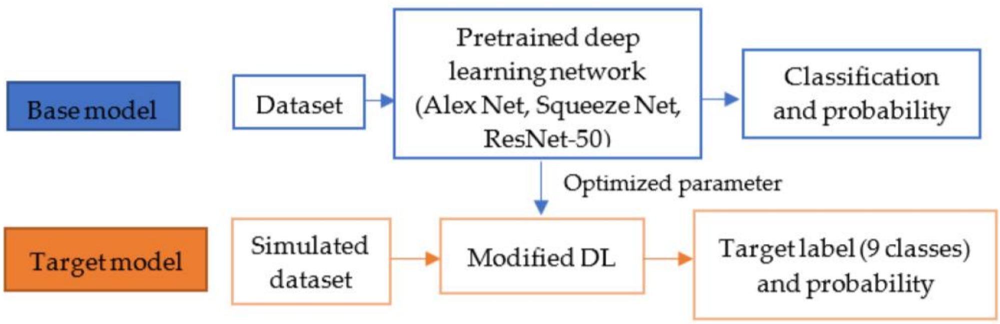

Figure 12. Data driven transfer learning (Letsoin, Purwestri, Rahmawan, et al., 2022).

Next, several parameters, i.e., learning rate, epoch, and min batch size were adjusted. The self-made dataset was divided into three kinds of purposes, namely data for training (data training), validation (data validation) and testing (data test) (Kneusel, R. T., 2021). The software was used in modelling experiments, such as MATLAB, spreadsheet and MATLAB scripts. In this stage, the experiment results were documented in a spreadsheet file. Finally, all results were evaluated based on metrics performance.

The experiment was designed as follows:

1) To validate the first objective, as well as the first and second hypotheses of this study, supported GIS software and dataset from Landsat were utilized. The estimation area was converted to an Excel file. The results were statistically evaluated using SPSS software. Thus, the changes, such as losses and gains, were also estimated.
2) Further, to achieve other objectives and hypotheses, MATLAB software with CNN deep learning models based on transfer learning techniques were used. The optimized parameters were defined through best practices from previous studies and by making some adjustments involving the number of epochs, initial learning rate, and min batch size. The results were used to test the third, fourth and fifth hypotheses of the study. The annotation images were labelled manually and in Mat-file, Common Object in Context (COCO) and Visual Geometry Group (VGG) JSON format.
3) Finally, metrics evaluation was carried out during the testing phase. The performance of the model was evaluated through the criteria of the confusion matrix and several metrics, i.e., F1-score, precision, sensitivity, specificity and accuracy, and also receiver operating characteristic (ROC) curves. The results were used to investigate the sixth hypothesis.

Figure 13 displays the overview of experiments in this study and the relation to each hypothesis and objective, as well as the publishing outcomes.

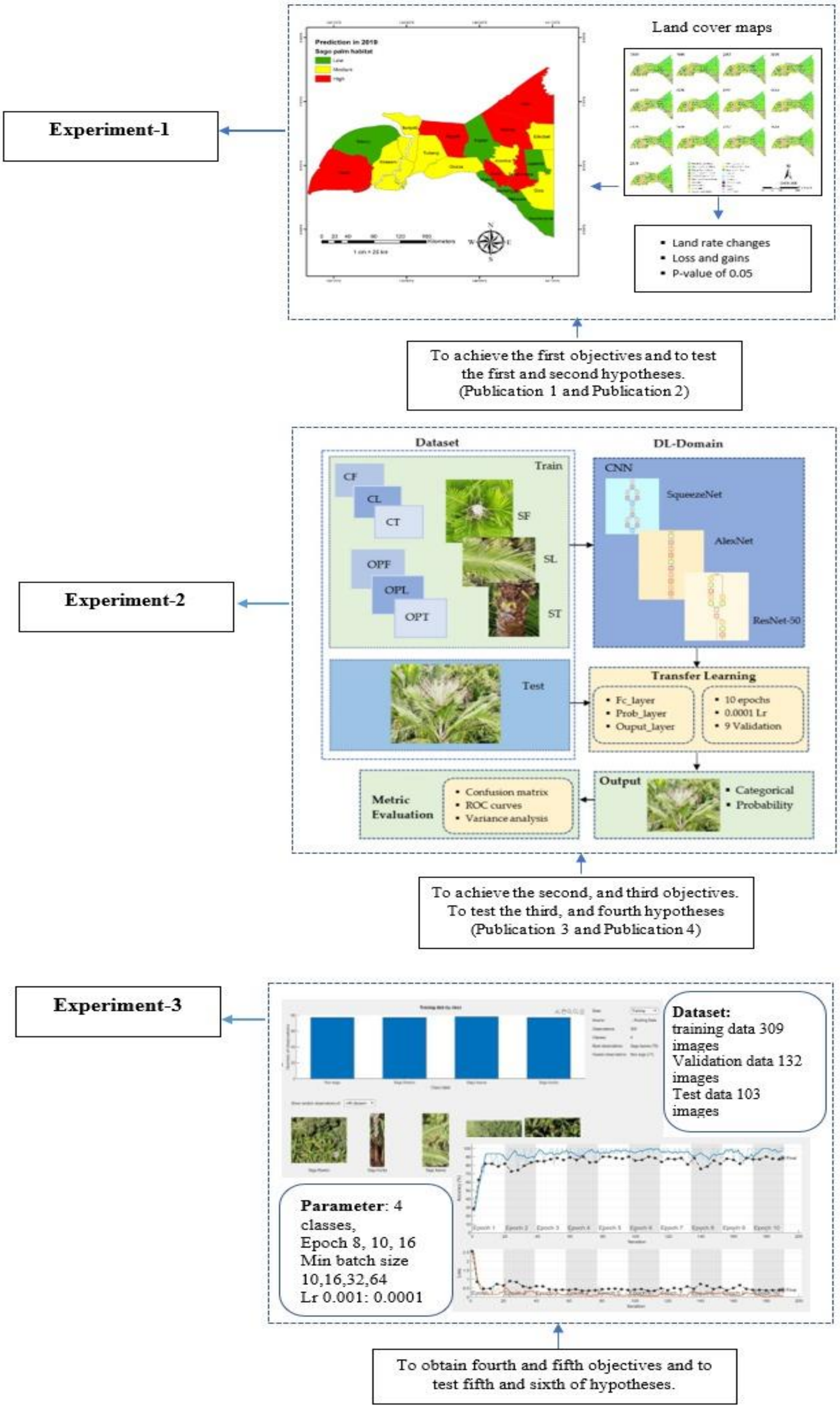

Figure 13. The relevance of the experiment, objectives, and hypotheses of study.

In experiment-2 and 3, MATLAB syntax was used to calculate the numeric confusion matrix, as follows:

```
[m,order] = confusionmat(Target1,Predict1);

figure
cm = confusionchart(Target1,Predict1, ...
    'Title',' Sago Model-1 (trainedNetwork_1) ', ...
    'RowSummary','row-normalized', ...
    'ColumnSummary','column-normalized');
```

And *pseudocode* for the testing process was defined as follows:

Start
Read image,
Display image,
Crop image,
Display image,
Process [Ypred, prob],
Display image,
Display Ypred
Display prob,
End

The test images will resize according to each backbone used, for instance, the Squeeze Net structure only allows a size of 227x227 pixels. The third experiment is principally based on the study approached in experiment-2 which was published in publication 2 and publication 3. Nevertheless, different parameters, namely epoch, learning rate and min batch size, was treated variously for four classes. Table 6 shows the dataset used in experiment-3. As displayed in Figure 13, the main effort in this experiment was used to test the fifth hypothesis as well as to support the previous finding in experiment-2.

Table 6. Dataset in experiment-3.

Dataset	Number of images	Description
Training		
Non-sago	110	Training images
Sago flowers	110	
Sago leaves	111	
Sago trunk	110	
Test		Testing images
Non-sago	23	
Sago flowers	16	
Sago leaves	53	
Sago trunk	11	
Validation	132	30% of total images

Different parameters of each base model are shown in Table 7. The backbone architecture designed from trainedNetwork-1 to trained Network-16 is SqueezeNet with transfer learning, while from trained Network-17 to trained Network-22, it is AlexNet with transfer learning. Moreover, from trained Network-17 to trained Network-22 are adopted from training setups used in trained Network-2, trained Network-3, trained Network-6, trained Network-13, trained Network-15, and trained Network-16 respectively.

Table 7**.** Parameters used in experiment-3.

Network name	**Training set up**		
	Epoch	**Learning rate**	**Min batch size**
trained Network-1	10	0.0001	32
trained Network-2	10	0.0001	64
trained Network-3	8	0.0001	32
trained Network-4	8	0.0001	64
trained Network-5	15	0.0001	32
trained Network-6	15	0.0001	64
trained Network-7	8	0.001	32
trained Network-8	8	0.001	64
trained Network-9	10	0.001	32
trained Network-10	10	0.001	64
trained Network-11	15	0.001	32
trained Network-12	15	0.001	64
trained Network-13	8	0.0001	16
trained Network-14	10	0.0001	16
trained Netwoork-15	10	0.0001	10
trained Network-16	8	0.0001	10
trained Network-17	10	0.0001	64
trained Network-18	8	0.0001	32
trained Network-19	15	0.0001	64
trained Network-20	8	0.0001	16
trained Network-21	10	0.0001	10
trained Network-22	8	0.0001	10

In this experiment, a validation frequency of 4 was used, corresponding to each category class, i.e., non-sago, sago flowers, sago leaves and sago trunks. Others parameters were related to experiment-2, for instance, momentum, learning rate bias coefficient, and learning rate coefficient. Further, the convolution layer used 3x3 filter size, weight Lr factor was 1, and bias Lr factor was 10. The batch size determines how many samples were used in one cycle training period of a model. Generally, there are three types, namely, batch gradient descent, stochastic and mini batch size.

5. RESULTS

5.1 Performing Remote Sensing Data to Investigate the Potential Habitat of Sago

The land cover area in *ha* and the percentage of change from 1990 to 2019 are presented in Table 8, Table 9 and Table 10 below. It is clearly visible that this regency has twenty-one land cover classes within six classes of forested areas and fifteen classes of non-forested areas. In 1990, about 50.3% of the regency was covered by forested areas. The areas of non-green cover were around 1% smaller than the forested areas (Table 8).

Table 8. Land cover area and the percentage of change from1990 to 2003.

LC Class	1990 (ha)	1996 (ha)	2000(ha)	2003 (ha)
Natural Forest				
Primary dryland forest	694,737	664,757	634,776	619,004
Secondary dryland forest	638,049	620,773	603,496	618,381
Primary mangrove forest	208,727	207,345	205,963	201,768
Secondary mangrove forest	25,345	24,209	23,073	25,776
Primary swamp forest	342,429	329,304	316,179	292,789
Secondary swamp forest	531,109	419,213	307,317	313,173
Total area (ha)	2,440,396	2,265,600	2,090,804	2,070,891
Percentage of change (%)	50.30	46.70	43.09	42.68
Change rate (ha/yr)	-	−7.1626	−7.715	−0.952
Non-Forest				
Bush/shrub	71,946	24,194	176,443	177,229
Estate crop plantation	-	-	-	101
Settlement area	3160	3366	3571	3667
Barren land	81,714	51,759	21,805	21,805
Cloud covered	764	764	764	764
Savanna/grassland	471,693	549,087	626,480	646,258
Water body	352,031	352,012	351.993	351,992
Swamp shrub	930,069	931,438	932,806	929,360
Dryland agriculture	14,377	15,368	16,358	16,772
Shrub-mixed dryland farm	43,462	49,013	54,563	54,563
Paddy field	10,932	10,932	10,932	10,974
Fishpond	-	-	-	-
Airport/harbor	159	159	159	159
Transmigration area	36,638	41,430	46.221	46,221
Swamp	394,375	456,596	518,816	521,051
Total area (ha)	2,411,319	2,586,115	2,760,912	2,780,824
Percentage of change (%)	49.70	53.30	56.91	57.32
Change rate (ha/yr)	-	7, 249	6, 759	0.721

The non-forested areas appear to have increased over the next six years, particularly in 1996, and continuously until 2014. In 2014 (Table 9), there was an 8% to9 % decrease in the forested areas compared to 1990. As mentioned previously, the forested areas play an important role as a habitat for native plants, such as sago.

Table 9. Land cover area and the percentage of change in two groups from 2006 to 2014.

LC Class	2006(ha)	2009(ha)	2011(ha)	2014 (ha)
Natural Forest				
Primary dryland forest	598,828	553,728	553,098	543,670
Secondary dryland forest	627,494	672,086	672,425	678,803
Primary mangrove forest	196,510	196,510	196,510	197,808
Secondary mangrove forest	23,678	23,574	23,574	23,675
Primary swamp forest	238,249	205,343	205,343	206,530
Secondary swamp forest	338,909	371,810	371,810	374,446
Total area (ha)	2,023,668	2,023,051	2,022,760	2,024,932
Percentage of change (%)	41.71	41.70	41.69	41.74
Change rate (ha/yr.)	-2280	-0.030	-0.014	-0.107
Non-Forest				
Bush/shrub	178,032	178,463	177,262	174,273
Estate crop plantation	101	101	1533	16,535
Settlement area	3891	3891	3891	3917
Barren land	21,853	21,853	21,913	23,501
Cloud covered	764	764	764	-
Savanna/grassland	655,175	704,034	704,044	708,703
Water body	351,995	351,994	351,994	322,264
Swamp shrub	949,786	900,908	900,838	906,111
Dryland agriculture	16,803	16,880	16,880	17,184
Shrub-mixed dryland farm	65,250	65,379	65,379	65,760
Paddy field	10,974	10,974	11,044	11,463
Fishpond	-	-	-	-
Airport/harbor	159	159	159	159
Transmigration area	46,221	46,221	46,221	46,440
Swamp	527,044	527,044	527,034	530,472
Total area (ha)	2,828,047	2,828,664	2,828,955	2,826,783
Percentage of change (%)	58.29	58.30	58.31	58.26
Change rate (ha/yr.)	1698	0.022	0.010	-0.077

From 2015 to 2018, green areas showed a decreasing trend, from 40.75% in 2015 to 39.46% in 2018 (Table 10). Nevertheless, in 2019 this percentage has risen to 42.97%.

Table 10. Land cover area and the percentage of change in two groups from 2015 to 2019.

LC Class	2015(ha)	2016 (ha)	2017(ha)	2018 (ha)	2019 (ha)
Natural Forest					
Primary dryland forest	529,715	522,977	519,144	401,879	500,359
Secondary dryland forest	664,888	654,663	652,518	732,934	631,295
Primary mangrove forest	196,758	195,162	195,007	195,660	195,384
Secondary mangrove forest	23,521	23,876	23,829	23,932	24,060
Primary swamp forest	202,799	200,958	200,400	202,694	202,193
Secondary swamp forest	359,399	356,270	358,089	357,151	531,266
Total changed area (ha)	1,977,080	1,953,906	1,948,987	1,914,250	2,084,557
Percentage of change (%)	40.75	40.27	40.17	39.46	42.97
Change rate (ha/yr)	−2363	−1172	−0.252	−1782	8897
Non-Forest					
Bush/shrub	169,262	166,111	170,801	169,656	29,465
Estate crop plantation	19,885	27,397	53,857	80,231	4359
Settlement area	3653	3878	3480	7216	7090
Barren land	263,859	75,081	56,539	77,994	88,946
Cloud covered	-	-	-	-	-
Savanna/grassland	568,723	700,156	603,422	576,528	555,274
Water body	322,282	351,749	351,734	349,816	349,884
Swamp shrub	860,813	917,482	969,770	978,818	942,998
Dryland agriculture	16,396	17,072	16,377	18,278	21,671
Shrub-mixed dryland farm	62,139	65,071	65,344	70,692	8600
Paddy field	11,459	11,388	11,388	48,795	45,505
Fishpond	-	-	-	448	80
Airport/harbor	159	159	159	175	175
Transmigration area	46,440	46,152	45,504	26,526	25,575
Swamp	529,565	516,113	554,354	532,291	37,538
Total area (ha)	2,874,635	2,897,809	2,902,728	2,937,465	2,767,158
Percentage of change (%)	59.25	59.73	59.83	60.54	57.03
Change rate (ha/yr)	1693	0.806	0.170	1197	-5798

The research also estimated the land cover losses and gains from 1990 to 2019, as presented in Table 11 below. The negative results indicate a decreasing number of areas; however, the positive number denotes an area of class expansion (Letsoin et al., 2020). Forested areas such as primary swamp forests demonstrated deterioration of about -40.95% of the lost areas. However, non-forested areas, for instance, settlement areas and paddy fields, increased by around 120% and 300%, respectively. Other forest groups, such as primary dryland, secondary dryland, primary mangrove, secondary mangrove, and primary swamp forest lost the areas, only secondary swamp forests increased slightly by 0.03% (Table 11). Conversely, in non-forested area groups, only two classes lost the areas, namely water bodies and transmigration areas.

Table 11**.** Land cover changes of each class in Merauke Regency from 1990 to 2019.

L.C. Class	Changed Rate (ha/yr.)			Total Changed Area	
	Gain (+)	**Loss (-)**	**Net (±)**	**Ha**	**%**
Primary dryland forest	8206.67	24,404.83	−16,198.17	−194,378.00	−27.98
Secondary dryland forest	12,976.92	13,539.75	−562,83	−6754.00	−1.06
Primary mangrove forest	162.58	1274.50	−1111.92	−13,343.00	−6.39
Secondary mangrove forest	282.60	389.74	−107,14	−1285.70	−5.07
Primary swamp forest	290.08	11,976.42	−11,686.33	−140,236.00	−40.95
Secondary swamp forest	20,255.25	20,242.17	13.08	157.00	0.03
Bush/shrub	9267.26	4474.00	4793.26	57,519.10	79.95
Estate crop plantation	7863.22	-	7863.22	94,358.60	-
Settlement area	393.19	65.68	327.52	3930.23	124.38
Barren land	22,871.75	22,269.04	602.71	7232.50	8.85
Cloud covered	-	63.64	−63.64	−763.65	−100
Grassland	30,703.58	23,738.50	6965.08	83,581.00	17.72
Water body	2462.99	2641.91	−178.93	−2147.15	−0.61
Swamp shrub	12,203.42	11,126.00	1077.42	12,929.00	1.39
Dryland agriculture	731.42	123.60	607.82	7293.80	50.73
Shrub-mixed dryland	2570.88	476.09	2094.78	25,137.40	57.84
Paddy field	3161.55	280.48	2881.08	34,572.90	316.26
Fishpond	37.35	30.71	6.64	79.67	-
Airport	1.38	0.02	1.36	16.30	10.27
Transmigration area	816.87	1738.78	−921.92	−11,063.00	−30.20
Swamp	14,529.00	10,932.08	3596.92	43,163.00	10.94

Table 12 shows the general features of the sago palm's prediction based on eight classes of sago's forecasted habitat, i.e., primary dryland, secondary dryland, primary swamp forest, secondary swamp forest, bash/shrub, grassland, swamp shrub, and swamp.

Table 12. General characteristics of the prediction of sago palm habitat in Merauke Regency (N=8).

District	1990	2019
Animha	16,975.06 ± 12,669.66 (125.05, 36,055.10)	16,983.27 ± 13,440.54 (437.21, 43,225.50)
Elikobel	18,216.17 ± 33,037.63 (0.00, 96,199.60)	17,495.36 ± 34,366.44 (0.00, 96,199.60)
Ilwayab	21,715.66 ± 27,109.94 (0,00, 80,960.40)	21,900.72 ± 21,947.41 (0.00, 80,960.40)
Jagebob	15,381.23 ± 21,832.78 (841.02, 6,459.20)	15,082.23 ± 23,852.07 (841.02, 64,359.20)
Kurik	8,312.54 ±7,576.85 (482.92, 20,296.30)	7,971.55 ± 6,519.25 (482.92, 20,296.30)
Kaptel	27,868.15 ± 22,683.46 (2,305.88, 63,204.40)	27,699.84 ± 20,332.62 (5,649.91, 63,317.30)
Kimaam	45,414.98 ± 63,137.85 (434.43, 181,539.00)	45,413,29 ± 64,595.09 (20.49, 1,9042.00)
Malind	4,975.18 ± 3,897.71 (0.00, 10,343.10)	4,883.73± 4,361.10 (0.00, 11,261.90)
Merauke	15,106.11 ± 22,450.10 (0.00, 60,288.60)	15,126.20 ± 18,966.08 (0.00, 60,228.60)
Muting	39,547.46 ± 46,345.29 (3,699.06, 118,800.00)	39,489.52 ± 41,776.44(3,954.98, 112,000.00)
Naukenjerai	10,682.42 ± 16,181.12 (0.00, 46,611.40)	9737.45 ± 10,263.51 (0.00, 50,872.70)
Ngguti	40,029 ±24,706.78(11,205.70, 70,419.90)	38,816.99 ±28,004.91(11,293.40, 89,504.20)
Okaba	17,481.54 ± 32,317.97 (37.903, 94,925.10)	18,900.30 ± 25,688,46 (505.92, 76,309.70)
Semangga	2,702.08 ± 3,717.96 (0.00, 10,013.90)	2,702.08 ± 3,978.13 (0.00, 11,292.90)
Sota	31,005.28 ± 35,952.15 (1,608.15, 110,369.00)	30,931.49 ± 29,605.80 (6,158.29, 99,919.30)
Tanah Miring	16,414.01±9,013.24 (4,923.28, 28,562.60)	16,359.38 ± 11,134.00 (347.94, 30,763.80)
Tabonji	33,038.64±40,211.73 (0.00, 111,643.00)	33,030.82±42,503.87 (0.00, 120,527.00)
Tubang	2,6192.51±108,655.74 (1,027.90, 73,437.70)	32,655.19±42,503.87 (8,534.63, 89,472.00)
Ulilin	56,469.20±108,655.74 (1,409.11, 315,111.00)	56,017.52±103,832.79 (742.51, 29,9073.00)
Waan	6,0482.52±60,071.43 (0.00, 165,196.00)	61,382.05±64,152.86 (742.51, 29,9073.00)

Table 13 displays the result of paired t-test on eight native habitats of sago in the regency. Accordingly, primary dry lands, grasslands, and swamp areas had a *p*-value less than 0.05.

Table 13**.** Land cover changes from the natural habitat of sago in 1990 and 2019.

LC	1990	2019	***P*-value**
Primary dryland	34,736.82 ±71,532.46 (0.00, 315,111.00)	27,686.42 ± 67,227.85(0, 299,073.00)	0.015
Secondary dryland	31,902.33 ±38,007.26 (1.02, 118,800.00)	33,604.22 ± 39,934.11(0, 112,000.00)	0.313
Primary swamp forest	17,126.28±23,169.16 (1,276.23,107615)	10,271.99± 8,519,85(531.72, 24,711.10)	0.107
Secondary swamp forest	26,555.19±24,072.41 (4,668.14, 94,925.10)	18,590.47± 23,439.27(949.07, 105.92)	0.152
Bush/shrub	3,597.31 ± 6,055.62 (0, 24,048.80)	8,923.07 ± 16,655.05(0, 63317.30)	0.081
Grassland	23,585.31 ± 36,748.43 (0, 111.643.00)	35,202.67 ± 42,540.96 (0, 152,745.00)	0.002
Swamp shrub	46,503 ± 52,913.31 (51.08, 181,539.00)	45,045.15±50,975.60(51.08, 190.427)	0.723
Swamp	19,197.62 ± 16,473.24 (79.92, 62,207.50)	25,707.58 ± 17,481.00(34.41, 68,235.40)	0.007

Nevertheless, land use cover changes in the regency were also determined to investigate statistically the changes in forested areas, crops and agriculture, and non-forested areas such as settlement areas, as demonstrated in Table 14. The result is measured using the Wilcoxon Signed-Rank test.

Table 14. Land use changes in five categories (Letsoin, Herak, & Purwestri, 2022).

LC	1990	2019	P-value
Forested areas	2,441,256.56 (1.02; 315,511.00)	2,172,113.451(1.02; 229,220.00)	0000
Crops and agriculture	68,771.00(28.10; 12,616.00)	122,078.93(15.08; 15,025.40)	0.001
Settlement area	39,797.74 (17.85; 8,696.00)	33,365.07 (19.82;5,700.00)	0.642
Water body	351,903.03(335.36; 58,824.67)	290,824.02 (802.50;51,772.81)	0.182
Barren land	80,942.58(18.07; 52,844.40)	77,527.85(608.75;20,717.90)	0.031

[1] Data are presented in total (minimum, maximum)

5.2 Designing the Transfer Learning Model for Sago Palm Recognition

Three CNN deep learning models are performed in this experiment, namely AlexNet, SqueezeNet and ResNet-50 to distinguish nine morphology classes of coconut fruits (CF), coconut leaves (CL), coconut trunks (CT), oil palm leaves (OPL), oil palm trunks (OPT), sago flowers (SF), sago leaves (SL), and sago trunks (ST). The parameters used in this study are shown in Table 15.

Table 15. Parameters in this study.

Parameter Name	Value
Epochs	10
Initial learning rate	0.0001
Validation frequency	9
Learning rate weight coefficient	10
Learning rate bias coefficient	10
Learning rate schedule	Constant
Momentum	0.9
L2 Regulation	0.0001
Min batch size	10

Data training used in these experiments was self-made from Unmanned Aerial Vehicles and ground photographs. A total of 231 images consisted of 70% allocates for training and 30% for testing and validation. The sample images of both data are displayed in Figure 14.

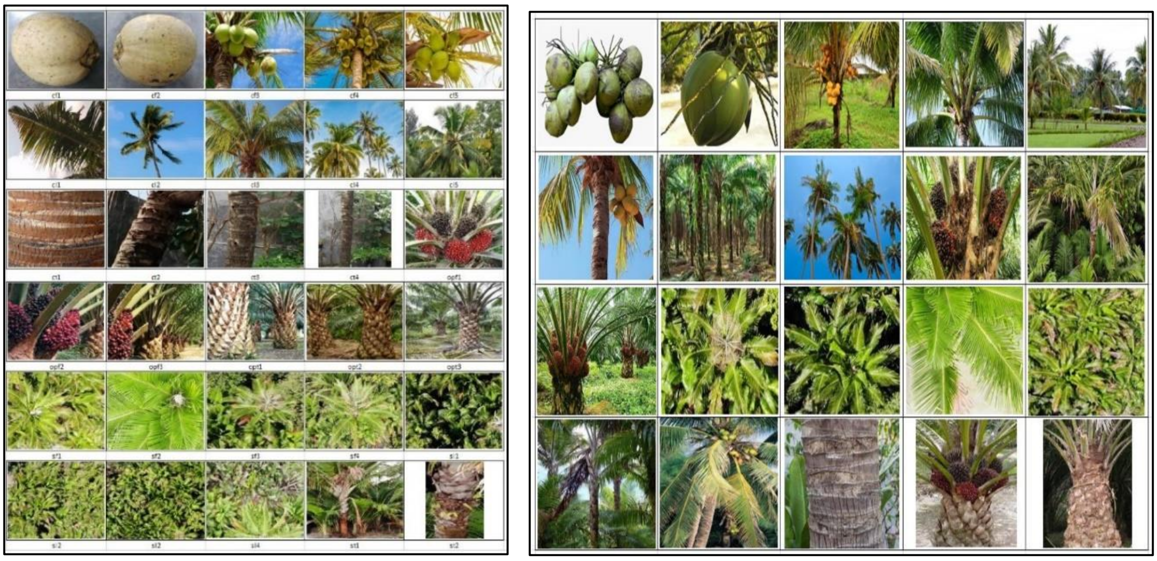

(a) (b)

Figure 14. The dataset provided in experiment-2, (a) sample data training, (b) sample data testing (Letsoin, Purwestri, Rahmawan, et al., 2022).

We examined three deep learning networks as explained before, then transmitted them to the target as part of transfer learning. The modified versions of this process shown in the last layers of each model were changed in the following ways to achieve the goals of this study and the new task via transfer learning. The fully connected layer, fc1000, was changed to fc and fc_new, followed by the SoftMax layer for converting values into probabilities, and finally, the classification layer predictions for 1000 output size were changed to class_output for categorizing into nine classes. The conv2d layer with nine num-filters was also changed. The network structures used in the second and third experiment are shown in Table 16 and Figure 15. All networks designed were published in the article publication 3 (Appendix E).

Table 16. Network structure in the second and third experiment (Letsoin, Purwestri, Rahmawan, et al., 2022).

Layer	Layer Name	Layer Type	Layer Details
1	Data	Image Input	227x227x3 images with zero center normalization
2	Conv1	Convolution	96 11x11x3 convolutions with stride [4 4] and padding [0 0 0 0]
3	Relu1	ReLU	ReLU
4	Norm1	Cross Channel Normalization	Cross channel normalization with 5 channels per element
5	Pool1	Max pooling	3x3 max pooling with stride [2 2] and padding [0 0 0 0]
6	Conv2	Grouped Convolution	2 groups of 128 5x5x48 conv with stride [1 1] and padding [2 2 2 2]
7	Relu2	ReLU	ReLU
8	Norm2	Cross Channel Normalization	Cross channels normalization with 5 channels per element
9	Pool2	Max Pooling	3x3 max pooling with stride [2 2] and padding [0 0 0 0]
10	Conv3	Convolution	384 3x3x256 convolutions with stride [1 1] and padding [1 1 1 1]
11	Relu3	ReLU	ReLU
12	Conv4	Grouped Convolution	2 groups of 192 3x3x192 convolutions with stride [1 1] and padding [1 1 1 1]
13	Relu4	ReLU	ReLU
14	Conv5	Grouped Convolution	2 groups of 128 3x3x192 convolutions with stride [1 1] and padding [1 1 1 1]
15	Relu5	ReLU	ReLU
16	Pool5	Max Pooling	3x3 max pooling with stride [2 2] and padding [0 0 0 0]
17	Fc6	Fully Connected	4096 fully connected layer
18	Relu6	ReLU	ReLU
19	Drop6	Dropout	50% dropout
20	Fc7	Fully Connected	4096 fully connected layer
21	Relu7	ReLU	ReLU
22	Drop7	Dropout	50% dropout
23	Fc_new	Fully Connected	9 fully connected layer 1x1x9
24	Prob	SoftMax	
25	Classoutput	Classification Output	

In multiclass classification problems, particularly to predict the probability of each instance, a SoftMax activation is applied in the output layer.

$$P(x_i) = \frac{e^{x_i}}{\sum_{j=1}^{n} e^{x_j}} \quad (2)$$

Here, x denotes the values from layers in the output of the i-dimension, and n represents the size of the dimension referring to the size of classes. In a classification task, the sum of the probabilities is equal to 1.

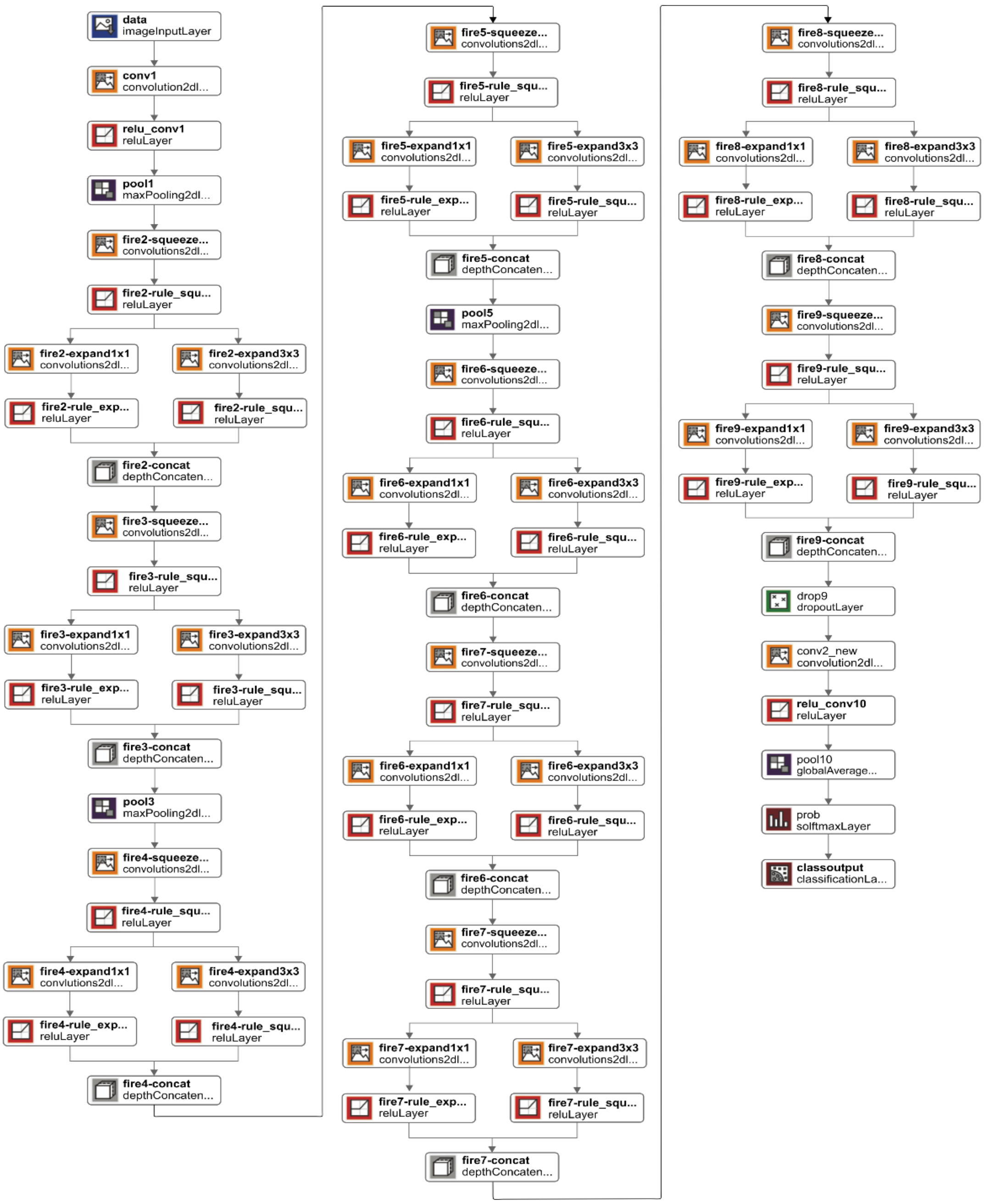

Figure 15. Network structure in the second and third experiment
(Letsoin, Purwestri, Rahmawan, et al., 2022).

A smaller loss function defines a good model. Otherwise, the model's parameters need to be adjusted to reduce the loss. The loss that happens during a single training process is called the loss function; on the other hand, the average loss across the whole training dataset is known as the cost function. Loss function in deep learning network can be estimated depending on its task, for instance, regression task by applying Mean Squared Error (MSE) or Mean Absolute Error (MAE) – in object detection task by utilizing focal loss, while in classification by using binary cross entropy or categorical cross entropy. Categorical cross entropy is used for multiclass classification with the following equation:

$$Loss = -\sum_{j=0}^{k} y_j \log(\hat{y}_j) \tag{3}$$

where, k is the number of classes in the data, and $j = 1, 2, \ldots k$.

$$Cost = \frac{1}{2}\sum_{i=1}^{n}\sum_{j=1}^{k}\left[y_{ij} \, log \, \hat{y}_{ij}\right] \tag{4}$$

k represents classes, y denotes the actual value, while $\hat{y}$ shows the prediction.

Another network used in this study is the residual network (ResNet-50), a 50-layer deep convolutional network variant of the ResNet model. It starts with a single convolution kernel size of 77 and finishes with an average pool, a fully connected layer, and a SoftMax layer. There are 48 convolutional layers in between these layers, each with a distinct kernel size. Thus, the completely linked layer's function, i.e., the fully connected layer, is to integrate all of the inputs from one layer linking to each activation unit of the following layer. The output layer (O), input layer (I), and residual map function (F(I_(i) W)) compose the residual block on the ResNet equation, which is shown below.

$$O = F(I_i W_i \;\; + I) \tag{5}$$

Figure 16 shows the training progress of each model, i.e., SqueezeNet, AlexNet, ResNet-50, with the accuracy of 76.60%, 76.60% and 82.98%, respectively.

(a)

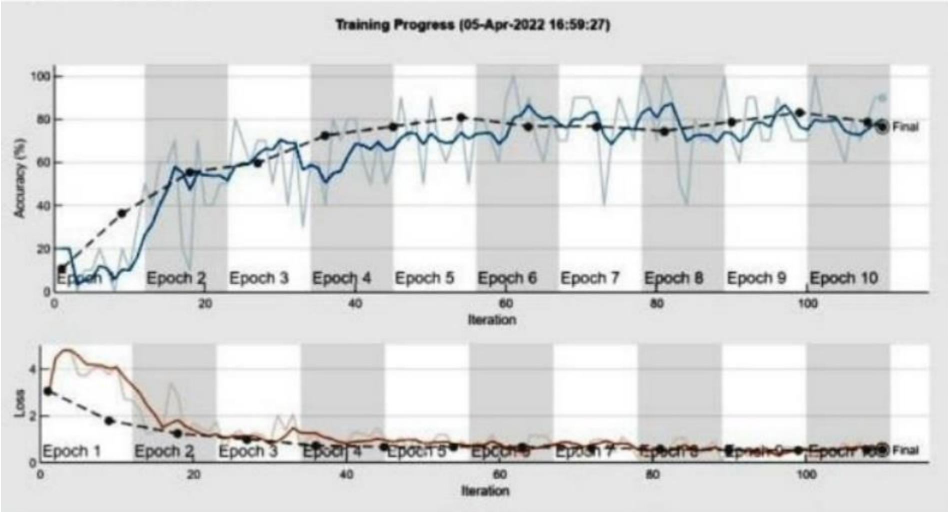

(b)

(c)

Figure 16. Training progress (a) SqueezeNet model, (b) Alexnet model, (c) ResNet-50 model.

The blue and orange colors, respectively, represent how smoothly the accuracy process goes along and how much training is lost, while bright blue and light orange-colored dots show the development of the training. Further, black colored dots along the black line help to demonstrate how the validation of the data trained and the loss are related. The three models' training progress was not quite as fluent; their accuracies were 76.60%, 76.60%, and 82.98%. With the highest accuracy of 82.98% among the models, the ResNet-50 model is more prevalent than the others. In epoch 5, the training progress improved while the training loss values for these models sharply reduced. Since the data training loss decreased during the course of the remaining steps in ResNet-50 and AlexNet, the validation accuracy and loss curves were afterwards more easily comprehended.

5.3 Investigating the Performance of Sago Palm Detection Model

After the training procedure described in Figure 16, all models were tested using the same data test, which was generated and placed differently than the trained data. To facilitate this testing process, we utilized several syntaxes supported by MATLAB2021, including *imresize*, *imshow*, prediction, classification and probability, as shown in Figure 17.

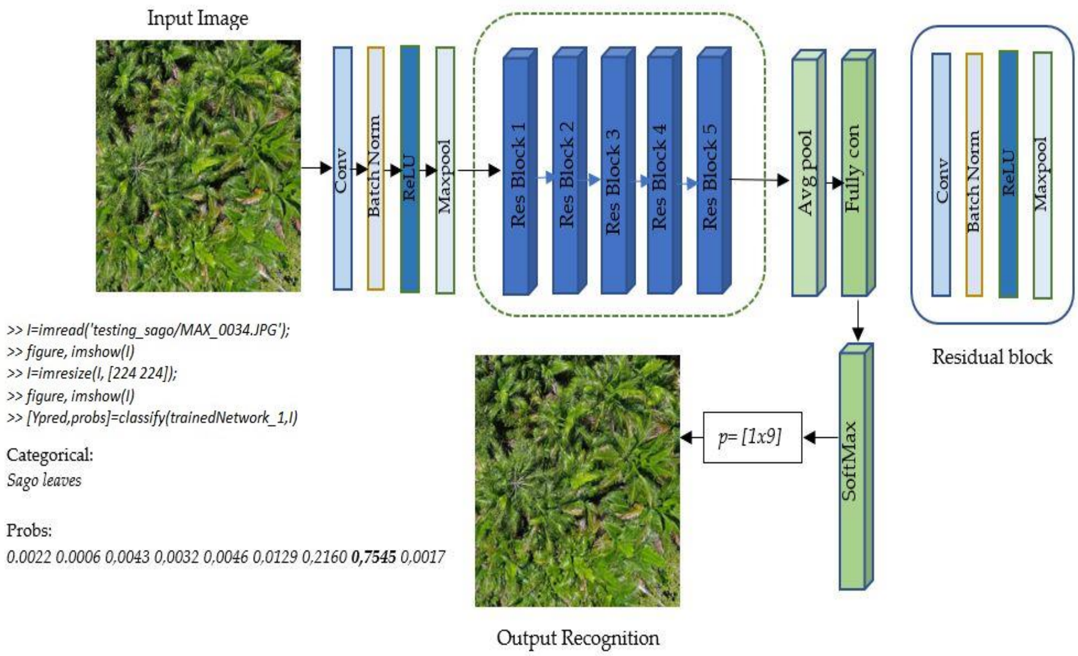

Figure 17. Sample testing phase: ResNet-50 model and sample testing script.

The confusion matrix of the three models is also tabulated, as displayed in Figure 18.

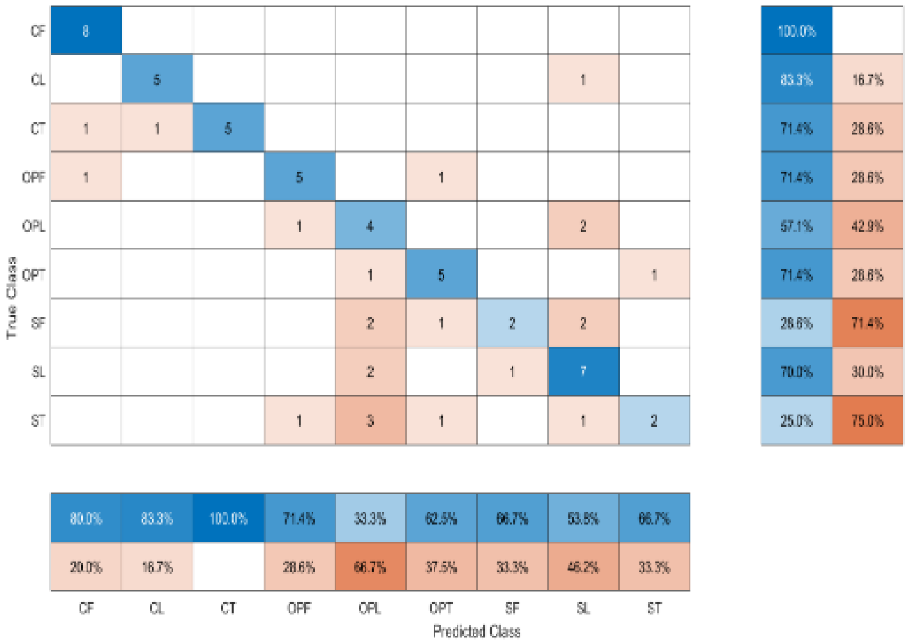

(a)

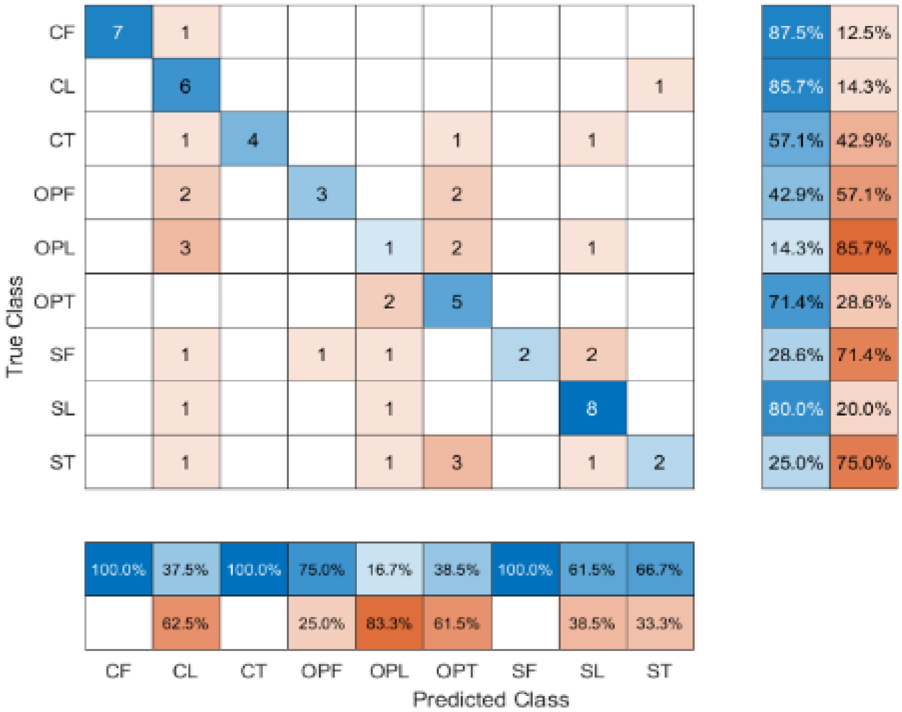

(b)

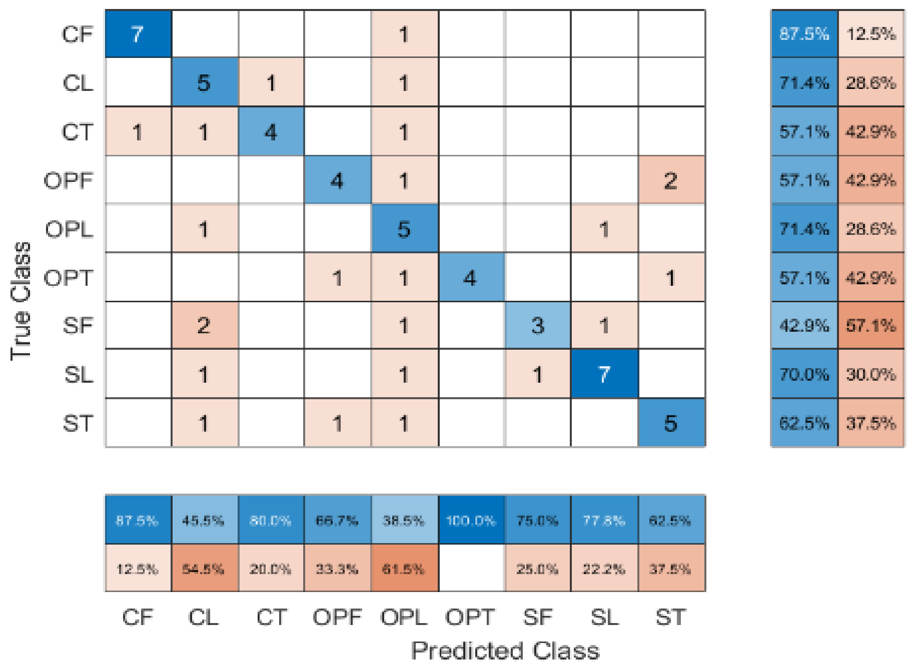

(c)

Figure 18. Confusion matrix of (a) SqueezeNet model, (b) Alexnet model, (c) ResNet-50 model.

Metric evaluation, for instance, recall (sensitivity), precision and F1 score are calculated and expressed in Figure 19, while ROC curves are depicted in Figure 20 (a-c) below. Based on the accuracy values, AlexNet outperformed the other models in detecting the sago flower (SF). However, the sensitivity is less adequate compared to, for example, ResNet-50. ResNet-50 performed better in terms of precision and sensitivity compared to the other models, specifically the detection of the sago trunk (ST) and sago leaves (SL). These findings show that the models can differentiate between the sago palm and other plants employed in this study. According to this result, the ResNet-50 can support the early detection of the sago palm.

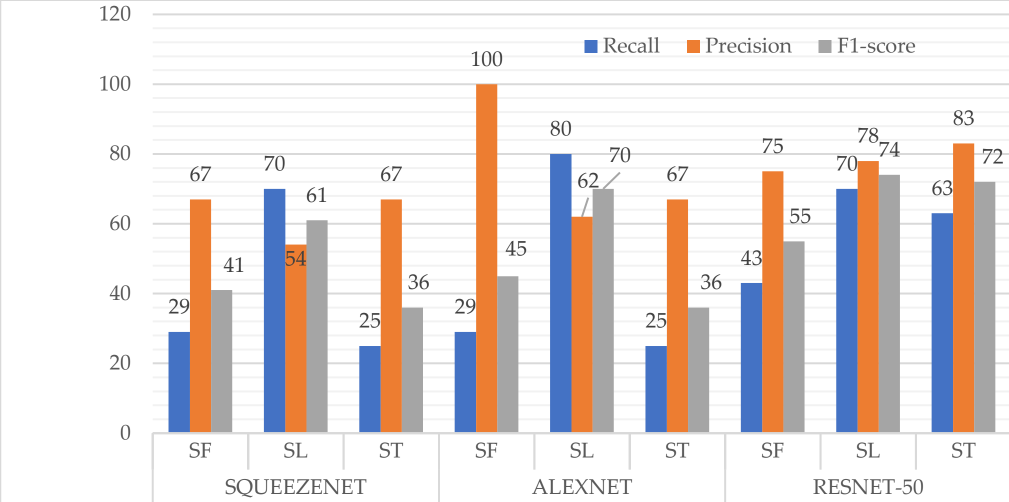

	SQUEEZENET SF	SQUEEZENET SL	SQUEEZENET ST	ALEXNET SF	ALEXNET SL	ALEXNET ST	RESNET-50 SF	RESNET-50 SL	RESNET-50 ST
Recall	29	70	25	29	80	25	43	70	63
Precision	67	54	67	100	62	67	75	78	83
F1-score	41	61	36	45	70	36	55	74	72

Figure 19. Metric evaluation of sago palm classifier in percentage.

ROC curves were used on the sago palm dataset to assess all tested models. The findings showed that all algorithms could accurately identify sago above coconut and oil palm (Figure 20a–c), with ResNet50 presenting the best model for identifying sago trees. While AlexNet was less likely to recognize it (as indicated by the line under the reference values), SqueezeNet and ResNet 50 were able to separate sago trunks from coconut and palm oil. The sensitivity is also known as the true positive rate (TPR), while (1-specificity) is referred to as the false positive rate (FPR).

(a)

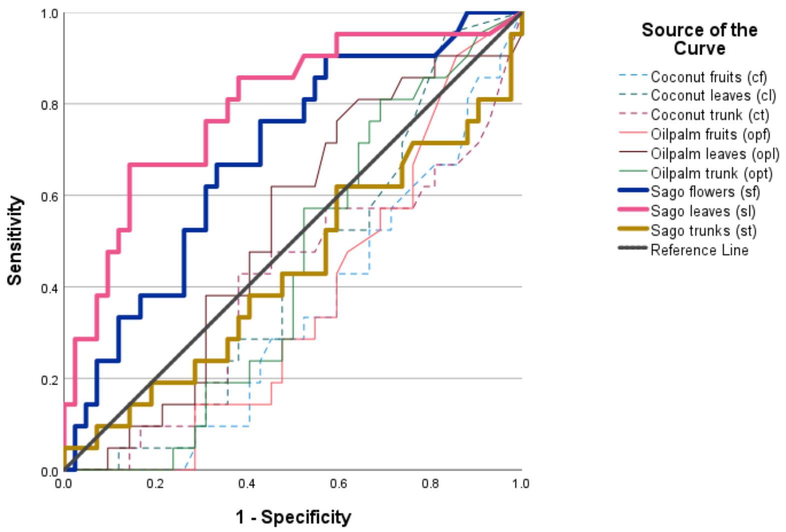

(b)

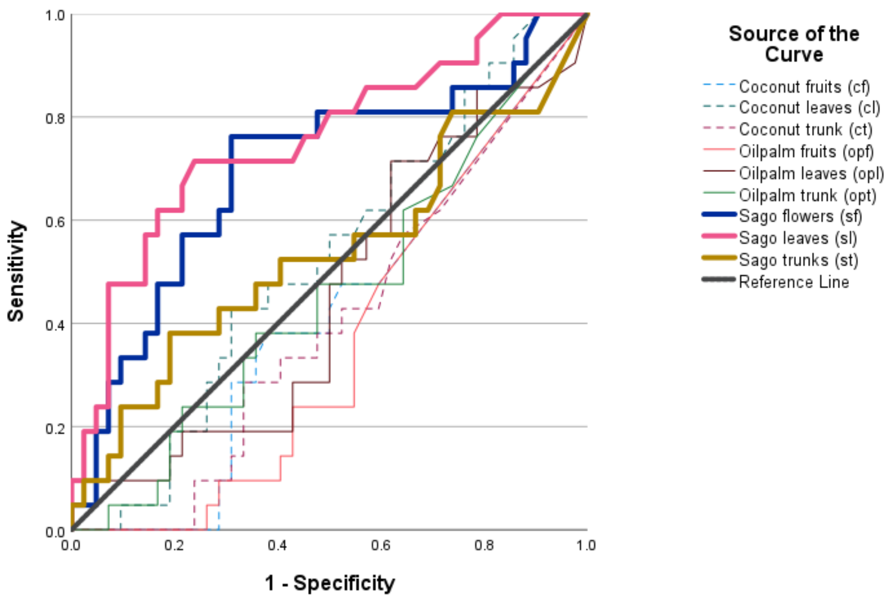

(c)

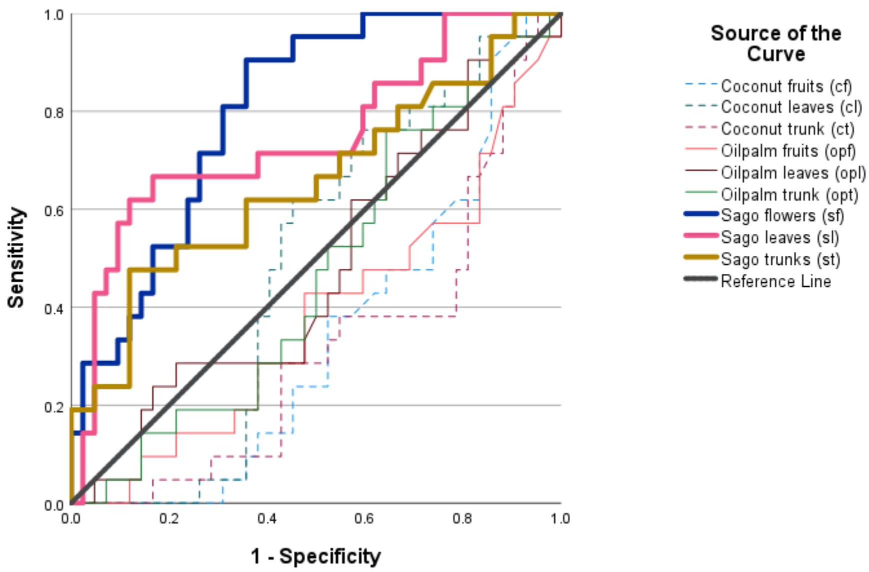

Figure 20. ROC curves of (a) AlexNet, (b) SqueezeNet, (c) ResNet-50.

5.4 Performing Various Learning Parameters

The training results of twenty-two trained networks are shown in Table 17. Network structure in trained Network-1 to trained Network-16 were trained based on the model as presented in Figure 15, while Networks 17 to 22 were trained according to the network structure displayed in Table 16.

Table 17. Learning results in third experiment.

Network trained name	Training accuracy	Training loss	Validation accuracy	Validation loss	Network iteration	Elapsed time
trained Network-1	93.75	0.1688	90.90	0.3580	90	17 min 21 sec
trained Network-2	93.75	0.1731	88.64	0.3533	40	8 min 9 sec
trained Network-3	96.82	0.0619	89.39	0.3652	72	6 min 37 sec
trained Network-4	85.94	0.3867	86.36	0.4627	32	3 min 49 sec
trained Network-5	100	0.0488	91.67	0.3496	135	29 min 3 sec
trained Network-6	95.31	0.0960	87.12	0.3349	60	10 min 1 sec
trained Network-7	96.88	0.053	94.70	0.1640	72	6 min 37 sec
trained Network-8	26.57	1.3861	25	1.3863	32	14 min 28 sec
trained Network-9	25	1.3861	25	1.3863	90	15 min 24 sec
trained Network-10	96.87	0.1884	84.85	0.8798	40	4 min 44 sec
trained Network-11	84.38	0.2620	72.72	0.7639	135	12 min 17 sec
trained Network-12	75	0.4209	71.97	0.8021	60	15 min 59 sec
trained Network-13	100	0.0242	90.15	0.3532	152	19 min 17 sec
trained Netwoork-14	100	0.0238	88.63	0.4014	190	552 min 16 sec
trained Network-15	100	0.0038	91.67	0.3120	300	33 min 21 sec
trained Network-16	100	0.0056	90.90	0.4908	240	59 min 39 sec
trained Network-17	89.06	0.2816	90.15	0.2766	40	3 min 44 sec
trained Network-18	90.62	0.1762	91.67	0.2689	32	11 min 52 sec
trained Network-19	96.87	0.1601	88.66	0.4384	60	5 min 55 sec
trained Network-20	100	0.0240	86.36	0.5317	152	20 min 8 sec
trained Network-21	90	0.1815	87.88	0.4128	300	43 min 48 sec
trained Network-22	80	0.3592	86.36	0.4761	240	31 min 40 sec

Some training progresses shown in Figure 21 (a-c) are as follows: the accuracy and loss values are distinguished by blue and orange color, respectively. Light blue colored dots represent the training accuracy, and light orange-colored dots refers to the training loss during the learning process. In addition, black colored dots denote validation accuracy and loss, while dark blue and dark orange colors define the sleekness of both accuracy and loss values, respectively. Training loss is calculated after each batch while validation loss is measured after each epoch. The impact of training and validation loss refers to underfitting, overfitting and proper fit. Proper fit happens when both the training loss and validation loss decrease and become firm at a specific position. Accordingly, underfitting describes that the training and validation losses are both similar at a particular point. However, the validation loss continues to be greater than the training loss. The overfitting illustrates typical circumstances where the validation loss tends to be always prominent than the training loss.

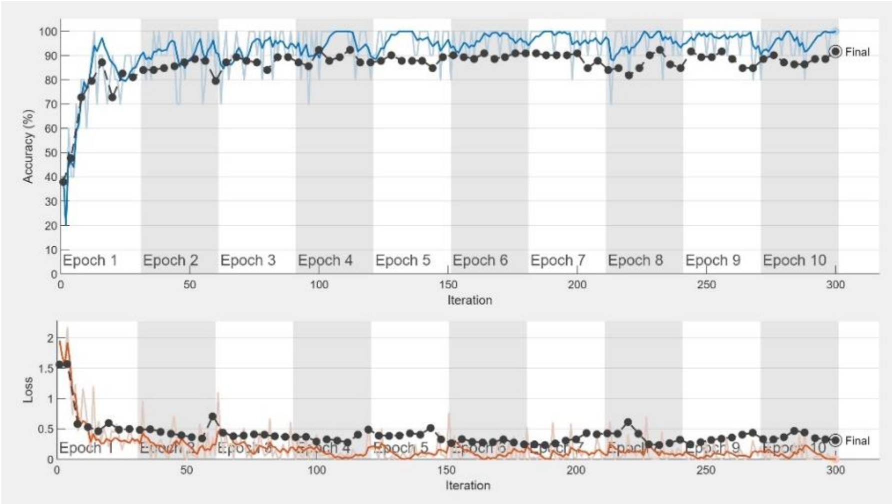

(a) trained Netwok-15.

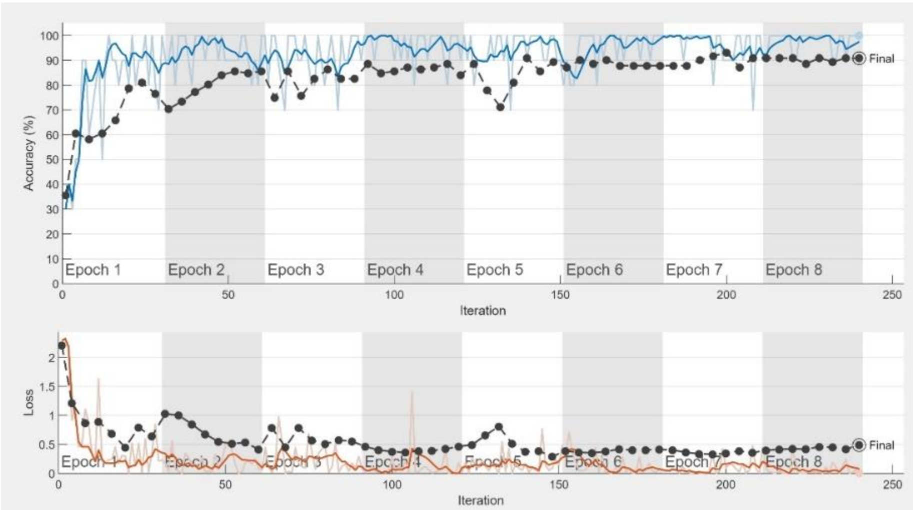

(b) trained Network-16.

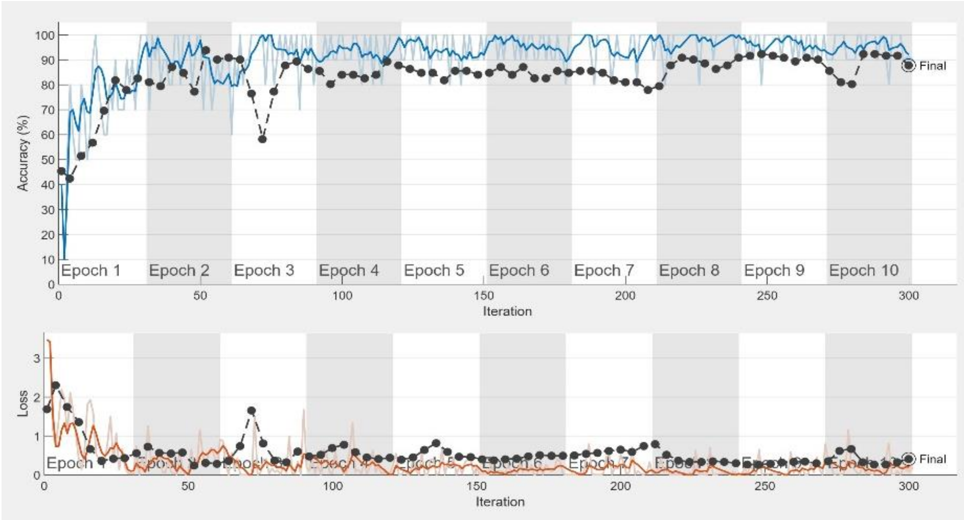

(c) trained Network-21.

Figure 21. Training progresses of (a) trainedNetwork-15,
(b) trainedNetwork16, (c) trainedNetwork-21.

After the learning process, 103 test images are used to investigate the performance of each trained model in predicting and classifying the input test image. The results are displayed in Appendixes (Appendix D). Afterwards, the confusion matrix is calculated as displayed in Figure 22. The sensitivity, precision and F1-score are measured based on values in the confusion matrix. The results are presented in Appendixes (Appendix D).

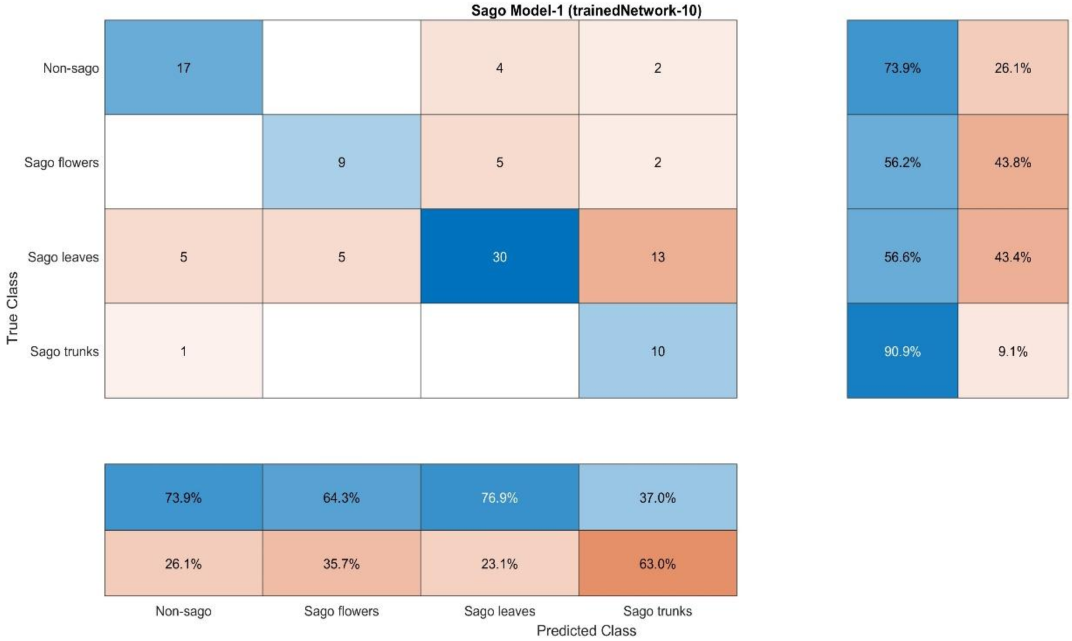

(a) trained Nework-10 (Epoch 10, 0.001 Lr, 64 min batch size).

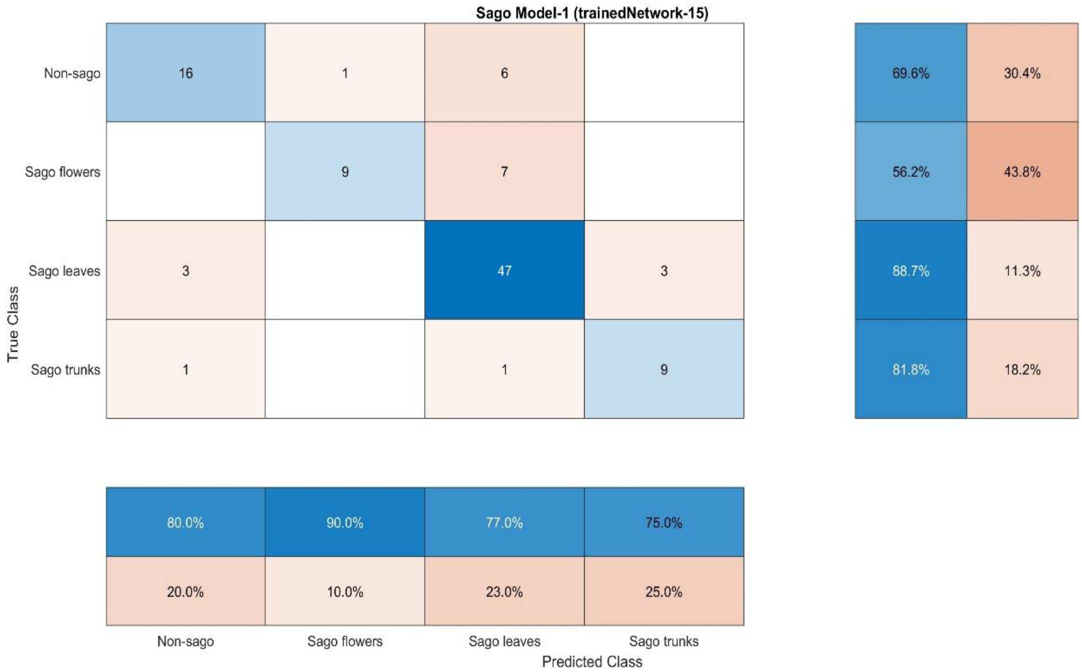

(b) trained Network-15 (Epoch 10, 0.0001 Lr, 10 min batch size).

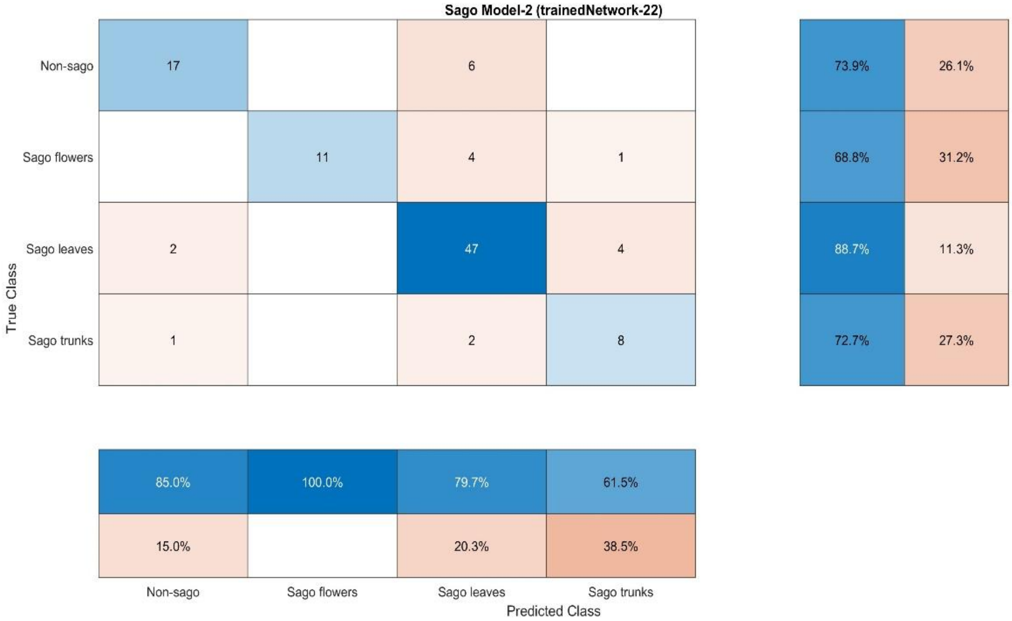

(c) trained Network-22 (Epoch 8, 0.0001 Lr, min batch size 10).

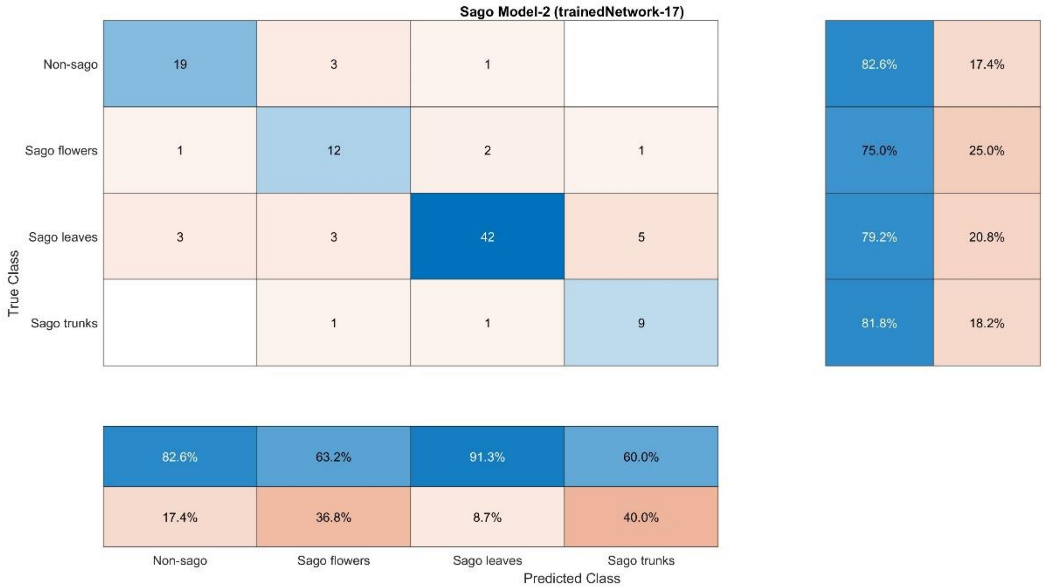

(d) trained Network-17 (Epoch 10, 0.0001 Lr, min batch size 64).

(e) trained Network-19 (Epoch 15, 0.0001 Lr, min batch size 64).

Figure 22. Confusion matrix of (a) trainedNetwork-10, (b) trainedNetwork15, (c) trainedNetwork-22, (d) trainedNetwork-17, (e) trainedNetwork-19.

6. DISCUSSION

To obtain the objectives of the study and test hypotheses, the research effort dealt with three experiments as described in Chapter 4 and Chapter 5. The first experiment explored remote sensing data supported by geographical information software and supervised classification to investigate the impact of land cover changes in the regency on the habitat of sago palm (Hypothesis 1), further, to assess the influence of the extension of non-forested areas, crops and agriculture on the changes in the sago's ecosystem (Hypothesis 2), likewise to achieve the first objective. The second experiment performed transfer learning technique based on the CNN deep learning model to differentiate the visual appearance of sago (Hypothesis 3) and to distinguish sago from other vegetation (Hypothesis 4). The third experiment covered different networks trained in a sago model; it examined them according to metric evaluation used, for instance, recall, precision and F1-score, which was calculated from the confusion matrix of each network. The results were used to test the influence of the parameters in designing a sago palm detection system (Hypothesis 5) and to evaluate the performance of each structure (Hypothesis 6).

6.1 Investigating results from Remote Sensing Data

This study investigated forest cover changes, as shown in Tables 8, 9, 10 and 11**.** This validation revealed that primary swamp forest and primary dryland forest saw greater area losses than other forest types, such as primary mangrove or secondary mangrove. Only the secondary swamp forest advantaged by about 0.03% over the study period. Nevertheless, as standardized by the Indonesian Government in Land cover classes in Indonesia (Table 1), primary swamp forest is purposed for native sago habitat. Consequently, this circumstance could contribute to decreased services to particular ecosystems such as sago. East Asian nations such as Malaysia also experienced changes in land use and how they affect biodiversity due to logging, agriculture growth and the expansion of the settlement area (Azari et al., 2022). As described in Table 13, other sago palm environments were investigated in twenty regions of our fieldwork by using paired t-tests. According to the mean values presented in Table 12**,** the results supported the general prediction of the sago palm habitat, as shown in Figure 23.

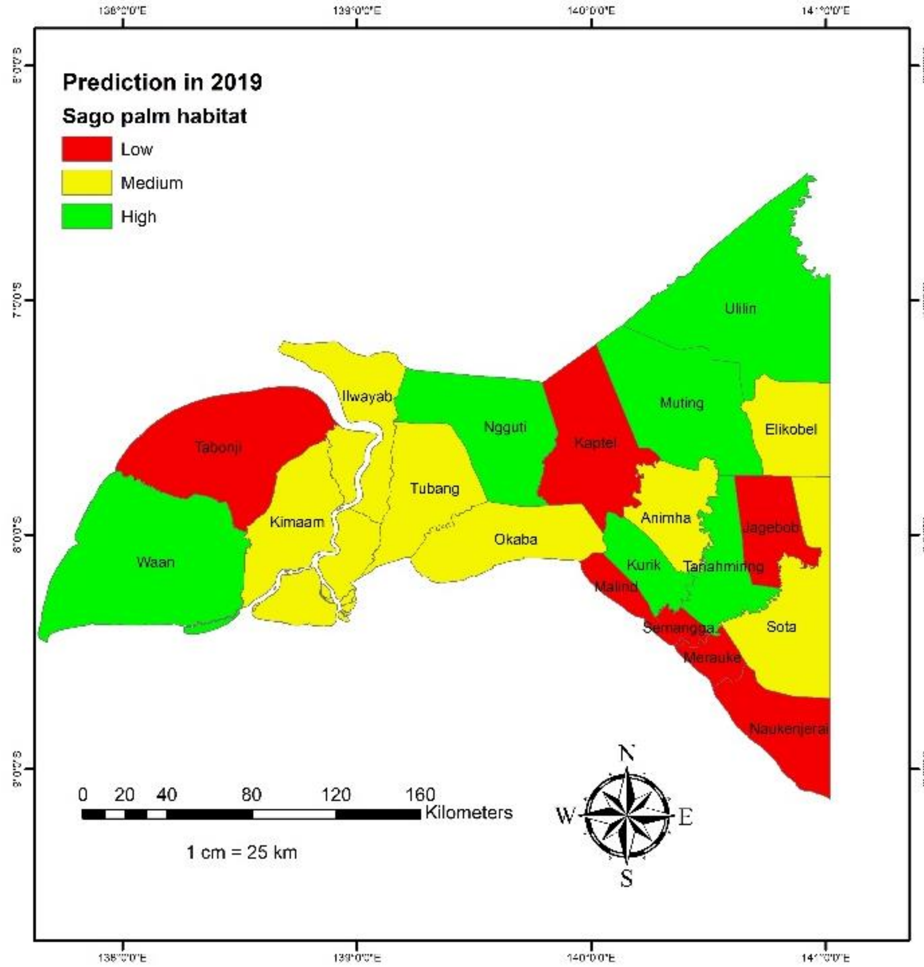

Figure 23. Sago habitat prediction (N=8) in Merauke Regency.

The investigation of five classes is presented in Table 14. The results demonstrated a notable reduction in the forested area with a *p*-value of 0.000, while the crops and agriculture were significantly larger, with a *p*-value of 0.001. The results approved our two hypotheses that the potential habitat of sago is possible to asses through the LULC changes, and the expansion of crops and agriculture could contribute to the changes in the sago's environment. Comparative studies were also conducted in African countries such as Tanzania, where it was found that the extension of agriculture and settlement area resulted in the decrease of ecological plants, birds and trees, for example (Seki et al., 2018). One of the biggest limitations to the research effort in this experiment was the lack of primary data from the local government regarding the sago area, which likely affected the general prediction of the experiments. However, parts of this research effort could provide prior valuable information concerning the prediction of the sago palm habitat for each regency region according to their land cover changes from 1990 to 2019.

6.2 Investigating results from Transfer Learning Model

In the second experiment, the research innovation was to differentiate the visual appearance of the sago palm and distinguish the palm from other vegetation. In this experiment, we also design a sago palm detection model. Some earlier studies detected the sago palm areas based mainly on satellite imageries and combined them with other methods, such as machine learning and image processing (Hidayat et al., 2018; Santillan & Makinano-Santillan, 2016). Nevertheless, the morphology of sago palms is considerably challenging due to the wild position. Therefore, in this experiment we involved a different approach, i.e., transfer learning based on CNN deep learning model. Sago palm images were captured by ground photographs and by an unmanned aerial vehicle (UAV). Several previous studies investigated the advantages of transfer learning. However, specifically the wild stand of sago palm was still not researched. A previous study in sago detection using CNN deep learning (Wahed et al., 2022) found the ability of this method to identify the maturity of sago palms. Conversely, another visible morphology of sago and similar plants was discovered. Three CNN deep models, SqueezeNet, AlexNet and ResNet050, were utilized as a transfer target to categorize and predict the three plants according to their visible morphology namely trunks, fruits and leaves. As a result, SqueezeNet achieved higher precision in detecting coconut palms than sago palm or oil palms (Figure 18). Considering the detection of sago palm, AlexNet was able to predict sago flowers at 100% (Figure 19). However, the sensitivity of this model to detect sago flowers was only 29%, quite less than the ResNet model. As one of the sago palm detection models in this experiment, ResNet was considerably better than others, as visualized in the ROC curve **(**Figure 20**)**. Sago fruits, sago leaves and trunks are in the upper area near the left corner (Grigorev, 2021; Kneusel, R. T., 2021). The relevant model based on improved ResNet was also examined in previous studies with different datasets and new tasks, for instance, detecting wood or a fault in rollers for bearing (Liu et al., 2023; Zou et al., 2023). According to these studies, ResNet was superior, with about 80% of the F1-score.

The dataset in the first experiments consisted of a self-made dataset of 231 images in total. Such a small dataset was also provided in several existing datasets, such as UW RGB-D object offering 300 general objects in 2.5 dataset (Minaee et al., 2021). The research effort in these experiments approved the hypotheses that the transfer learning technique is able to differentiate the visible morphology of sago with a small dataset (Hypothesis-3) and the ability of the designed network to detect and predict self-made dataset of sago palm from UAV and ground photographs (Hypothesis 4). In this experiment, all models were trained with a similar parameter, as shown in Table 15. This parameter was based on the best practice from some previous studies (J. Huang et al., 2022; Thenmozhi & Srinivasulu Reddy, 2019). Nevertheless, the parameter changes such as learning rate, epoch and min batch size need to be considered. Therefore, in the next experiment, we adjusted different parameters in the sago model designed in this experiment.

6.3 Interpreting the Effect of Parameter Changes to the Model

In the third experiment, the dataset and parameters, as described in Table 6 and Table 7**,** were performed. Further, network structures with 68 layers (Figure 15) as sago model-1 and 24 layers (Table 16) as sago model-2 were examined. As can be seen from the learning results presented in Table 17, trained Network-8 and trained Network-9 achieved lowest training and validation accuracy as well as the greatest loss during the validation and training process. On the one hand, trained Network-11 and trained Network-12 showed that the validation loss was greater than the training loss, which could indicate underfitting. Underfitting refers to a network that did not learn adequately the task and performed poorly on a training dataset and inadequately on an unsuccessful sample. Overfitting then represents a network accomplishing well on training dataset but insufficiently on a holdout sample. In experiment-3, some trained Network performed in a good fit, for instance, trained Network-17 and trained Network-18. A good fit represents a network that adequately obtains the training dataset and applies it appropriately to the task. In addition, trained Network-19 and trained Network-22 achieved around 0.2 differentiation between training loss and validation loss and similarly less than 9% of differentiation between training accuracy and validation accuracy. As displayed in the confusion matrix (Figure 22), the sensitivity and precision are calculated as depicted in Figure 24.

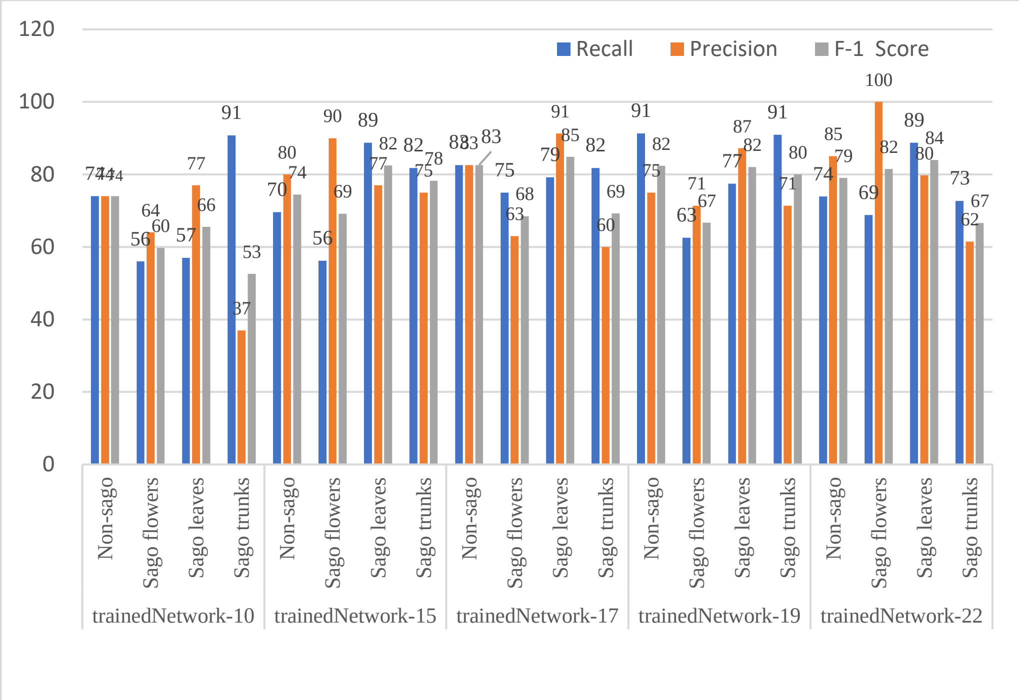

Figure 24. Sensitivity and precision of trainedNetwork-10, 15, 17, 19 and 22.

It can be seen that the precision and the sensitivity of each class were performed better in trained Network-17, trained Network-19 and trained Network-22. Although the sensitivity (recall) in trained Network-10 was 91% for sago trunks, the precision was only about 37%. Conversely, in trainedNetwork-15, the precision of sago flowers was 90%, but the sensitivity was only about 56%, which means that around 56% of the network was able to detect the instances of specific classes. In this experiment, trained Network-15 was trained using similar parameters as in experiment-2, i.e., 10 epochs, Lr 0.0001- and 10-min batch size. However, experiment-3 reached better results. The most significant differentiation between these two experiments was the size of dataset provided which was larger than in the second experiment. Even though transfer learning can work in a small dataset, the proper amount of datasets helps to achieve specific purposes (Jahja et al., 2023; Mimi et al., 2023).

The third experiment also recognized the loss that happened during the training and validation process. For example, we compared the trained Network-10, which consisted of epoch 10, Lr 0.001- and 64-min batch size, to trained Network-2 which also contained epoch 10- and 64-min batch size (Appendix D). The precision and sensitivity calculation results confirmed that trainedNetwork-2 performed better than trainedNetwork-10. The learning rate is the most significant difference between these two-network structures; the trained Network was adjusted at 0.0001 Lr rather than 0.001. If the loss value changes rather than drops, the model may not be learning at all. Nevertheless, if it declines in the training set but not in the validation set (or if it declines but there is a significant difference), the model may be overfitting. To overcome this circumstance in deep learning as well as transfer learning techniques, is to merely decrease the learning rate (Lin et al., 2023; Mukoya et al., 2023).

Passing a complete dataset through the network constitutes an epoch, thus, the total number of training samples in a single min-batch is referred to as the batch size. Adapting a larger batch size requires higher hardware processing; therefore, splitting it into min batch sizes is foremost. An updating of the model's weights during training is referred to as an iteration. The number of batches required to finish one epoch is equal to the number of iterations. In this experiment, we define four kinds of min batch size, i.e., 10, 16, 32, 64, combined with three groups of epochs, i.e., 8, 10, and 15, with 309 images in the dataset (training images). For example, a trained Network-17 splits into a 64 min batch size with 10 epochs (Table 7). Thus 309 images divided by 64 min batch size turn to approximately 4.8 or around 4 images in one epoch. Then, it will take 40 network iterations to complete 10 epochs (4 images x 10 epochs) (Table 14). Thus, if we set up a high Lr or a fast-learning process, the model is not able to read accurately. As a result, the model fails to learn, particularly if the loss not decreased, as explained previously (Kumar et al., 2022). The results achieved from the second and third experiment proved that parameters such as epoch and min batch size in a network structure are necessary for a sago palm detection model (Hypothesis 5). Further, the confusion matrix and the metric values are helpful to examine the performance of a model as arranged in the second and third experiments.

The whole study effort also involved some research on the potential uses of the palm, in health aspects, bioeconomy and food supply. These studies were based on a literature review with principal stages as follows:

(1) Identification. In this stage some keywords were used, for instance, “sago” AND “supplementation”, “sago” AND “glycemic”, or “sago” AND “food” from publications on science direct, articles indexed by Scopus facilitated by Infozdroje (CULS), also google scholar written in English, German and Indonesian. However, the Indonesian bioeconomy policy, particularly a document addressing sago forest management, is still unavailable.

(2) Screening and skimming. All the articles are screened according to the study objective, accessibility and relevance of the studies.

As a result, from the point of health aspect, sago's resistant starch promotes beneficial physiological reactions, which may result from its reduced glycemic index and quicker absorption. Additionally, the prebiotic qualities of sago's resistant starch promote a healthy composition of the intestinal microbiota, raising the levels of short chain fatty acids and improving intestinal epithelial protection. Consumption of sago starches positively affects metabolic parameters like enhanced pancreatic beta-cell and insulin functioning as well as lipid panels. Sago-based meals are an excellent source of supplements for maintaining physical performance and accelerating recuperation during the post-exercise phase (Setiawan, Fetriyuna, Letsoin, et al., 2022).

Further, the study's document evaluation and analysis revealed that neither the region nor the nations where sago primarily grows had formed a single policy on the bioeconomy. Only Malaysia and Thailand have a national bioeconomic policy. In Indonesia and the Philippines, the concepts are covered by several different ministries. Sago's promotion and the development of its value-added products, particularly into bioenergy, align with Malaysia and Thailand's strategic plans for their respective bio-economies. Though they are rarely mentioned in the documents under study, sustainable biomass production and preserving the wooded landscape, including sago areas, are important aspects of mitigating climate change (Fetriyuna, 2022). Nevertheless, Sago forests provide the potential to be great carbon sinks for absorbing carbon, lowering the greenhouse effect and preventing global warming (Chew et al., 1999; Trisia et al., 2016). Therefore, research to enhance the usefulness of sago refining and preservation should also be taken into account (Nurhasan et al., 2022).

7. CONCLUSIONS

In summation, the research effort aimed to investigate the use of remote sensing data, Indonesian land cover categories, and peatland classes to examine and predict the potential habitat of sago in the regency. As far as we know, the sago area data in this regency has not been provided periodically yet and is still unresearched. Therefore, this research effort can be considered an unprecedented prior study. Further, the study attempted to design a sago palm detection model, using transfer learning based on deep learning CNN models with a self-made dataset captured by UAV and ground photographs from the fieldwork, which can distinguish sago palm from other vegetation. To the best knowledge and references in the related work mentioned in Section 2.9, the methods, parameters, dataset, metric evaluation, and network structure are considerably different. Although one of the earlier studies has investigated transfer learning in sago detection in Malaysia using the same CNN backbone network, namely AlexNet and ResNet, the layer in this research effort was arranged distinctively. Moreover, the investigation in various parameters such as epoch and min batch size, as attempted in the third experiment, was not examined in the earlier study. Therefore, this research effort is noticeably contributing to this whole study. Accordingly, the study effort resulted in addressing the hypotheses subsequently:

Hypotheses-1: **The potential habitat of sago can be evaluated through the Land Use Land Cover (LULC) changes and supported by stakeholders' data.**

The research effort in utilizing remote sensing data, Indonesian land cover categories, and peatland classes resulted in the prediction of eight potential habitats of sago palm, namely, primary and secondary dryland, bush/shrub, grasslands, swamp shrub, swamp, primary and secondary swamp forest. The results revealed statistically significant changes in primary dryland, grassland and swamp with a *p*-value less than 0.05. The results of mean values demonstrated that 12 of the 20 districts of Merauke Regency lost the natural habitat of sago palm, while a larger potential area is in 6 districts. This study effort also produced a land cover map of the regency from 1990 to 2019.

Hypotheses-2: The expansion of crops and agriculture areas, the settlement sector and also the degradation of the forested areas based on LULC data could contribute to the changes in the sago's ecosystem in the fieldwork.

To evaluate remote sensing data, Indonesian land cover categories were also derived from examining the land rate changes of several categories: forested areas, crops and agriculture, settlement area, water body and barren land. The statistical results demonstrated a significant decrease in the forested area, an extension of crops and agriculture, and a reduction of barren land during the observed years with *p-values* 0000, 0.001, and 0.031, respectively. Nevertheless, one of the forested areas, such as the swamp forest, was noticed as the sago's habitat.

Hypothesis 3: Transfer learning techniques are able to differentiate the physical appearance of sago compared to other vegetation with small datasets.

Transfer learning approaches are used to transfer the learning model into a new task, i.e., to distinguish the visual morphology of sago. The visible morphology experiment (experiment-2) consisted of 231 images divided into nine classes of coconut fruits, coconut leaves, coconut trunks, oil palm fruits, oil palm leaves, oil palm trunks, sago flowers, sago leaves and sago trunks. The proposed ResNet-50 surpassed other networks.

Hypothesis 4: CNN deep learning networks are able to detect, and predict sago palms captured by a UAV and ground photographs.

The three deep CNN models were arranged using transfer learning with 50 layers, 68 layers, and 25 layers within ResNet, SqueezeNet and Alex, respectively; further, with 10 epoch, 10 min batch size and 0.0001 learning rate. The results showed that 68 and 50 layers performed well in detecting and predicting sago palms captured from UAV and ground photographs as provided in the dataset.

Hypothesis 5: In designing the sago palm detection, parameters and network structure must be considered.

The research work in experiment-3 led to adjusting various parameters in two network structures i.e., 68 layers (sago model-1) and 25 layers (sago model-2). Network parameters in this study were described through epoch, min batch size, learning rate and network iteration. Network iteration processed the data training according to the number of images in the data trained, then split it into min batch size. Afterwards, the result was multiplied according to the number of epochs. The sago palm model in this study enabled good fit conditions with about 0.2 differentiation between training loss and validation loss, also less than 9% of differentiation between training accuracy and validation accuracy. In this case, early stopping during training progress could be involved to avoid underfitting or overfitting. Thus, according to the prediction results and metric evaluation in this third experiment, the learning rate of these two models is preferably 0.0001.

Hypothesis 6: The evaluation of the model is essential to ensure the model is performing in accordance with the expected output.

The model was evaluated by performing a confusion matrix, then from this tabular matrix, the sensitivity, precision and F1-score were calculated in the two experiments. To add this, the evaluation result is visualized through the ROC curves in the second experiment.

7.1 Research Contribution

The significant contributions achieved from the whole study effort are concluded in the following outcomes:

a. **Identification of available data sources in the regency, specifically in sago habitat, Indonesia Land Cover and** p**eatland land cover from Peatland Restoration Agency**.

   The most considerable limitation identified was the inadequacy of data on sago areas, and sago yield areas in the regency. The first experiment was performed using remote sensing data to evaluate the land use changes in the regency and the impact on the sago habitat. The data source derived from remote sensing was documented in spreadsheet file, and ArcGIS files, which enabled to predict the future changes periodically. As mentioned in our research problem the study site has a shortage of regular documentation specifically in sago palm areas. The research effort gained from the first experiment was useful for gaining dynamic changes of various environments. In this regard, the regional and national governments require annual land use changes data to monitor and assess specific land uses. Once the habitat is damaged over time due to the lack of thorough study research, this Province and Indonesia suffer from the depletion of numerous natural plants such as sago.

b. **Development of land cover maps of the area, forest cover changes map and prediction of the potential sago habitat in each region in the regency.**

In Papua, forest areas are crucial as a prerequisite for the sago palm to grow; meanwhile, the changes in the forested areas contribute to the sago palm's existence. On the one hand, land cover maps and the rate changes from 1990 to 20109 that examined in this study can be utilized to support the local government's decision-making for the preservation and management of natural resources. Further, the research effort predicted the potential area of sago in this regency, which can be useful to support the community, business sector and researchers in developing further applications. Our studies reviewed the potential uses of sago palm, such as health aspects or food industry and bioeconomy; it is proven that sago has added value that can be expanded beyond its original usage as a basic food source. Sago has been processed in the food business using various techniques that may enhance its physicochemical, nutritional, and palatable qualities. Sago can also be useful in the non-food sector of the economy, particularly in the field of bioenergy, as experimented by (Jonatan et al., 2017); it can support the local community in providing low household energy. Sago's potential advantages and uses led to its use in both food and non-food products. As a result, it supports sustainable production, sago forest preservation, and regional bioeconomy development. Sago food production can ensure that society consumes sufficient quantities of food, while the growth of sago based on industrial production might contribute to the emergence of new business ventures and employment prospects. Hence, monitoring the natural resources through land use changes is also beneficial not only for the Government's regulation or preventive programs, but also to enrich the research itself, and to improve the business sector and community lives.

c. **Provision of sago palm dataset from South Papua in our GitHub repository in format JSON, VGG and original images**.

   The images captured by UAV and ground photographs in our fieldwork, namely Tambat, a region in Tanah Miring of Merauke Regency that is well known as sago producer in the regency. A different dataset provided by research is essential to support further application in sago palm detection in Papua Province. In general, the dataset provided in this research did not contain sago palm only , other plants were also involved, for instance, coconut, palm oil and other non-sago. The results of the second and third experiments revealed that the model was able to distinguish them compared to sago. Meanwhile, the research contribution was also able to support other detection, for example, coconut, palm oil and non-sago.

d. **Development of an alternative technique based on transfer learning approaches to establish a sago detection model that can differentiate the palm through their visible morphology.**

   An earlier study in sago palm detection, as presented in section 2.9, was arranged differently from our research effort: (1) The previous study aimed to distinguish the maturity of sago palms in Malaysia. (2) The dataset gained from UAV containing harvestable sago, non-harvestable sago and other objects, such as rivers and cars, was divided into five groups. However, this research effort, specifically the second and third experiment was focused on detecting sago palms based on visual morphology of sago. The dataset was derived from UAV and photo ground of sago leaves, flowers, trunks, non-sago objects, coconut leaves, coconut trunks, coconut fruits, as well as oil pam leaves, oil palm fruits and oil palm trunks. In the second experiment, nine groups were utilized, while in the third experiment four groups were labelled. Another different point of view was (3) that the training and the validation samples were divided based on 80:20, i.e., 756 images in the training phase and 189 images in the validation set, while our dataset was arranged based on 70:30 in each experiment. Further, (4) the AlexNet based model in the previous studies consisted of 11 layers, while this study included 25 layers and 50 layers. Thus, (5) in the previous study, metric evaluation with fivefold validation was implemented; in this research effort, a confusion matrix was performed to calculate the accuracy, sensitivity and F1-score, as well as to present the performance through the ROC curve.

7.2 Further Work

Due to time and resources restrictions, further experiments are recommended as the most encouraged future research, as follows:

a. Adding additional features for detection.

Improving the transfer learning technique by performing different network structures, for instance, semantic segmentation network and different syntaxes. It is important to keep the accuracy in learning and do the task in classifying or predicting the palm not only from the images but also from the moving object. Future applications such as disease identification, unnourished sago classification, and sago yield estimation based on sago flowers, could potentially facilitate sago palm protection for sago palm farmers, business sector, and relevant stakeholders.

b. Acquiring the benefist from mobile or handheld devices.

One of the most significant motivations in this research is how the community employed a conventional method to detect the harvest time, i.e., visual detection. This research effort proved the ability to detect with confidence sago palm images. This designed model could be connected to a mobile or web-based application, enabling the community, farmers or government to access it widely. Future studies will include connectivity with the Internet of Things (IoT), such as for recognizing sago weeds, particularly if commercial sago planting is envisioned.

c. New collaboration with government.

All data employed in this research was collected before the new structure of Papua was announced. As mentioned earlier, the most challenging in this study is the limited amount of data related to sago areas and sago yield areas. This study relied on remote sensing data. Related work enabled us to gain the historical data presented in this study. Therefore, to improve the prediction of sago palms in each region, collaboration with the new government could potentially affect the discovery of new data.

8. REFERENCES

1. Aliani, H., Malmir, M., Sourodi, M., & Kafaky, S. B. (2019). Change detection and prediction of urban land use changes by CA–Markov model (case study: Talesh County). *Environmental Earth Sciences*, *78*(17), 546. https://doi.org/10.1007/s12665-019-8557-9.
2. Allworth, J., Windrim, L., Bennett, J., & Bryson, M. (2021). A transfer learning approach to space debris classification using observational light curve data. *Acta Astronautica*, *181*, 301–315. https://doi.org/10.1016/j.actaastro.2021.01.048.
3. Amin, N., Sabli, N., Izhar, S., & Yoshida, H. (1841). *Sago Wastes and Its Applications*. 22.
4. Artasanchez, A., & Joshi, P. (2020). *Artificial intelligence with Python: Your complete guide to building intelligent apps using Python 3.x* (Second edition). Packt.
5. Ashouri, M., & Hashemi, A. (2022). A transfer learning metamodel using artificial neural networks for natural convection flows in enclosures. *Case Studies in Thermal Engineering*, *36*, 102179. https://doi.org/10.1016/j.csite.2022.102179.
6. Awais, M., Li, W., Cheema, M. J. M., Zaman, Q. U., Shaheen, A., Aslam, B., Zhu, W., Ajmal, M., Faheem, M., Hussain, S., Nadeem, A. A., Afzal, M. M., & Liu, C. (2023). UAV-based remote sensing in plant stress imagine using high-resolution thermal sensor for digital agriculture practices: A meta-review. *International Journal of Environmental Science and Technology*, *20*(1), 1135–1152. https://doi.org/10.1007/s13762-021-03801-5.
7. Awg-Adeni, D. S., Abd-Aziz, S., Bujang, K., & Hassan, M. A. (n.d.). *Bioconversion of sago residue into value added products*. 6.
8. Azari, M., Billa, L., & Chan, A. (2022). Multi-temporal analysis of past and future land cover change in the highly urbanized state of Selangor, Malaysia. *Ecological Processes*, *11*(1), 2. https://doi.org/10.1186/s13717-021-00350-0
9. Baumann, M., Koch, C., & Staudacher, S. (2022). Application of Neural Networks and Transfer Learning to Turbomachinery Heat Transfer. *Aerospace*, *9*(2), 49. https://doi.org/10.3390/aerospace9020049.

10. Berger, K., Machwitz, M., Kycko, M., Kefauver, S. C., Van Wittenberghe, S., Gerhards, M., Verrelst, J., Atzberger, C., van der Tol, C., Damm, A., Rascher, U., Herrmann, I., Paz, V. S., Fahrner, S., Pieruschka, R., Prikaziuk, E., Buchaillot, Ma. L., Halabuk, A., Celesti, M., … Schlerf, M. (2022). Multi-sensor spectral synergies for crop stress detection and monitoring in the optical domain: A review. *Remote Sensing of Environment*, *280*, 113198. https://doi.org/10.1016/j.rse.2022.113198.
11. Directorate General of Estate Crops (2020), *Statisitical of National Leading Estate Scrops Commodity 2019-2021*. Secretariate of Directorate General of Estate Crops: Ministry of Agriculture. Accessed online: https://drive.google.com/file/d/1ZpXeZogAQYfClNBOgVLhYi8X_vujJdHx/view. May 14th, 2023. 14:43 CEST time.
12. Chen, J., Chen, S., Fu, R., Li, D., Jiang, H., Wang, C., Peng, Y., Jia, K., & Hicks, B. J. (2022). Remote Sensing Big Data for Water Environment Monitoring: Current Status, Challenges, and Future Prospects. *Earth's Future*, *10*(2). https://doi.org/10.1029/2021EF002289.
13. Cheng, K., & Wang, J. (2019). Forest Type Classification Based on Integrated Spectral-Spatial-Temporal Features and Random Forest Algorithm—A Case Study in the Qinling Mountains. *Forests*, *10*(7), 559. https://doi.org/10.3390/f10070559.
14. Chew, T.-A., Isa, A. H. B. Md., & Mohayidin, Mohd. G. B. (1999). Sago (*Metroxylon sagu Rottboll*), the Forgotten Palm. *Journal of Sustainable Agriculture*, *14*(4), 5–17. https://doi.org/10.1300/J064v14n04_03.
15. Chollet, F. (2018). *Deep learning with Python*. Manning Publications Co.
16. Dimara, P. A., Purwanto, R. H., & Sunarta, S. (2021). The spatial distribution of sago palm landscape Sentani watershed in Jayapura District, Papua Province, Indonesia. *Biodiversitas Journal of Biological Diversity*, *22*(9). https://doi.org/10.13057/biodiv/d220926.
17. Ehara, H., Toyoda, Y., & Johnson, D. V. (Eds.). (2018). *Sago Palm: Multiple Contributions to Food Security and Sustainable Livelihoods*. Springer Singapore. https://doi.org/10.1007/978-981-10-5269-9.
18. Entwistle, C., Mora, M. A., & Knight, R. (2018). Estimating coastal wetland gain and losses in Galveston County and Cameron County, Texas, USA:

Wetland Gains and Losses in 2 Texas Coastal Counties. *Integrated Environmental Assessment and Management*, *14*(1), 120–129. https://doi.org/10.1002/ieam.1973.

19. Ferchichi, A., Abbes, A. B., Barra, V., & Farah, I. R. (2022). Forecasting vegetation indices from spatio-temporal remotely sensed data using deep learning-based approaches: A systematic literature review. *Ecological Informatics*, *68*, 101552. https://doi.org/10.1016/j.ecoinf.2022.101552.
20. Fetriyuna, F. (2022). *Potential uses of underutilized sago to support the sustainability of food supply and bioeconomy*. *2022*.
21. García-Pardo, K. A., Moreno-Rangel, D., Domínguez-Amarillo, S., & García-Chávez, J. R. (2022). Remote sensing for the assessment of ecosystem services provided by urban vegetation: A review of the methods applied. *Urban Forestry & Urban Greening*, *74*, 127636. https://doi.org/10.1016/j.ufug.2022.127636.
22. Gondwe, M. F., Cho, M. A., Chirwa, P. W., & Geldenhuys, C. J. (2019). Land use land cover change and the comparative impact of co-management and government-management on the forest cover in Malawi (1999-2018). *Journal of Land Use Science*, *14*(4–6), 281–305. https://doi.org/10.1080/1747423X.2019.1706654.
23. Grigorev, A. (2021). *Machine Learning Bookcamp*. Manning Publications Co.
24. Guo, Y., Fang, G., Xu, Y.-P., Tian, X., & Xie, J. (2020). Identifying how future climate and land use/cover changes impact streamflow in Xinanjiang Basin, East China. *Science of The Total Environment*, *710*, 136275. https://doi.org/10.1016/j.scitotenv.2019.136275.
25. Halmy, M. W. A., Gessler, P. E., Hicke, J. A., & Salem, B. B. (2015). Land use/land cover change detection and prediction in the north-western coastal desert of Egypt using Markov-CA. *Applied Geography*, *63*, 101–112. https://doi.org/10.1016/j.apgeog.2015.06.015.
26. Hamad, R., Balzter, H., & Kolo, K. (2018). Predicting Land Use/Land Cover Changes Using a CA-Markov Model under Two Different Scenarios. *Sustainability*, *10*(10), 3421. https://doi.org/10.3390/su10103421.
27. Han, B., Hu, Z., Su, Z., Bai, X., Yin, S., Luo, J., & Zhao, Y. (2022). Mask_LaC R-CNN for measuring morphological features of fish. *Measurement*, *203*,

111859. https://doi.org/10.1016/j.measurement.2022.111859.

28. Han, L., Zhao, Y., Chen, H., & Chandrasekar, V. (2022). Advancing Radar Nowcasting Through Deep Transfer Learning. *IEEE Transactions on Geoscience and Remote Sensing*, *60*, 1–9. https://doi.org/10.1109/TGRS.2021.3056470.
29. Hao, R., Namdar, K., Liu, L., & Khalvati, F. (2021). A Transfer Learning–Based Active Learning Framework for Brain Tumor Classification. *Frontiers in Artificial Intelligence*, *4*, 635766. https://doi.org/10.3389/frai.2021.635766.
30. He, K., Gkioxari, G., Dollár, P., & Girshick, R. (2018). *Mask R-CNN* (arXiv:1703.06870). arXiv. http://arxiv.org/abs/1703.06870.
31. Hidayat, S., Matsuoka, M., Baja, S., & Rampisela, D. A. (2018). Object-Based Image Analysis for Sago Palm Classification: The Most Important Features from High-Resolution Satellite Imagery. *Remote Sensing*, *10*(8), 1319. https://doi.org/10.3390/rs10081319.
32. Hu, G., Wang, T., Wan, M., Bao, W., & Zeng, W. (2022). UAV remote sensing monitoring of pine forest diseases based on improved Mask R-CNN. *International Journal of Remote Sensing*, *43*(4), 1274–1305. https://doi.org/10.1080/01431161.2022.2032455.
33. Huang, J., Lu, X., Chen, L., Sun, H., Wang, S., & Fang, G. (2022). Accurate Identification of Pine Wood Nematode Disease with a Deep Convolution Neural Network. *Remote Sensing*, *14*(4), 913. https://doi.org/10.3390/rs14040913.
34. Huang, M.-L., Chuang, T.-C., & Liao, Y.-C. (2022). Application of transfer learning and image augmentation technology for tomato pest identification. *Sustainable Computing: Informatics and Systems*, *33*, 100646. https://doi.org/10.1016/j.suscom.2021.100646.
35. Huang, Y., Chen, Z., Yu, T., Huang, X., & Gu, X. (2018). Agricultural remote sensing big data: Management and applications. *Journal of Integrative Agriculture*, *17*(9), 1915–1931. https://doi.org/10.1016/S2095-3119(17)61859-8.
36. Jafarbiglu, H., & Pourreza, A. (2022). A comprehensive review of remote sensing platforms, sensors, and applications in nut crops. *Computers and Electronics in Agriculture*, *197*, 106844.

https://doi.org/10.1016/j.compag.2022.106844.

37. Jahja, H. D., Yudistira, N., & Sutrisno. (2023). Mask usage recognition using vision transformer with transfer learning and data augmentation. *Intelligent Systems with Applications*, *17*, 200186. https://doi.org/10.1016/j.iswa.2023.200186.
38. J.J. Lal. (2003). *Encyclopedia of Food Sciences and Nutrition*. Elsevier.
39. Jonatan, N. J., Ekayuliana, A., Dhiputra, I. M. K., & Nugroho, Y. S. (2017). The Utilization of Metroxylon Sago (Rottb.) Dregs for Low Bioethanol as Fuel Households Needs in Papua Province Indonesia. *KnE Life Sciences*, *3*(5), 150. https://doi.org/10.18502/kls.v3i5.987.
40. Karim, A. A., Tie, A. P.-L., Manan, D. M. A., & Zaidul, I. S. M. (2008). Starch from the Sago (*Metroxylon sagu*) Palm TreeProperties, Prospects, and Challenges as a New Industrial Source for Food and Other Uses. *Comprehensive Reviews in Food Science and Food Safety*, *7*(3), 215–228. https://doi.org/10.1111/j.1541-4337.2008.00042.x.
41. Kho, E. P., Chua, S. N. D., Lim, S. F., Lau, L. C., & Gani, M. T. N. (2022). Development of young sago palm environmental monitoring system with wireless sensor networks. *Computers and Electronics in Agriculture*, *193*, 106723. https://doi.org/10.1016/j.compag.2022.106723.
42. Kneusel, R. T. (2021). *Practical Deep Learning: A Python-Based Introduction* (First). No Starch Press, Inc.
43. Kumar, J. S., Anuar, S., & Hassan, N. H. (2022). Transfer Learning based Performance Comparison of the Pre-Trained Deep Neural Networks. *International Journal of Advanced Computer Science and Applications*, *13*(1). https://doi.org/10.14569/IJACSA.2022.0130193.
44. Lamba, A., Cassey, P., Segaran, R. R., & Koh, L. P. (2019). Deep learning for environmental conservation. *Current Biology*, *29*(19), R977–R982. https://doi.org/10.1016/j.cub.2019.08.016.
45. Letsoin, S. M. A., Herak, D., & Purwestri, R. C. (2022). Evaluation Land Use Cover Changes Over 29 Years in Papua Province of Indonesia Using Remote Sensing Data. *IOP Conference Series: Earth and Environmental Science*, *1034*(1), 012013. https://doi.org/10.1088/1755-1315/1034/1/012013.

46. Letsoin, S. M. A., Herak, D., Rahmawan, F., & Purwestri, R. C. (2020). Land Cover Changes from 1990 to 2019 in Papua, Indonesia: Results of the Remote Sensing Imagery. *Sustainability*, *12*(16), 6623. https://doi.org/10.3390/su12166623.
47. Letsoin, S. M. A., Purwestri, R. C., & Herák, D. (2022). Combining the Surveillance of Unmanned Aerial Vehicle and Deep Learning Methods in Sago Palm Detection. *8th TAE 2022*.
48. Letsoin, S. M. A., Purwestri, R. C., Rahmawan, F., & Herak, D. (2022). Recognition of Sago Palm Trees Based on Transfer Learning. *Remote Sensing*, *14*(19), 4932. https://doi.org/10.3390/rs14194932.
49. Li, W., Huang, R., Li, J., Liao, Y., Chen, Z., He, G., Yan, R., & Gryllias, K. (2022). A perspective survey on deep transfer learning for fault diagnosis in industrial scenarios: Theories, applications and challenges. *Mechanical Systems and Signal Processing*, *167*, 108487. https://doi.org/10.1016/j.ymssp.2021.108487.
50. Li, Z., Kristoffersen, E., & Li, J. (2022). Deep transfer learning for failure prediction across failure types. *Computers & Industrial Engineering*, *172*, 108521. https://doi.org/10.1016/j.cie.2022.108521.
51. Li, Z., Shen, H., Weng, Q., Zhang, Y., Dou, P., & Zhang, L. (2022). Cloud and cloud shadow detection for optical satellite imagery: Features, algorithms, validation, and prospects. *ISPRS Journal of Photogrammetry and Remote Sensing*, *188*, 89–108. https://doi.org/10.1016/j.isprsjprs.2022.03.020.
52. Lim, L. W. K., Chung, H. H., Hussain, H., & Bujang, K. (2019). *Sago Palm (Metroxylon sagu Rottb.): Now and Beyond*.
53. Lin, K., Zhao, Y., Wang, L., Shi, W., Cui, F., & Zhou, T. (2023). MSWNet: A visual deep machine learning method adopting transfer learning based upon ResNet 50 for municipal solid waste sorting. *Frontiers of Environmental Science & Engineering*, *17*(6), 77. https://doi.org/10.1007/s11783-023-1677-1.
54. Liu, Y., Xiang, H., Jiang, Z., & Xiang, J. (2023). A Domain Adaption ResNet Model to Detect Faults in Roller Bearings Using Vibro-Acoustic Data. *Sensors*, *23*(6), 3068. https://doi.org/10.3390/s23063068.

55. Lu, T., Han, B., & Yu, F. (2021). Detection and classification of marine mammal sounds using AlexNet with transfer learning. *Ecological Informatics*, *62*, 101277. https://doi.org/10.1016/j.ecoinf.2021.101277.
56. Martínez, M. L., Pérez-Maqueo, O., Vázquez, G., Castillo-Campos, G., García-Franco, J., Mehltreter, K., Equihua, M., & Landgrave, R. (2009). Effects of land use change on biodiversity and ecosystem services in tropical montane cloud forests of Mexico. *Forest Ecology and Management*, *258*(9), 1856–1863. https://doi.org/10.1016/j.foreco.2009.02.023.
57. Mathewos, M., Lencha, S. M., & Tsegaye, M. (2022). Land Use and Land Cover Change Assessment and Future Predictions in the Matenchose Watershed, Rift Valley Basin, Using CA-Markov Simulation. *Land*, *11*(10), 1632. https://doi.org/10.3390/land11101632.
58. Mehmood, M., Shahzad, A., Zafar, B., Shabbir, A., & Ali, N. (2022). Remote Sensing Image Classification: A Comprehensive Review and Applications. *Mathematical Problems in Engineering*, *2022*, 1–24. https://doi.org/10.1155/2022/5880959.
59. Meraner, A., Ebel, P., Zhu, X. X., & Schmitt, M. (2020). Cloud removal in Sentinel-2 imagery using a deep residual neural network and SAR-optical data fusion. *ISPRS Journal of Photogrammetry and Remote Sensing*, *166*, 333–346. https://doi.org/10.1016/j.isprsjprs.2020.05.013.
60. Metaragakusuma, A. P., Katsuya, O., & Bai, H. (2016). An Overview of The Traditional Use of Sago for Sago-based Food Industry in Indonesia. *KnE Life Sciences*, *3*(3), 119. https://doi.org/10.18502/kls.v3i3.382.
61. Mimi, A., Zohura, S. F. T., Ibrahim, M., Haque, R. R., Farrok, O., Jabid, T., & Ali, M. S. (2023). Identifying selected diseases of leaves using deep learning and transfer learning models. *Machine Graphics and Vision*, *32*(1), 55–71. https://doi.org/10.22630/MGV.2023.32.1.3.
62. Minaee, S., Boykov, Y. Y., Porikli, F., Plaza, A. J., Kehtarnavaz, N., & Terzopoulos, D. (2021). Image Segmentation Using Deep Learning: A Survey. *IEEE Transactions on Pattern Analysis and Machine Intelligence*, 1–1. https://doi.org/10.1109/TPAMI.2021.3059968.
63. Mofu, S. S., & Abbas, B. (2015). Development of Sago Palm Research and Agroindustry in University of Papua. *Proceeding of the 12th International*

Sago Symposium in Tokyo, Japan. Japan Society for the Promotion Science.

64. Mukoya, E., Rimiru, R., Kimwele, M., Gakii, C., & Mugambi, G. (2023). Accelerating deep learning inference via layer truncation and transfer learning for fingerprint classification. *Concurrency and Computation: Practice and Experience*, *35*(8). https://doi.org/10.1002/cpe.7619
65. Nurhasan, M., Maulana, A. M., Ariesta, D. L., Usfar, A. A., Napitupulu, L., Rouw, A., Hurulean, F., Hapsari, A., Heatubun, C. D., & Ickowitz, A. (2022). Toward a Sustainable Food System in West Papua, Indonesia: Exploring the Links Between Dietary Transition, Food Security, and Forests. *Frontiers in Sustainable Food Systems, 5,* 789186. https://doi.org/10.3389/fsufs.2021.789186.
66. Orchi, H., Sadik, M., Khaldoun, M., & Sabir, E. (2023). Automation of Crop Disease Detection through Conventional Machine Learning and Deep Transfer Learning Approaches. *Agriculture*, *13*(2), 352. https://doi.org/10.3390/agriculture13020352.
67. Ornek, A. H., & Ceylan, M. (2022). Medical thermograms' classification using deep transfer learning models and methods. *Multimedia Tools and Applications*, *81*(7), 9367–9384. https://doi.org/10.1007/s11042-021-11852-6.
68. BPS. *Papua in Figures 2021*. BPS-Statistics of Papua Province, BPS: Jakarta, Indonesia.
69. Rasyid, T. H., Kusumawaty, Y., & Hadi, S. (2020). The utilization of sago waste: Prospect and challenges. *IOP Conference Series: Earth and Environmental Science*, *415*(1), 012023. https://doi.org/10.1088/1755-1315/415/1/012023.
70. Reuters, T. (2016). *Artificial Intelligence in Law: The State of Play 2016*. p 6.
71. Salosa, S. T. (2016). Challenge Of Sago (Metroxylon Sp) As Papua Food Identity. *KnE Social Sciences*, *1*(1). https://doi.org/10.18502/kss.v1i1.435.
72. Santillan, J. R., & Makinano-Santillan, M. (2016). Recent Distribution of Sago Palms in the Philippines. *Paluga, M.J.D., Ed.; University of the Philippines: Mindanao, Philippines*, 186.
73. Seki, H. A., Shirima, D. D., Courtney Mustaphi, C. J., Marchant, R., & Munishi, P. K. T. (2018). The impact of land use and land cover change on biodiversity within and adjacent to Kibasira Swamp in Kilombero Valley,

Tanzania. *African Journal of Ecology*, *56*(3), 518–527. https://doi.org/10.1111/aje.12488.

74. Setiawan, B., Fetriyuna, F., Letsoin, S. M. A., Purwestri, R. C., & Jati, I. R. A. P. (2022). A Sago Positive Character: A Literature Review. *Jurnal Ilmiah Kedokteran Wijaya Kusuma*, *11*(2), 145. https://doi.org/10.30742/jikw.v11i2.2443.
75. Shafique, A., Cao, G., Khan, Z., Asad, M., & Aslam, M. (2022). Deep Learning-Based Change Detection in Remote Sensing Images: A Review. *Remote Sensing*, *14*(4), 871. https://doi.org/10.3390/rs14040871.
76. Shivaprakash, K. N., Swami, N., Mysorekar, S., Arora, R., Gangadharan, A., Vohra, K., Jadeyegowda, M., & Kiesecker, J. M. (2022). Potential for Artificial Intelligence (AI) and Machine Learning (ML) Applications in Biodiversity Conservation, Managing Forests, and Related Services in India. *Sustainability*, *14*(12), 7154. https://doi.org/10.3390/su14127154.
77. Sidiq, F. F., Coles, D., Hubbard, C., Clark, B., & Frewer, L. J. (2021). Sago and the indigenous peoples of Papua, Indonesia: A review. *Journal of Agriculture and Applied Biology*, *2*(2), 138–149. https://doi.org/10.11594/jaab.02.02.08.
78. Singhal, R. S., Kennedy, J. F., Gopalakrishnan, S. M., Kaczmarek, A., Knill, C. J., & Akmar, P. F. (2008). Industrial production, processing, and utilization of sago palm-derived products. *Carbohydrate Polymers*, *72*(1), 1–20. https://doi.org/10.1016/j.carbpol.2007.07.043.
79. Thenmozhi, K., & Srinivasulu Reddy, U. (2019). Crop pest classification based on deep convolutional neural network and transfer learning. *Computers and Electronics in Agriculture*, *164*, 104906. https://doi.org/10.1016/j.compag.2019.104906.
80. Tripathy, P., & Kumar, A. (2019). Monitoring and modelling spatio-temporal urban growth of Delhi using Cellular Automata and geoinformatics. *Cities*, *90*, 52–63. https://doi.org/10.1016/j.cities.2019.01.021.
81. Trisia, M. A., Metaragakusuma, A. P., Osozawa, K., & Bai, H. (2016). Local Actions to Foster Climate Change adaption Through Sago Palm Development Initiatives: Examining the Case of South Sulawesi, Indonesia. *European Journal of Sustainable Development*, *5*(4).

https://doi.org/10.14207/ejsd.2016.v5n4p312.

82. Tůma, L., Kumhálová, J., Kumhála, F., & Krepl, V. (2022). The noise-reduction potential of Radar Vegetation Index for crop management in the Czech Republic. *Precision Agriculture*, *23*(2), 450–469. https://doi.org/10.1007/s11119-021-09844-5.
83. Vallentin, C., Harfenmeister, K., Itzerott, S., Kleinschmit, B., Conrad, C., & Spengler, D. (2022). Suitability of satellite remote sensing data for yield estimation in northeast Germany. *Precision Agriculture*, *23*(1), 52–82. https://doi.org/10.1007/s11119-021-09827-6.
84. Vasilev, I., Slater, D., Spacagna, G., Roelants, P., & Zocca, V. (2019). *Python deep learning: Exploring deep learning techniques and neural network architectures with PyTorch, Keras, and TensorFlow* (Second edition). Packt Publishing Limited.
85. Velastegui-Montoya, A., Montalván-Burbano, N., Peña-Villacreses, G., de Lima, A., & Herrera-Franco, G. (2022). Land Use and Land Cover in Tropical Forest: Global Research. *Forests*, *13*(10), 1709. https://doi.org/10.3390/f13101709
86. Wahed, Z., Joseph, A., Zen, H., & Kipli, K. (2022). Sago Palm Detection and its Maturity Identification Based on Improved Convolution Neural Network. *Pertanika Journal of Science and Technology*, *30*(2), 1219–1236. https://doi.org/10.47836/pjst.30.2.20.
87. Whittle, M., Quegan, S., Uryu, Y., Stüewe, M., & Yulianto, K. (2012). Detection of tropical deforestation using ALOS-PALSAR: A Sumatran case study. *Remote Sensing of Environment*, *124*, 83–98. https://doi.org/10.1016/j.rse.2012.04.027.
88. Xu, X., Zhao, M., Shi, P., Ren, R., He, X., Wei, X., & Yang, H. (2022). Crack Detection and Comparison Study Based on Faster R-CNN and Mask R-CNN. *Sensors*, *22*(3), 1215. https://doi.org/10.3390/s22031215.
89. Yao, X., Guo, Q., Li, A., & Shi, L. (2022). Optical remote sensing cloud detection based on random forest only using the visible light and near-infrared image bands. *European Journal of Remote Sensing*, *55*(1), 150–167. https://doi.org/10.1080/22797254.2021.2025433.

90. Yasir, M., Jianhua, W., Shanwei, L., Sheng, H., Mingming, X., & Hossain, M. (2023). Coupling of deep learning and remote sensing: A comprehensive systematic literature review. *International Journal of Remote Sensing*, *44*(1), 157–193. https://doi.org/10.1080/01431161.2022.2161856.
91. Zhang, B., Zhu, J., & Su, H. (2023). Toward the third generation artificial intelligence. *Science China Information Sciences*, *66*(2), 121101. https://doi.org/10.1007/s11432-021-3449-x.
92. Zhang, L., Wang, M., Fu, Y., & Ding, Y. (2022). A Forest Fire Recognition Method Using UAV Images Based on Transfer Learning. *Forests*, *13*(7), 975. https://doi.org/10.3390/f13070975.
93. Zheng, J., Fu, H., Li, W., Wu, W., Yu, L., Yuan, S., Tao, W. Y. W., Pang, T. K., & Kanniah, K. D. (2021). Growing status observation for oil palm trees using Unmanned Aerial Vehicle (UAV) images. *ISPRS Journal of Photogrammetry and Remote Sensing*, *173*, 95–121. https://doi.org/10.1016/j.isprsjprs.2021.01.008.
94. Zheng, J., Song, X., Yang, G., Du, X., Mei, X., & Yang, X. (2022). Remote Sensing Monitoring of Rice and Wheat Canopy Nitrogen: A Review. *Remote Sensing*, *14*(22), 5712. https://doi.org/10.3390/rs14225712.
95. Zhuang, F., Qi, Z., Duan, K., Xi, D., Zhu, Y., Zhu, H., Xiong, H., & He, Q. (2021). A Comprehensive Survey on Transfer Learning. *Proceedings of the IEEE*, *109*(1), 43–76. https://doi.org/10.1109/JPROC.2020.3004555.
96. Zou, X., Wu, C., Liu, H., & Yu, Z. (2023). Improved ResNet-50 model for identifying defects on wood surfaces. *Signal, Image and Video Processing*. https://doi.org/10.1007/s11760-023-02533-y.

APPENDIX A

Land cover maps of the regency as displayed in Figure A.1. The land cover maps were produced from the first experiment and were published in research publication-1 and publication-2. The publications are listed in appendix E.

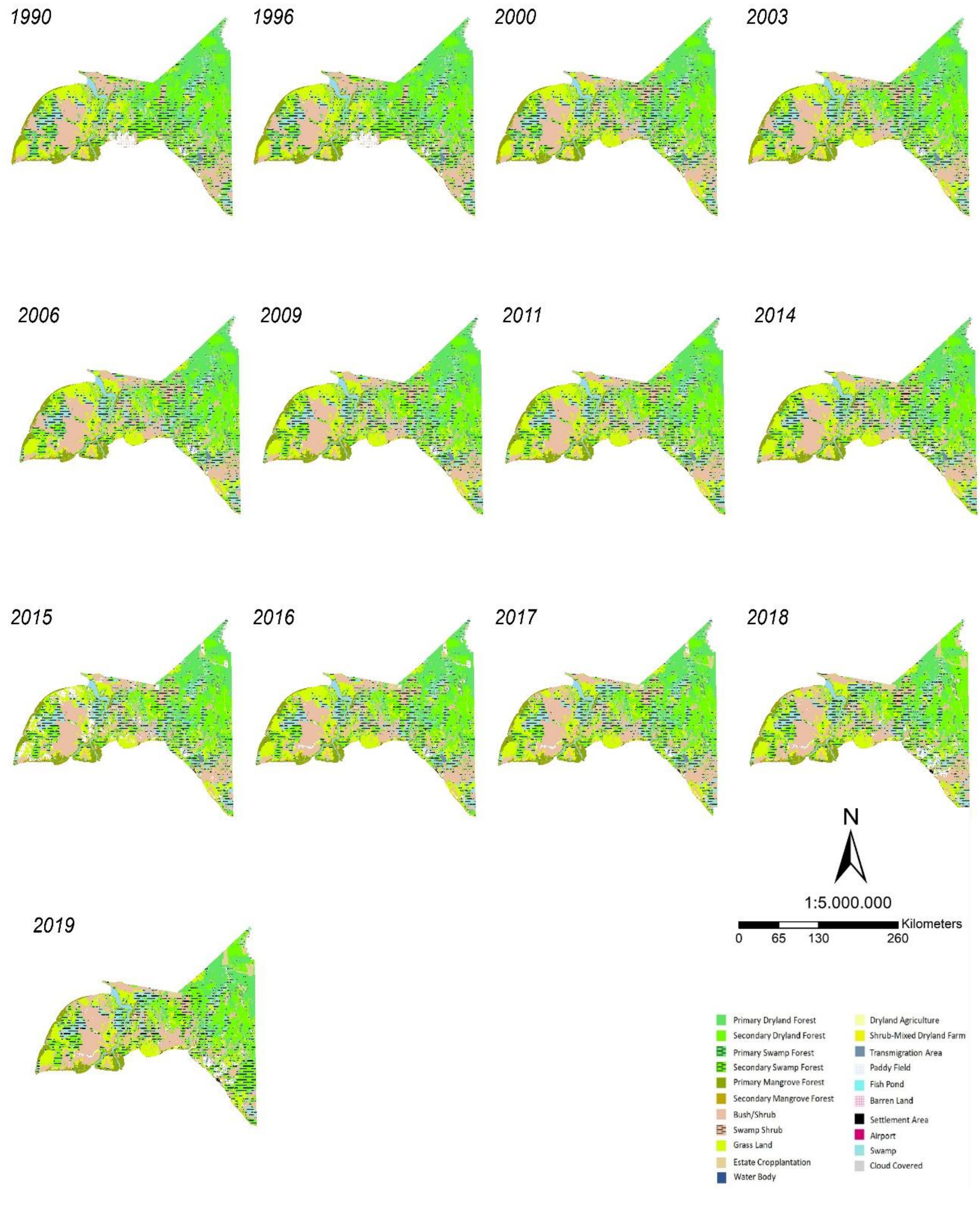

Figure A.1. Land cover maps of the regency from 1990 to 2019.

Forest cover changes in the regency as shown in Figure A.2.

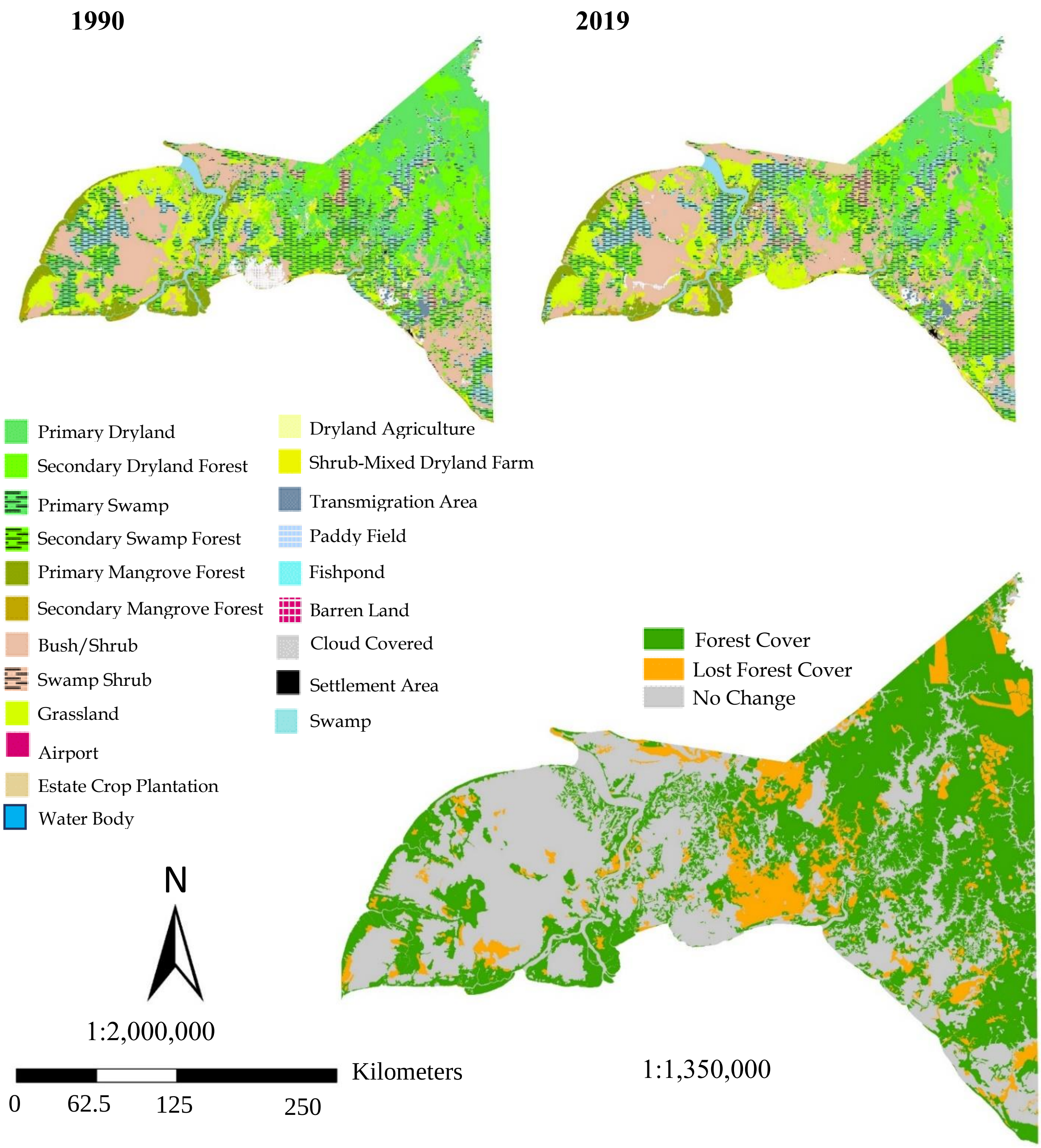

Figure A.2 . Forest cover changes in Merauke Regency.

APPENDIX B

The results in this appendix were derived from experiment-1. The rate changes (Table 11) were calculated in the following formula (Entwistle et al., 2018; Gondwe et al., 2019; Martínez et al., 2009):

$$the\ change\ rate = \frac{Area\ (f) - Area\ (i)}{Area\ (i)} \tag{6}$$

Area (f) and *Area (i)* are the areas of a specific land type at final and beginning period of study, respectively.

Table B.1 Land cover area (Ha).

Merauke Regency														
No	**LC Classes**	**Area Estimation per Year (Hektar)**												
		1990	**1996**	**2000**	**2003**	**2006**	**2009**	**2011**	**2014**	**2015**	**2016**	**2017**	**2018**	**2019**
1	Primary Dryland Forest	694,737	664,757	634,776	619,004	598,828	553,728	553,098	543,670	529,715	522,977	519,144	401,879	500,359
2	Secondary Dryland Forest	638,049	620,773	603,496	618,381	627,494	672,086	672,425	678,803	664,888	654,663	652,518	732,934	631,295
3	Primary Mangrove Forest	208,727	207,345	205,963	201,768	196,510	196,510	196,510	197,808	196,758	195,162	195,007	195,660	195,384
4	Primary Swamp Forest	342,429	329,304	316,179	292,789	238,249	205,343	205,343	206,530	202,799	200,958	200,400	202,694	202,193
5	Bush/Shrub	71,946	124,194	176,443	177,229	178,032	178,463	177,262	174,273	169,262	166,111	170,801	169,656	129,465
6	Secondary Mangrove Forest	25,345	24,209	23,073	25,776	23,678	23,574	23,574	23,675	23,521	23,876	23,829	23,932	24,060
7	Secondary Swamp Forest	531,109	419,213	307,317	313,173	338,909	371,810	371,810	374,446	359,399	356,270	358,089	357,151	531,266
8	Estate Cropplantation	-	-	-	101	101	101	1,533	16,535	19,885	27,397	53,857	80,231	94,359

9	Settlement Area	3,160	3,366	3,571	3,667	3,891	3,891	3,891	3,917	3,653	3,878	3,480	7,216	7,090
10	Barren Land	81,714	51,759	21,805	21,805	21,853	21,853	21,913	23,501	263,859	75,081	56,539	77,994	88,946
11	Cloud Covered	764	764	764	764	764	764	764	-	-	-	-	-	-
12	Grass Land	471,693	549,087	626,480	646,258	655,175	704,034	704,044	708,703	568,723	700,156	603,422	576,528	555,274
13	Water Body	352,031	352,012	351,993	351,992	351,995	351,994	351,994	322,264	322,282	351,749	351,734	349,816	349,884
14	Swamp Shrub	930,069	931,438	932,806	929,360	949,786	900,908	900,838	906,111	860,813	917,482	969,770	978,818	942,998
15	Dryland Agriculture	14,377	15,368	16,358	16,722	16,803	16,880	16,880	17,184	16,396	17,072	16,377	18,278	21,671
16	Shrub-Mixed Dryland Farm	43,462	49,013	54,563	54,563	65,250	65,379	65,379	65,760	62,139	65,071	65,344	70,692	68,600
17	Rice Field	10,932	10,932	10,932	10,932	10,974	10,974	11,044	11,463	11,459	11,388	11,388	48,795	45,505
18	Fish Pond	-	-	-	-	-	-	-	-	-	-	-	448	80
19	Airport	159	159	159	159	159	159	159	159	159	159	159	175	175
20	Transmigration Area	36,638	41,430	46,221	46,221	46,221	46,221	46,221	46,440	46,440	46,152	45,504	26,526	25,575
21	Swamp	394,375	456,596	518,816	521,051	527,044	527,044	527,034	530,472	529,565	516,113	554,354	532,291	437,538

[1]Land cover area of each region, loss and gain calculation (in spreadsheet files), also our publication (Publication-1 and Publication-2) regarding the first experiment was uploaded to our git repository.

[1]https://github.com/sriletsoin/LC-results

The total area of the regency is 4.851.715 ha and each region area were displayed in Table B.2.

Table B.2 The regency area (Ha).

District	Waan	Tabonji	Kimaam	Ilwayab	Ngguti	Tubang	Okaba
Area (Ha)	644,097	332,619	507,591	233,099	334,982	290,296	183,168

District	Kurik	Animha	Tanah Miring	Semangga	Merauke	Naukenjerai	Sota
Area (Ha)	93,189	138,480	143,275	39,467	152,339	133,555	256,785

District	Elikobel	Muting	Ulilin	Kaptel	Malin	Jagebob
Area (Ha)	147,066	331,280	460,551	225,478	74,853	129,545

Thus, the percentage of two categories of land cover changes in the regency were presented in Figure B.1.

Figure B.1 The percentage of two classes.

APPENDIX C

The workflow in the third experiment, for example trained Network-22 was as follows:

Number of layers: 25
Number of connections: 24
Training setup file: D:\Dissertation work- Sri\Data set\Data set dissertation-experiment-2\AlexNet\params_2023_05_19__14_21_24.mat

Run this script to create the network layers, import training and validation data, and train the network. The network layers are stored in the workspace variable layers. The trained network is stored in the workspace variable net.

1. Load Initial Parameters

Load parameters for network initialization.

```
trainingSetup = load ("D:\Dissertation work- Sri\Data set\Data set dissertation-experiment-2\AlexNet\params_2023_05_19__14_21_24.mat");
```

2. Import Data

Import training and validation data.

```
imdsTrain = imageDatastore("C:\Program Files\MATLAB\Training Data","IncludeSubfolders",true,"LabelSource","foldernames");
[imdsTrain, imdsValidation] = splitEachLabel(imdsTrain,0.7);
```

3. Augmentation Settings

```
imageAugmenter = imageDataAugmenter(...
    "RandRotation",[-90 90],...
    "RandScale",[1 2],...
    "RandXReflection",true);
% Resize the images to match the network input layer.
augimdsTrain = augmentedImageDatastore([227 227 3],imdsTrain,"DataAugmentation",imageAugmenter);
augimdsValidation = augmentedImageDatastore([227 227 3],imdsValidation);
```

4. Set Training Options

Specify options to use when training.

```
%training parameter used

opts = trainingOptions("sgdm",...
    "ExecutionEnvironment","auto",...
    "InitialLearnRate",0.0001,...
    "MaxEpochs",8,...
    "MiniBatchSize",10,...
    "Shuffle","every-epoch",...
    "ValidationFrequency",4,...
    "Plots","training-progress",...
    "ValidationData",augimdsValidation);
```

5. **Create Array of Layers**

```
%network layers
layers = [
    imageInputLayer([227 227 3],"Name","Input","Mean",trainingSetup.Input.Mean)
    convolution2dLayer([11 11],96,"Name","conv1","BiasLearnRateFactor",2,"Stride",[4
4],"Bias",trainingSetup.conv1.Bias,"Weights",trainingSetup.conv1.Weights)
    reluLayer("Name","relu1")
    crossChannelNormalizationLayer(5,"Name","norm1","K",1)
    maxPooling2dLayer([3 3],"Name","pool1","Stride",[2 2])
    groupedConvolution2dLayer([5 5],128,2,"Name","conv2","BiasLearnRateFactor",2,"Padding",[2 2 2
2],"Bias",trainingSetup.conv2.Bias,"Weights",trainingSetup.conv2.Weights)
    reluLayer("Name","relu2")
    crossChannelNormalizationLayer(5,"Name","norm2","K",1)
    maxPooling2dLayer([3 3],"Name","pool2","Stride",[2 2])
    convolution2dLayer([3 3],384,"Name","conv3","BiasLearnRateFactor",2,"Padding",[1 1 1
1],"Bias",trainingSetup.conv3.Bias,"Weights",trainingSetup.conv3.Weights)
    reluLayer("Name","relu3")
    groupedConvolution2dLayer([3 3],192,2,"Name","conv4","BiasLearnRateFactor",2,"Padding",[1 1 1
1],"Bias",trainingSetup.conv4.Bias,"Weights",trainingSetup.conv4.Weights)
    reluLayer("Name","relu4")
    groupedConvolution2dLayer([3 3],128,2,"Name","conv5","BiasLearnRateFactor",2,"Padding",[1 1 1
1],"Bias",trainingSetup.conv5.Bias,"Weights",trainingSetup.conv5.Weights)
    reluLayer("Name","relu5")
    maxPooling2dLayer([3 3],"Name","pool5","Stride",[2 2])

fullyConnectedLayer(4096,"Name","fc6","BiasLearnRateFactor",2,"Bias",trainingSetup.fc6.Bias,"Weights",trainingSet
up.fc6.Weights)
    reluLayer("Name","relu6")
    dropoutLayer(0.5,"Name","drop6")

fullyConnectedLayer(4096,"Name","fc7","BiasLearnRateFactor",2,"Bias",trainingSetup.fc7.Bias,"Weights",trainingSet
up.fc7.Weights)
    reluLayer("Name","relu7")
    dropoutLayer(0.5,"Name","drop7")
    fullyConnectedLayer(4,"Name","fc","BiasLearnRateFactor",10,"WeightLearnRateFactor",10)
    softmaxLayer("Name","prob")
    classificationLayer("Name","classoutput")];
```

Train Network

Train the network using the specified options and training data.

```
[net, traininfo] = trainNetwork(augimdsTrain,layers,opts);
```

Followed by testing process and confusion matrix calculation.

APPENDIX D

The estimation results, confusion matrix and metric evaluation from experiment-3 were presented, as follows:

Table D.1 The prediction result of trained Network-13.

Parameter training setup		No	Test Image	Target13	Predict13	Non-sago	Sago flowers	Sago leaves	Sago trunks
Parameter name	**Value**	1	10-rev	Sago trunks	Sago leaves	0.0002	0.0004	**0.9907**	0.0088
Epoch	8	2	11-rev	Sago trunks	Sago trunks	0.0000	0.0000	0.0001	**0.9999**
Initial Learning rate	0.0001	3	12	Sago flowers	Sago leaves	0.0014	0.2323	**0.7643**	0.0020
Validation freq	4	4	12-rev	Sago flowers	Sago leaves	0.0014	0.1862	**0.8107**	0.0016
Learning rate weight coeff	10	5	14	Sago leaves	Sago leaves	0.0000	0.0001	**0.9999**	0.0000
Learning rate bias coeff	10	6	15	Sago leaves	Sago leaves	0.0048	0.0152	**0.9752**	0.0048
Momentum	0.9	7	15-rev	Sago leaves	Sago leaves	0.0041	0.0143	**0.9776**	0.0040
L2 Regulation	0.0001	8	19-rev	Sago leaves	Sago trunks	0.0000	0.0001	0.0000	**0.9999**
Min Batch size	16	9	20-rev	Sago leaves	Sago trunks	0.0000	0.0000	0.0000	**1.0000**
		10	DJI_0081	Sago leaves	Sago leaves	0.0004	0.0016	**0.9976**	0.0003
		11	DJI_0100	Sago trunks	Sago trunks	0.0241	0.0317	0.2087	**0.7354**
		12	DJI_0101	Sago trunks	Sago trunks	0.0000	0.0000	0.0000	**1.0000**
trainedNetwork_13		13	DJI_0103	Sago trunks	Non-sago	**0.6493**	0.0832	0.1840	0.0834
		14	DJI_0106	Sago flowers	Sago flowers	0.0081	**0.8845**	0.1037	0.0037
Accuracy		15	DJI_0107	Sago flowers	Sago flowers	0.0030	**0.9481**	0.0474	0.0015
validation accuracy=90.15%		16	DJI_0108	Sago flowers	Sago flowers	0.0000	**0.9996**	0.0004	0.0000
elapsed time=19 min 17 sec		17	DJI_0121	Sago flowers	Sago flowers	0.0001	**0.9519**	0.0479	0.0001
		18	DJI_0122	Sago flowers	Sago flowers	0.0007	**0.9195**	0.0792	0.0006
		19	DJI_0123	Sago flowers	Sago flowers	0.0048	**0.9621**	0.0310	0.0021
		20	img1	Sago trunks	Sago trunks	0.0009	0.0013	0.1159	**0.8819**
		21	MAX_0001	Sago leaves	Sago leaves	0.0000	0.0001	**0.9999**	0.0000
		22	MAX_0002	Non-sago	Non-sago	**1.0000**	0.0000	0.0000	0.0000
		23	MAX_0003	Sago leaves	Sago leaves	0.0000	0.0001	**0.9999**	0.0000
		24	MAX_0004	Sago leaves	Sago leaves	0.0000	0.0000	**1.0000**	0.0000
		25	MAX_0006	Sago leaves	Sago leaves	0.0007	0.0025	**0.9962**	0.0006
		26	MAX_0007	Sago leaves	Sago leaves	0.0000	0.0000	**1.0000**	0.0000
		27	MAX_0008	Non-sago	Sago leaves	0.1316	0.2654	**0.5552**	0.0478
		28	MAX_0009	Non-sago	Sago leaves	0.0027	0.0964	**0.8990**	0.0018
		29	MAX_0010	Sago leaves	Sago trunks	0.0040	0.0300	0.0721	**0.8939**
		30	MAX_0011	Sago flowers	Sago leaves	0.0001	0.0004	**0.9993**	0.0002

	31	MAX_0012	Sago leaves	Sago leaves	0.0254	0.0633	**0.7733**	0.1380
	32	MAX_0013	Non-sago	Non-sago	**0.9990**	0.0003	0.0004	0.0003
	33	MAX_0014	Sago leaves	Sago flowers	0.0581	**0.5962**	0.2222	0.1234
	34	MAX_0015	Non-sago	Non-sago	**1.0000**	0.0000	0.0000	0.0000
	35	MAX_0016	Sago leaves	Sago leaves	0.0251	0.0663	**0.6969**	0.2118
	36	MAX_0017	Sago leaves	Sago leaves	0.1044	0.3263	**0.4642**	0.1051
	37	MAX_0018	Non-sago	Non-sago	**0.9984**	0.0004	0.0009	0.0004
	38	MAX_0019	Sago leaves	Sago trunks	0.0018	0.0435	0.0049	**0.9497**
	39	MAX_0020	Sago leaves	Sago trunks	0.0185	0.0595	0.1198	**0.8021**
	40	MAX_0021	Non-sago	Non-sago	**1.0000**	0.0000	0.0000	0.0000
	41	MAX_0022	Sago leaves	Sago leaves	0.1346	0.0592	**0.5517**	0.2545
	42	MAX_0023	Sago leaves	Sago leaves	0.0000	0.0000	**1.0000**	0.0000
	43	MAX_0024	Sago leaves	Sago leaves	0.0026	0.0047	**0.9907**	0.0020
	44	MAX_0025	Sago leaves	Non-sago	**0.9903**	0.0024	0.0033	0.0040
	45	MAX_0026	Non-sago	Sago flowers	0.1247	**0.3659**	0.1957	0.3137
	46	MAX_0027	Non-sago	Sago leaves	0.2383	0.3443	**0.3930**	0.0245
	47	MAX_0028	Sago leaves	Sago leaves	0.0000	0.0002	**0.9997**	0.0000
	48	MAX_0029	Sago leaves	Sago leaves	0.1119	0.1055	**0.4563**	0.3263
	49	MAX_0030	Sago leaves	Sago leaves	0.0000	0.0000	**1.0000**	0.0000
	50	MAX_0031	Non-sago	Sago leaves	0.1241	0.1509	**0.6159**	0.1091
	51	MAX_0032	Sago leaves	Sago leaves	0.0142	0.0148	**0.9576**	0.0133
	52	MAX_0033	Sago leaves	Sago leaves	0.0000	0.0000	**1.0000**	0.0000
	53	MAX_0034	Sago leaves	Sago leaves	0.0000	0.0000	**1.0000**	0.0000
	54	MAX_0035	Sago leaves	Sago leaves	0.0000	0.0000	**1.0000**	0.0000
	55	MAX_0036	Non-sago	Non-sago	**1.0000**	0.0000	0.0000	0.0000
	56	MAX_0037	Sago leaves	Sago leaves	0.0015	0.0028	**0.9952**	0.0005
	57	MAX_0038	Non-sago	Non-sago	**0.9978**	0.0007	0.0010	0.0005
	58	MAX_0039	Non-sago	Non-sago	**0.9985**	0.0005	0.0005	0.0005
	59	MAX_0040	Sago leaves	Sago leaves	0.0004	0.0008	**0.9902**	0.0086
	60	MAX_0041	Sago leaves	Sago leaves	0.0082	0.0114	**0.9546**	0.0258
	61	MAX_0042	Sago leaves	Sago leaves	0.0042	0.0047	**0.9866**	0.0045
	62	MAX_0043	Non-sago	Non-sago	**0.9997**	0.0000	0.0002	0.0000
	63	MAX_0044	Sago leaves	Sago leaves	0.0001	0.0002	**0.9997**	0.0001
	64	MAX_0045	Sago flowers	Sago flowers	0.0000	**1.0000**	0.0000	0.0000
	65	MAX_0046	Sago flowers	Sago flowers	0.0000	**0.9993**	0.0005	0.0002
	66	MAX_0047	Sago flowers	Sago leaves	0.0593	0.1496	**0.7326**	0.0585
	67	MAX_0048	Sago flowers	Sago leaves	0.0089	0.0760	**0.8931**	0.0221
	68	MAX_0468	Sago leaves	Sago leaves	0.0063	0.0134	**0.9748**	0.0055
	69	MAX_0469	Sago leaves	Sago leaves	0.0183	0.0187	**0.9491**	0.0139

	70	MAX_0470	Sago leaves	Sago leaves	0.0002	0.0002	**0.9998**	0.0000
	71	MAX_0471	Sago leaves	Non-sago	**0.9383**	0.0079	0.0491	0.0047
	72	MAX_0536	Sago leaves	Sago leaves	0.0013	0.0144	**0.9818**	0.0024
	73	MAX_0537	Sago leaves	Non-sago	**0.6536**	0.0218	0.3072	0.0174
	74	MAX_0538	Non-sago	Non-sago	**0.6801**	0.0050	0.3108	0.0040
	75	MAX_0539	Sago leaves	Sago trunks	0.0019	0.0034	0.0065	**0.9881**
	76	MAX_0540	Sago leaves	Sago leaves	0.0368	0.0306	**0.9159**	0.0167
	77	MAX_0541	Sago leaves	Sago leaves	0.0000	0.0000	**1.0000**	0.0000
	78	MAX_0542	Sago leaves	Sago leaves	0.3400	0.0684	**0.5419**	0.0498
	79	MAX_0543	Sago leaves	Non-sago	**0.6430**	0.0295	0.2991	0.0283
	80	MAX_0544	Sago leaves	Sago leaves	0.0039	0.0056	**0.9885**	0.0190
	81	MAX_0546	Non-sago	Sago leaves	0.0160	0.1539	**0.8223**	0.0079
	82	MAX_0547	Sago leaves	Sago leaves	0.0030	0.0319	**0.9609**	0.0042
	83	MAX_0549	Sago leaves	Sago leaves	0.0018	0.0035	**0.9930**	0.0018
	84	no	Non-sago	Non-sago	**1.0000**	0.0000	0.0000	0.0000
	85	non	Non-sago	Sago leaves	0.0178	0.0566	**0.9192**	0.0064
	86	nonsa	Non-sago	Sago leaves	0.1173	0.2458	**0.6044**	0.0325
	87	nonsag	Non-sago	Sago leaves	0.0048	0.0625	**0.9311**	0.0016
	88	sf	Sago flowers	Sago leaves	0.0000	0.0005	**0.9945**	0.0001
	89	sf1	Sago flowers	Sago flowers	0.0008	**0.7867**	0.2058	0.0067
	90	sff	Sago flowers	Sago flowers	0.0001	**0.9983**	0.0016	0.0001
	91	sl	Sago leaves	Sago leaves	0.0000	0.0027	**0.9972**	0.0001
	92	sl1	Sago leaves	Sago leaves	0.0037	0.0183	**0.9633**	0.0148
	93	sl2	Sago leaves	Sago leaves	0.0000	0.0000	**1.0000**	0.0000
	94	testnon	Non-sago	Non-sago	**0.9961**	0.0010	0.0021	0.0007
	95	testnons	Non-sago	Non-sago	**0.4411**	0.1047	0.4095	0.0447
	96	testnonss	Non-sago	Non-sago	**1.0000**	0.0000	0.0000	0.0000
	97	testrunk	Sago trunks	Sago trunks	0.0000	0.0000	0.0005	**0.9995**
	98	testsag	Sago leaves	Sago leaves	0.0184	0.0751	**0.8268**	0.0798
	99	testsl	Sago leaves	Sago leaves	0.0004	0.0016	**0.9976**	0.0003
	100	testtr	Sago trunks	Sago trunks	0.0000	0.0000	0.0005	**0.9995**
	101	trunk	Sago trunks	Sago trunks	0.0000	0.0000	0.0000	**1.0000**
	102	trunks	Sago trunks	Sago trunks	0.0000	0.0000	0.0000	**1.0000**
	103	trunkss	Sago trunks	Sago trunks	0.0000	0.0000	0.0000	**1.0000**

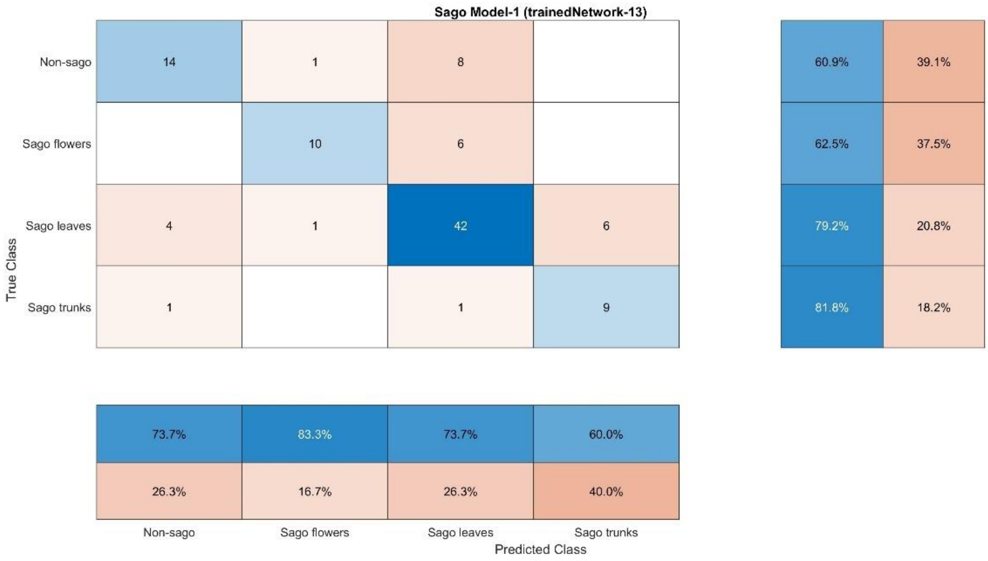

Figure D.1. Confusion matrix of trained Network-13.

Table D.2 The prediction result of trained Network-8.

Parameter training setup		**No**	**Test Image**	**Target8**	**Predict8**	**Non-sago**	**Sago flowers**	**Sago leaves**	**Sago trunks**
Parameter name	**Value**	1	10-rev	Sago trunks	Non-sago	**0.2500**	0.2500	0.2500	0.2500
Epoch	8	2	11-rev	Sago trunks	Non-sago	**0.2500**	0.2500	0.2500	0.2500
Initial Learning rate	0.001	3	12	Sago flowers	Non-sago	**0.2500**	0.2500	0.2500	0.2500
Validation freq	4	4	12-rev	Sago flowers	Non-sago	**0.2500**	0.2500	0.2500	0.2500
Learning rate weight coeff	10	5	14	Sago leaves	Non-sago	**0.2500**	0.2500	0.2500	0.2500
Learning rate bias coeff	10	6	15	Sago leaves	Non-sago	**0.2500**	0.2500	0.2500	0.2500
Momentum	0.9	7	15-rev	Sago leaves	Non-sago	**0.2500**	0.2500	0.2500	0.2500
L2 Regulation	0.001	8	19-rev	Sago leaves	Non-sago	**0.2500**	0.2500	0.2500	0.2500
Min Batch size	64	9	20-rev	Sago leaves	Non-sago	**0.2500**	0.2500	0.2500	0.2500
		10	DJI_0081	Sago leaves	Non-sago	**0.2500**	0.2500	0.2500	0.2500
		11	DJI_0100	Sago trunks	Non-sago	**0.2500**	0.2500	0.2500	0.2500
		12	DJI_0101	Sago trunks	Non-sago	**0.2500**	0.2500	0.2500	0.2500
trainedNetwork_8		13	DJI_0103	Sago trunks	Non-sago	**0.2500**	0.2500	0.2500	0.2500
		14	DJI_0106	Sago flowers	Non-sago	**0.2500**	0.2500	0.2500	0.2500
Accuracy		15	DJI_0107	Sago flowers	Non-sago	**0.2500**	0.2500	0.2500	0.2500
validation accuracy=25%		16	DJI_0108	Sago flowers	Non-sago	**0.2500**	0.2500	0.2500	0.2500
elapsed time= 14 min 28 sec		17	DJI_0121	Sago flowers	Non-sago	**0.2500**	0.2500	0.2500	0.2500
		18	DJI_0122	Sago flowers	Non-sago	**0.2500**	0.2500	0.2500	0.2500
		19	DJI_0123	Sago flowers	Non-sago	**0.2500**	0.2500	0.2500	0.2500

	20	img1	Sago trunks	Non-sago	**0.2500**	0.2500	0.2500	0.2500
	21	MAX_0001	Sago leaves	Non-sago	**0.2500**	0.2500	0.2500	0.2500
	22	MAX_0002	Non-sago	Non-sago	**0.2500**	0.2500	0.2500	0.2500
	23	MAX_0003	Sago leaves	Non-sago	**0.2500**	0.2500	0.2500	0.2500
	24	MAX_0004	Sago leaves	Non-sago	**0.2500**	0.2500	0.2500	0.2500
	25	MAX_0006	Sago leaves	Non-sago	**0.2500**	0.2500	0.2500	0.2500
	26	MAX_0007	Sago leaves	Non-sago	**0.2500**	0.2500	0.2500	0.2500
	27	MAX_0008	Non-sago	Non-sago	**0.2500**	0.2500	0.2500	0.2500
	28	MAX_0009	Non-sago	Non-sago	**0.2500**	0.2500	0.2500	0.2500
	29	MAX_0010	Sago leaves	Non-sago	**0.2500**	0.2500	0.2500	0.2500
	30	MAX_0011	Sago flowers	Non-sago	**0.2500**	0.2500	0.2500	0.2500
	31	MAX_0012	Sago leaves	Non-sago	**0.2500**	0.2500	0.2500	0.2500
	32	MAX_0013	Non-sago	Non-sago	**0.2500**	0.2500	0.2500	0.2500
	33	MAX_0014	Sago leaves	Non-sago	**0.2500**	0.2500	0.2500	0.2500
	34	MAX_0015	Non-sago	Non-sago	**0.2500**	0.2500	0.2500	0.2500
	35	MAX_0016	Sago leaves	Non-sago	**0.2500**	0.2500	0.2500	0.2500
	36	MAX_0017	Sago leaves	Non-sago	**0.2500**	0.2500	0.2500	0.2500
	37	MAX_0018	Non-sago	Non-sago	**0.2500**	0.2500	0.2500	0.2500
	38	MAX_0019	Sago leaves	Non-sago	**0.2500**	0.2500	0.2500	0.2500
	39	MAX_0020	Sago leaves	Non-sago	**0.2500**	0.2500	0.2500	0.2500
	40	MAX_0021	Non-sago	Non-sago	**0.2500**	0.2500	0.2500	0.2500
	41	MAX_0022	Sago leaves	Non-sago	**0.2500**	0.2500	0.2500	0.2500
	42	MAX_0023	Sago leaves	Non-sago	**0.2500**	0.2500	0.2500	0.2500
	43	MAX_0024	Sago leaves	Non-sago	**0.2500**	0.2500	0.2500	0.2500
	44	MAX_0025	Sago leaves	Non-sago	**0.2500**	0.2500	0.2500	0.2500
	45	MAX_0026	Non-sago	Non-sago	**0.2500**	0.2500	0.2500	0.2500
	46	MAX_0027	Non-sago	Non-sago	**0.2500**	0.2500	0.2500	0.2500
	47	MAX_0028	Sago leaves	Non-sago	**0.2500**	0.2500	0.2500	0.2500
	48	MAX_0029	Sago leaves	Non-sago	**0.2500**	0.2500	0.2500	0.2500
	49	MAX_0030	Sago leaves	Non-sago	**0.2500**	0.2500	0.2500	0.2500
	50	MAX_0031	Non-sago	Non-sago	**0.2500**	0.2500	0.2500	0.2500
	51	MAX_0032	Sago leaves	Non-sago	**0.2500**	0.2500	0.2500	0.2500
	52	MAX_0033	Sago leaves	Non-sago	**0.2500**	0.2500	0.2500	0.2500
	53	MAX_0034	Sago leaves	Non-sago	**0.2500**	0.2500	0.2500	0.2500
	54	MAX_0035	Sago leaves	Non-sago	**0.2500**	0.2500	0.2500	0.2500
	55	MAX_0036	Non-sago	Non-sago	**0.2500**	0.2500	0.2500	0.2500
	56	MAX_0037	Sago leaves	Non-sago	**0.2500**	0.2500	0.2500	0.2500
	57	MAX_0038	Non-sago	Non-sago	**0.2500**	0.2500	0.2500	0.2500

	58	MAX_0039	Non-sago	Non-sago	**0.2500**	0.2500	0.2500	0.2500
	59	MAX_0040	Sago leaves	Non-sago	**0.2500**	0.2500	0.2500	0.2500
	60	MAX_0041	Sago leaves	Non-sago	**0.2500**	0.2500	0.2500	0.2500
	61	MAX_0042	Sago leaves	Non-sago	**0.2500**	0.2500	0.2500	0.2500
	62	MAX_0043	Non-sago	Non-sago	**0.2500**	0.2500	0.2500	0.2500
	63	MAX_0044	Sago leaves	Non-sago	**0.2500**	0.2500	0.2500	0.2500
	64	MAX_0045	Sago flowers	Non-sago	**0.2500**	0.2500	0.2500	0.2500
	65	MAX_0046	Sago flowers	Non-sago	**0.2500**	0.2500	0.2500	0.2500
	66	MAX_0047	Sago flowers	Non-sago	**0.2500**	0.2500	0.2500	0.2500
	67	MAX_0048	Sago flowers	Non-sago	**0.2500**	0.2500	0.2500	0.2500
	68	MAX_0468	Sago leaves	Non-sago	**0.2500**	0.2500	0.2500	0.2500
	69	MAX_0469	Sago leaves	Non-sago	**0.2500**	0.2500	0.2500	0.2500
	70	MAX_0470	Sago leaves	Non-sago	**0.2500**	0.2500	0.2500	0.2500
	71	MAX_0471	Sago leaves	Non-sago	**0.2500**	0.2500	0.2500	0.2500
	72	MAX_0536	Sago leaves	Non-sago	**0.2500**	0.2500	0.2500	0.2500
	73	MAX_0537	Sago leaves	Non-sago	**0.2500**	0.2500	0.2500	0.2500
	74	MAX_0538	Non-sago	Non-sago	**0.2500**	0.2500	0.2500	0.2500
	75	MAX_0539	Sago leaves	Non-sago	**0.2500**	0.2500	0.2500	0.2500
	76	MAX_0540	Sago leaves	Non-sago	**0.2500**	0.2500	0.2500	0.2500
	77	MAX_0541	Sago leaves	Non-sago	**0.2500**	0.2500	0.2500	0.2500
	78	MAX_0542	Sago leaves	Non-sago	**0.2500**	0.2500	0.2500	0.2500
	79	MAX_0543	Sago leaves	Non-sago	**0.2500**	0.2500	0.2500	0.2500
	80	MAX_0544	Sago leaves	Non-sago	**0.2500**	0.2500	0.2500	0.2500
	81	MAX_0546	Non-sago	Non-sago	**0.2500**	0.2500	0.2500	0.2500
	82	MAX_0547	Sago leaves	Non-sago	**0.2500**	0.2500	0.2500	0.2500
	83	MAX_0549	Sago leaves	Non-sago	**0.2500**	0.2500	0.2500	0.2500
	84	no	Non-sago	Non-sago	**0.2500**	0.2500	0.2500	0.2500
	85	non	Non-sago	Non-sago	**0.2500**	0.2500	0.2500	0.2500
	86	nonsa	Non-sago	Non-sago	**0.2500**	0.2500	0.2500	0.2500
	87	nonsag	Non-sago	Non-sago	**0.2500**	0.2500	0.2500	0.2500
	88	sf	Sago flowers	Non-sago	**0.2500**	0.2500	0.2500	0.2500
	89	sf1	Sago flowers	Non-sago	**0.2500**	0.2500	0.2500	0.2500
	90	sff	Sago flowers	Non-sago	**0.2500**	0.2500	0.2500	0.2500
	91	sl	Sago leaves	Non-sago	**0.2500**	0.2500	0.2500	0.2500
	92	sl1	Sago leaves	Non-sago	**0.2500**	0.2500	0.2500	0.2500
	93	sl2	Sago leaves	Non-sago	**0.2500**	0.2500	0.2500	0.2500
	94	testnon	Non-sago	Non-sago	**0.2500**	0.2500	0.2500	0.2500
	95	testnons	Non-sago	Non-sago	**0.2500**	0.2500	0.2500	0.2500

	No	Test Image	Target	Predict	Non-sago	Sago flowers	Sago leaves	Sago trunks
	96	testnonss	Non-sago	Non-sago	**0.2500**	0.2500	0.2500	0.2500
	97	testrunk	Sago trunks	Non-sago	**0.2500**	0.2500	0.2500	0.2500
	98	testsag	Sago leaves	Non-sago	**0.2500**	0.2500	0.2500	0.2500
	99	testsl	Sago leaves	Non-sago	**0.2500**	0.2500	0.2500	0.2500
	100	testtr	Sago trunks	Non-sago	**0.2500**	0.2500	0.2500	0.2500
	101	trunk	Sago trunks	Non-sago	**0.2500**	0.2500	0.2500	0.2500
	102	trunks	Sago trunks	Non-sago	**0.2500**	0.2500	0.2500	0.2500
	103	trunkss	Sago trunks	Non-sago	**0.2500**	0.2500	0.2500	0.2500

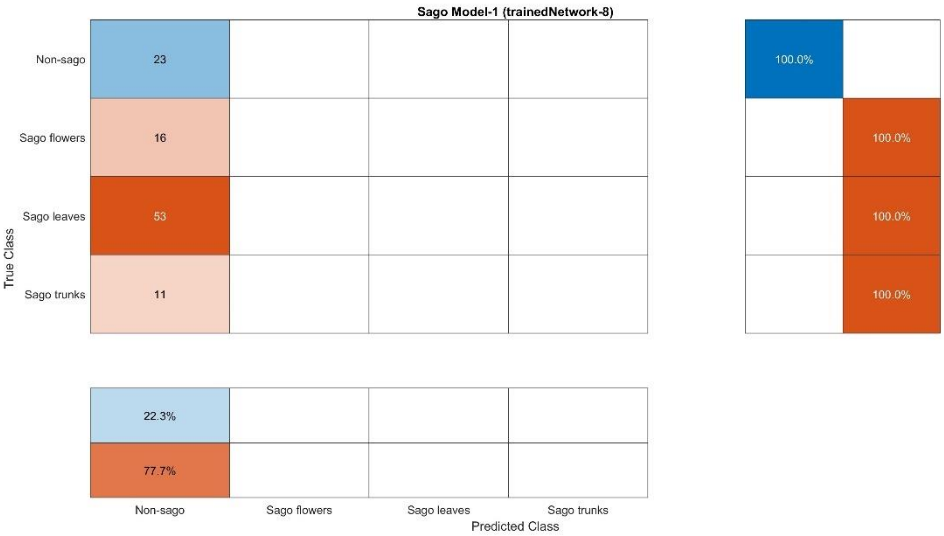

Figure D.2. Confusion matrix of trained Network-8.

Table D.3 The prediction result of trained Network-2.

Parameter Training setup		**No**	**Test Image**	**Target2**	**Predict2**	**Non-sago**	**Sago flowers**	**Sago leaves**	**Sago trunks**
Parameter name	**Value**	1	10-rev	Sago trunks	Sago leaves	0.0011	0.0041	**0.9778**	0.0170
Epoch	10	2	11-rev	Sago trunks	Sago trunks	0.0012	0.0005	0.0003	**0.9979**
Initial Learning rate	0.0001	3	12	Sago flowers	Sago leaves	0.0031	0.1786	**0.8142**	0.0040
Validation freq	4	4	12-rev	Sago flowers	Sago leaves	0.0029	0.1977	**0.7959**	0.0035
Learning rate weight coeff	10	5	14	Sago leaves	Sago leaves	0.0001	0.0040	**0.9957**	0.0002
Learning rate bias coeff	10	6	15	Sago leaves	Sago leaves	0.0039	0.0828	**0.9081**	0.0052
Momentum	0.9	7	15-rev	Sago leaves	Sago leaves	0.0043	0.0944	**0.8966**	0.0047
L2 Regulation	0.0001	8	19-rev	Sago leaves	Sago trunks	0.0001	0.0005	0.0002	**0.9992**
Min Batch size	64	9	20-rev	Sago leaves	sago trunks	0.0000	0.0000	0.0000	**1.0000**
		10	DJI_0081	Sago leaves	Sago leaves	0.0033	0.0134	**0.9804**	0.0029

	11	DJI_0100	Sago trunks	Sago trunks	0.0213	0.0398	0.0216	**0.9173**
epoch 10,	12	DJI_0101	Sago trunks	Sago trunks	0.0000	0.0000	0.0000	**1.0000**
trainedNetwork_2	13	DJI_0103	Sago trunks	Non-sago	**0.6718**	0.0601	0.2131	0.0550
	14	DJI_0106	Sago flowers	Sago flowers	0.0100	**0.8770**	0.1090	0.0040
	15	DJI_0107	Sago flowers	Sago flowers	0.0025	**0.9829**	0.0137	0.0009
Accuracy	16	DJI_0108	Sago flowers	Sago flowers	0.0001	**0.9977**	0.0022	0.0001
validation accuracy=88.64%	17	DJI_0121	Sago flowers	Sago flowers	0.0003	**0.7400**	0.2593	0.0004
elapsed time=8 min 9 sec	18	DJI_0122	Sago flowers	Sago leaves	0.0016	0.1662	**0.8308**	0.0014
	19	DJI_0123	Sago flowers	Sago flowers	0.0340	**0.7050**	0.2541	0.0069
	20	img1	Sago trunks	Sago trunks	0.0002	0.0038	0.0010	**0.9950**
	21	MAX_0001	Sago leaves	Sago leaves	0.0001	0.0006	**0.9993**	0.0001
	22	MAX_0002	Non-sago	Non-sago	**0.9999**	0.0000	0.0000	0.0000
	23	MAX_0003	Sago leaves	Sago leaves	0.0003	0.0016	**0.9980**	0.0001
	24	MAX_0004	Sago leaves	Sago leaves	0.0000	0.0000	**1.0000**	0.0000
	25	MAX_0006	Sago leaves	Sago leaves	0.0097	0.0397	**0.9449**	0.0057
	26	MAX_0007	Sago leaves	Sago leaves	0.0000	0.0001	**0.9990**	0.0000
	27	MAX_0008	Non-sago	Sago leaves	0.1403	0.2455	**0.3333**	0.2809
	28	MAX_0009	Non-sago	Sago leaves	0.0119	0.2160	**0.7647**	0.0075
	29	MAX_0010	Sago leaves	Sago leaves	0.0073	0.0983	**0.8139**	0.0860
	30	MAX_0011	Sago flowers	Sago leaves	0.0004	0.0036	**0.9955**	0.0005
	31	MAX_0012	Sago leaves	Sago leaves	0.0015	0.0033	**0.9912**	0.0040
	32	MAX_0013	Non-sago	Non-sago	**0.9925**	0.0035	0.0022	0.0018
	33	MAX_0014	Sago leaves	Sago leaves	0.0337	0.2701	**0.6259**	0.0703
	34	MAX_0015	Non-sago	Non-sago	**0.9998**	0.0001	0.0001	0.0000
	35	MAX_0016	Sago leaves	Sago leaves	0.0028	0.0154	**0.9759**	0.0059
	36	MAX_0017	Sago leaves	Sago leaves	0.0568	0.1367	**0.7842**	0.0223
	37	MAX_0018	Non-sago	Non-sago	**0.9791**	0.0089	0.0056	0.0064
	38	MAX_0019	Sago leaves	Sago trunks	0.0097	0.0488	0.2531	**0.6884**
	39	MAX_0020	Sago leaves	Sago leaves	0.0092	0.0118	**0.8867**	0.0923
	40	MAX_0021	Non-sago	Non-sago	**1.0000**	0.0000	0.0000	0.0000
	41	MAX_0022	Sago leaves	Sago leaves	0.0397	0.0206	**0.9137**	0.0261
	42	MAX_0023	Sago leaves	Sago leaves	0.0000	0.0001	**0.9999**	0.0000
	43	MAX_0024	Sago leaves	Sago leaves	0.0019	0.0055	**0.9915**	0.0011
	44	MAX_0025	Sago leaves	Non-sago	**0.9926**	0.0024	0.0019	0.0032
	45	MAX_0026	Non-sago	Sago trunks	0.2503	0.2237	0.2239	**0.3021**
	46	MAX_0027	Non-sago	Non-sago	**0.6025**	0.2339	0.1403	0.0234

	47	MAX_0028	Sago leaves	Sago leaves	0.0001	0.0018	**0.9981**	0.0001
	48	MAX_0029	Sago leaves	Sago leaves	0.0276	0.0366	**0.9098**	0.0260
	49	MAX_0030	Sago leaves	Sago leaves	0.0001	0.0002	**0.9983**	0.0015
	50	MAX_0031	Non-sago	Non-sago	**0.6998**	0.0834	0.1007	0.1160
	51	MAX_0032	Sago leaves	Sago leaves	0.0268	0.0215	**0.9373**	0.0144
	52	MAX_0033	Sago leaves	Sago leaves	0.0000	0.0000	**1.0000**	0.0000
	53	MAX_0034	Sago leaves	Sago leaves	0.0000	0.0000	**1.0000**	0.0000
	54	MAX_0035	Sago leaves	Sago leaves	0.0000	0.0000	**1.0000**	0.0000
	55	MAX_0036	Non-sago	Non-sago	**0.9995**	0.0003	0.0001	0.0002
	56	MAX_0037	Sago leaves	Sago leaves	0.0042	0.0048	**0.9903**	0.0007
	57	MAX_0038	Non-sago	Non-sago	**0.9974**	0.0012	0.0080	0.0006
	58	MAX_0039	Non-sago	Non-sago	**0.9953**	0.0025	0.0011	0.0011
	59	MAX_0040	Sago leaves	Sago leaves	0.0001	0.0004	**0.9994**	0.0001
	60	MAX_0041	Sago leaves	Sago leaves	0.0262	0.0399	**0.9075**	0.0264
	61	MAX_0042	Sago leaves	Sago leaves	0.0097	0.0070	**0.9763**	0.0070
	62	MAX_0043	Non-sago	Non-sago	**0.9998**	0.0001	0.0001	0.0000
	63	MAX_0044	Sago leaves	Sago leaves	0.0001	0.0008	**0.9987**	0.0004
	64	MAX_0045	Sago flowers	Sago flowers	0.0003	**0.9976**	0.0007	0.0014
	65	MAX_0046	Sago flowers	Sago flowers	0.0219	**0.7325**	0.1331	0.1125
	66	MAX_0047	Sago flowers	Sago leaves	0.2652	0.1151	**0.5286**	0.0911
	67	MAX_0048	Sago flowers	Sago leaves	0.0321	0.0805	**0.8307**	0.0567
	68	MAX_0468	Sago leaves	Sago leaves	0.0256	0.0104	**0.9590**	0.0051
	69	MAX_0469	Sago leaves	Sago leaves	0.1199	0.0480	**0.8088**	0.0234
	70	MAX_0470	Sago leaves	Sago leaves	0.0002	0.0022	**0.9973**	0.0003
	71	MAX_0471	Sago leaves	Non-sago	**0.9946**	0.0019	0.0024	0.0011
	72	MAX_0536	Sago leaves	Sago flowers	0.0143	**0.6940**	0.2721	0.0195
	73	MAX_0537	Sago leaves	Non-sago	**0.9517**	0.0111	0.0326	0.0046
	74	MAX_0538	Non-sago	Non-sago	**0.9780**	0.0066	0.0114	0.0041
	75	MAX_0539	Sago leaves	Sago trunks	0.0012	0.0033	0.0110	**0.9845**
	76	MAX_0540	Sago leaves	Sago leaves	0.1444	0.1691	**0.6559**	0.0306
	77	MAX_0541	Sago leaves	Sago leaves	0.0003	0.0016	**0.9964**	0.0017
	78	MAX_0542	Sago leaves	Non-sago	**0.8184**	0.0565	0.1070	0.0182
	79	MAX_0543	Sago leaves	Non-sago	**0.9183**	0.0105	0.0698	0.0060
	80	MAX_0544	Sago leaves	Sago leaves	0.0064	0.0147	**0.9768**	0.0021
	81	MAX_0546	Non-sago	Sago leaves	0.0217	0.0895	**0.8813**	0.0075
	82	MAX_0547	Sago leaves	Sago leaves	0.0019	0.0347	**0.9619**	0.0015

	83	MAX_0549	Sago leaves	Sago leaves	0.0026	0.0140	**0.9812**	0.0022
	84	no	Non-sago	Non-sago	**1.0000**	0.0000	0.0000	0.0000
	85	non	Non-sago	Sago leaves	0.3627	0.2175	**0.3670**	0.0528
	86	nonsa	Non-sago	Sago leaves	0.2046	0.2751	**0.4636**	0.0568
	87	nonsag	Non-sago	Sago leaves	0.2435	0.1581	**0.5718**	0.0267
	88	sf	Sago flowers	Sago leaves	0.0005	0.0088	**0.9900**	0.0007
	89	sf1	Sago flowers	Sago flowers	0.0010	**0.9174**	0.0690	0.0126
	90	sff	Sago flowers	Sago flowers	0.0006	**0.9952**	0.0036	0.0005
	91	sl	Sago leaves	Sago leaves	0.0013	0.4839	**0.5097**	0.0050
	92	sl1	Sago leaves	Sago leaves	0.0075	0.0740	**0.8719**	0.0467
	93	sl2	Sago leaves	Sago leaves	0.0000	0.0054	**0.9945**	0.0001
	94	testnon	Non-sago	Non-sago	**0.9913**	0.0032	0.0035	0.0020
	95	testnons	Non-sago	Non-sago	**0.9002**	0.0295	0.0525	0.0178
	96	testnonss	Non-sago	Non-sago	**1.0000**	0.0000	0.0000	0.0000
	97	testrunk	Sago trunks	Sago trunks	0.0000	0.0000	0.0000	**0.9999**
	98	testsag	Sago leaves	Sago leaves	0.0131	0.1064	**0.8019**	0.0786
	99	testsl	Sago leaves	Sago leaves	0.0034	0.0134	**0.9804**	0.0029
	100	testtr	Sago trunks	Sago trunks	0.0000	0.0003	0.0004	**0.9993**
	101	trunk	Sago trunks	Sago trunks	0.0000	0.0000	0.0000	**1.0000**
	102	trunks	Sago trunks	Sago trunks	0.0000	0.0000	0.0000	**1.0000**
	103	trunkss	Sago trunks	Sago trunks	0.0000	0.0000	0.0000	**1.0000**

Table D.4. The prediction result of trained Network-10.

Parameter training setup		**No**	**Test Image**	**Target10**	**Predict10**	**Non-sago**	**Sago flowers**	**Sago leaves**	**Sago trunks**
Parameter name	**Value**	1	10-rev	Sago trunks	Sago trunks	0.0271	0.0330	0.0440	**0.8599**
Epoch	10	2	11-rev	Sago trunks	Sago trunks	0.1121	0.0259	0.0061	**0.8559**
Initial Learning rate	0.001	3	12	Sago flowers	Sago flowers	0.0153	**0.8348**	0.1261	0.0238
Validation freq	4	4	12-rev	Sago flowers	Sago flowers	0.0097	**0.9079**	0.0693	0.0130
Learning rate weight coeff	10	5	14	Sago leaves	Sago leaves	0.1196	0.1836	**0.5709**	0.1259
Learning rate bias coeff	10	6	15	Sago leaves	Sago leaves	0.0968	0.3549	**0.4370**	0.1113
Momentum	0.9	7	15-rev	Sago leaves	Sago flowers	0.1012	**0.4018**	0.3785	0.1185
L2 Regulation	0.001	8	19-rev	Sago leaves	Sago trunks	0.0000	0.0005	0.0000	**0.9995**
Min Batch size	64	9	20-rev	Sago leaves	Sago trunks	0.0000	0.0000	0.0000	**1.0000**
		10	DJI_0081	Sago leaves	Sago leaves	0.0268	0.3354	**0.9108**	0.0270
Accuracy		11	DJI_0100	Sago trunks	Sago trunks	0.0001	0.0001	0.0001	**0.9997**
validation accuracy=84.85%		12	DJI_0101	Sago trunks	Sago trunks	0.0000	0.0000	0.0000	**1.0000**

elapsed time=4 min 44 sec	13	DJI_0103	Sago trunks	Non-sago	**0.6892**	0.1877	0.0172	0.1059
	14	DJI_0106	Sago flowers	Sago flowers	0.0937	**0.8789**	0.0186	0.0088
trainedNetwork_10	15	DJI_0107	Sago flowers	Sago flowers	0.0141	**0.9806**	0.0032	0.0020
	16	DJI_0108	Sago flowers	Sago flowers	0.0011	**0.9971**	0.0007	0.0011
	17	DJI_0121	Sago flowers	Sago flowers	0.0128	**0.9150**	0.0593	0.0128
	18	DJI_0122	Sago flowers	Sago leaves	0.0646	0.1296	**0.7447**	0.0611
	19	DJI_0123	Sago flowers	Sago leaves	0.0308	0.1233	**0.8253**	0.0206
	20	img1	Sago trunks	Sago trunks	0.0000	0.0001	0.0000	**0.9998**
	21	MAX_0001	Sago leaves	Sago leaves	0.0059	0.0063	**0.9815**	0.0062
	22	MAX_0002	Non-sago	Non-sago	**1.0000**	0.0000	0.0000	0.0000
	23	MAX_0003	Sago leaves	Sago leaves	0.0004	0.0002	**0.9992**	0.0002
	24	MAX_0004	Sago leaves	Sago leaves	0.0047	0.0072	**0.9835**	0.0046
	25	MAX_0006	Sago leaves	Sago leaves	0.0332	0.0598	**0.8864**	0.0207
	26	MAX_0007	Sago leaves	Sago leaves	0.0544	0.0675	**0.8206**	0.0575
	27	MAX_0008	Non-sago	Sago trunks	0.0027	0.0291	0.0091	**0.9591**
	28	MAX_0009	Non-sago	Sago leaves	0.0431	0.0628	**0.8617**	0.0325
	29	MAX_0010	Sago leaves	Sago trunks	0.0045	0.0138	0.0045	**0.9772**
	30	MAX_0011	Sago flowers	Sago flowers	0.0360	**0.6102**	0.3040	0.0498
	31	MAX_0012	Sago leaves	Sago trunks	0.0000	0.0000	0.0000	**1.0000**
	32	MAX_0013	Non-sago	Non-sago	**1.0000**	0.0000	0.0000	0.0000
	33	MAX_0014	Sago leaves	Sago trunks	0.0304	0.2253	0.0320	**0.7123**
	34	MAX_0015	Non-sago	Non-sago	**1.0000**	0.0000	0.0000	0.0000
	35	MAX_0016	Sago leaves	Sago trunks	0.0796	0.2804	0.0879	**0.5522**
	36	MAX_0017	Sago leaves	Sago flowers	0.0636	**0.7935**	0.0628	0.0802
	37	MAX_0018	Non-sago	Non-sago	**0.9997**	0.0000	0.0003	0.0000
	38	MAX_0019	Sago leaves	Sago trunks	0.0000	0.0000	0.0000	**1.0000**
	39	MAX_0020	Sago leaves	Sago trunks	0.0000	0.0000	0.0000	**1.0000**
	40	MAX_0021	Non-sago	Non-sago	**1.0000**	0.0000	0.0000	0.0000
	41	MAX_0022	Sago leaves	Sago trunks	0.0003	0.0009	0.0003	**0.9985**
	42	MAX_0023	Sago leaves	Sago leaves	0.0761	0.0946	**0.7532**	0.0761
	43	MAX_0024	Sago leaves	Sago leaves	0.0197	0.0302	**0.9335**	0.0166
	44	MAX_0025	Sago leaves	Sago trunks	0.0667	0.0161	0.0135	**0.9036**
	45	MAX_0026	Non-sago	Sago trunks	0.0746	0.0733	0.1390	**0.7131**
	46	MAX_0027	Non-sago	Non-sago	**0.9945**	0.0000	0.0054	0.0000
	47	MAX_0028	Sago leaves	Sago leaves	0.0426	0.0751	**0.8397**	0.0426
	48	MAX_0029	Sago leaves	Sago trunks	0.0330	0.0891	0.0334	**0.8444**
	49	MAX_0030	Sago leaves	Sago leaves	0.1113	0.1199	**0.4472**	0.3216

	50	MAX_0031	Non-sago	Sago leaves	0.2066	0.0127	**0.7681**	0.0127
	51	MAX_0032	Sago leaves	Sago leaves	0.0666	0.0246	**0.8842**	0.0246
	52	MAX_0033	Sago leaves	Sago leaves	0.1500	0.2499	**0.4373**	0.1629
	53	MAX_0034	Sago leaves	Sago leaves	0.0710	0.0711	**0.7793**	0.0787
	54	MAX_0035	Sago leaves	Sago leaves	0.0622	0.0635	**0.7253**	0.1489
	55	MAX_0036	Non-sago	Non-sago	**1.0000**	0.0000	0.0000	0.0000
	56	MAX_0037	Sago leaves	Sago leaves	0.0961	0.0164	**0.8719**	0.0156
	57	MAX_0038	Non-sago	Non-sago	**1.0000**	0.0000	0.0000	0.0000
	58	MAX_0039	Non-sago	Non-sago	**1.0000**	0.0000	0.0000	0.0000
	59	MAX_0040	Sago leaves	Sago trunks	0.0709	0.0709	0.4061	**0.4520**
	60	MAX_0041	Sago leaves	Sago leaves	0.0479	0.0439	**0.6896**	0.2186
	61	MAX_0042	Sago leaves	Sago leaves	0.1774	0.0290	**0.7577**	0.0360
	62	MAX_0043	Non-sago	Non-sago	**1.0000**	0.0000	0.0000	0.0000
	63	MAX_0044	Sago leaves	Sago leaves	0.0230	0.0259	**0.9198**	0.0313
	64	MAX_0045	Sago flowers	Sago trunks	0.0004	0.0024	0.0005	**0.9968**
	65	MAX_0046	Sago flowers	Sago trunks	0.0001	0.0003	0.0001	**0.9995**
	66	MAX_0047	Sago flowers	Sago leaves	0.0974	0.0999	**0.7252**	0.0775
	67	MAX_0048	Sago flowers	Sago leaves	0.1160	0.1303	**0.4533**	0.3004
	68	MAX_0468	Sago leaves	Sago leaves	0.0009	0.0000	**0.9990**	0.0000
	69	MAX_0469	Sago leaves	Sago leaves	0.0070	0.0000	**0.9930**	0.0000
	70	MAX_0470	Sago leaves	Sago leaves	0.0002	0.0002	**0.9994**	0.0002
	71	MAX_0471	Sago leaves	Non-sago	**1.0000**	0.0000	0.0000	0.0000
	72	MAX_0536	Sago leaves	Sago flowers	0.0301	**0.8898**	0.0545	0.0257
	73	MAX_0537	Sago leaves	Non-sago	**0.9999**	0.0000	0.0001	0.0000
	74	MAX_0538	Non-sago	Non-sago	**0.9986**	0.0001	0.0013	0.0001
	75	MAX_0539	Sago leaves	Sago trunks	0.0004	0.0117	0.0004	**0.9874**
	76	MAX_0540	Sago leaves	Non-sago	**0.9796**	0.0036	0.0146	0.0022
	77	MAX_0541	Sago leaves	Sago flowers	0.0804	**0.4141**	0.1772	0.3283
	78	MAX_0542	Sago leaves	Non-sago	**0.9999**	0.0000	0.0001	0.0000
	79	MAX_0543	Sago leaves	Non-sago	**1.0000**	0.0000	0.0000	0.0000
	80	MAX_0544	Sago leaves	Sago leaves	0.1275	0.0734	**0.7428**	0.0563
	81	MAX_0546	Non-sago	Non-sago	**0.9657**	0.0319	0.0010	0.0013
	82	MAX_0547	Sago leaves	Sago leaves	0.1010	0.3478	**0.3543**	0.1969
	83	MAX_0549	Sago leaves	Sago leaves	0.0433	0.0339	**0.8907**	0.0321
	84	no	Non-sago	Non-sago	**1.0000**	0.0000	0.0000	0.0000
	85	non	Non-sago	Sago leaves	0.0002	0.0002	**0.9994**	0.0002
	86	nonsa	Non-sago	Non-sago	**0.7722**	0.0875	0.1045	0.0359

	87	nonsag	Non-sago	Sago leaves	0.0787	0.0163	**0.8892**	0.0159
	88	sf	Sago flowers	Sago leaves	0.0424	0.1909	**0.6900**	0.0767
	89	sf1	Sago flowers	Sago flowers	0.0220	**0.9097**	0.0462	0.0220
	90	sff	Sago flowers	Sago flowers	0.0468	**0.8955**	0.0321	0.0257
	91	sl	Sago leaves	Sago leaves	0.1624	0.1869	**0.4877**	0.1630
	92	sl1	Sago leaves	Sago flowers	0.0965	**0.5363**	0.2526	0.1146
	93	sl2	Sago leaves	Sago leaves	0.0015	0.0015	**0.9958**	0.0012
	94	testnon	Non-sago	Non-sago	**1.0000**	0.0000	0.0000	0.0000
	95	testnons	Non-sago	Non-sago	**0.5901**	0.0058	0.3990	0.0050
	96	testnonss	Non-sago	Non-sago	**1.0000**	0.0000	0.0000	0.0000
	97	testrunk	Sago trunks	Sago trunks	0.0000	0.0000	0.0000	**1.0000**
	98	testsag	Sago leaves	Sago leaves	0.1065	0.2972	**0.4469**	0.1494
	99	testsl	Sago leaves	Sago leaves	0.0268	0.0354	**0.9108**	0.0270
	100	testtr	Sago trunks	Sago trunks	0.0021	0.0841	0.0021	**0.9118**
	101	trunk	Sago trunks	Sago trunks	0.0000	0.0000	0.0000	**1.0000**
	102	trunks	Sago trunks	Sago trunks	0.0000	0.0000	0.0000	**1.0000**
	103	trunkss	Sago trunks	Sago trunks	0.0000	0.0000	0.0000	**1.0000**

Table D.5. The prediction result of trained Network-11.

Parameter training setup		**No**	**Test Image**	**Target11**	**Predict11**	**Non-sago**	**Sago flowers**	**Sago leaves**	**Sago trunks**
Parameter name	**Value**	1	10-rev	Sago trunks	Sago trunks	0.0573	0.0573	0.0573	**0.8281**
Epoch	15	2	11-rev	Sago trunks	Sago trunks	0.0000	0.0000	0.0000	**1.0000**
Initial Learning rate	0.001	3	12	Sago flowers	Sago flowers	0.0011	**0.9966**	0.0011	0.0011
Validation freq	4	4	12-rev	Sago flowers	Sago flowers	0.0005	**0.9984**	0.0005	0.0005
Learning rate weight coeff	10	5	14	Sago leaves	Sago flowers	0.2498	**0.2507**	0.2498	0.2498
Learning rate bias coeff	10	6	15	Sago leaves	Non-sago	**0.2500**	0.2500	0.2500	0.2500
Momentum	0.9	7	15-rev	Sago leaves	Non-sago	**0.2500**	0.2500	0.2500	0.2500
L2 Regulation	0.001	8	19-rev	Sago leaves	Sago trunks	0.0000	0.0000	0.0000	**1.0000**
Min Batch size	32	9	20-rev	Sago leaves	Sago trunks	0.0000	0.0000	0.0000	**1.0000**
		10	DJI_0081	Sago leaves	Non-sago	**0.2500**	0.2500	0.2500	0.2500
		11	DJI_0100	Sago trunks	Sago trunks	0.0003	0.0003	0.0003	**0.9990**
validation accurcy=72.83%		12	DJI_0101	Sago trunks	Sago trunks	0.0000	0.0000	0.0000	**1.0000**
elapsed time= 12 mins 17 ssec		13	DJI_0103	Sago trunks	Sago trunks	0.3218	0.1592	0.1740	**0.3451**
		14	DJI_0106	Sago flowers	Sago flowers	0.0479	**0.8623**	0.0449	0.0449
trainedNetwork_11		15	DJI_0107	Sago flowers	Sago flowers	0.0050	**0.9855**	0.0048	0.0048

	16	DJI_0108	Sago flowers	Sago flowers	0.0011	**0.9967**	0.0011	0.0011
	17	DJI_0121	Sago flowers	Sago flowers	0.0000	**1.0000**	0.0000	0.0000
	18	DJI_0122	Sago flowers	Sago flowers	0.0002	**0.9994**	0.0002	0.0002
	19	DJI_0123	Sago flowers	Sago flowers	0.0043	**0.9876**	0.0041	0.0041
	20	img1	Sago trunks	Sago trunks	0.0000	0.0000	0.0000	**1.0000**
	21	MAX_0001	Sago leaves	Non-sago	**0.2500**	0.2500	0.2500	0.2500
	22	MAX_0002	Non-sago	Non-sago	**1.0000**	0.0000	0.0000	0.0000
	23	MAX_0003	Sago leaves	Non-sago	**0.2500**	0.2500	0.2500	0.2500
	24	MAX_0004	Sago leaves	Non-sago	**0.2500**	0.2500	0.2500	0.2500
	25	MAX_0006	Sago leaves	Non-sago	**0.2606**	0.2465	0.2465	0.2465
	26	MAX_0007	Sago leaves	Non-sago	**0.2500**	0.2500	0.2500	0.2500
	27	MAX_0008	Non-sago	Sago flowers	0.0011	**0.9956**	0.0010	0.0023
	28	MAX_0009	Non-sago	Sago flowers	0.2478	**0.2567**	0.2478	0.2478
	29	MAX_0010	Sago leaves	Sago trunks	0.0119	0.0119	0.0119	**0.9643**
	30	MAX_0011	Sago flowers	Sago trunks	0.2495	0.2495	0.2495	**0.2516**
	31	MAX_0012	Sago leaves	Sago trunks	0.1158	0.1158	0.1158	**0.6526**
	32	MAX_0013	Non-sago	Non-sago	**1.0000**	0.0000	0.0000	0.0000
	33	MAX_0014	Sago leaves	Sago trunks	0.1394	0.1394	0.1394	**0.5818**
	34	MAX_0015	Non-sago	Non-sago	**0.9993**	0.0002	0.0002	0.0002
	35	MAX_0016	Sago leaves	Sago trunks	0.2400	0.2400	0.2400	**0.2800**
	36	MAX_0017	Sago leaves	Non-sago	**0.2507**	0.2498	0.2498	0.2498
	37	MAX_0018	Non-sago	Non-sago	**0.9900**	0.0033	0.0033	0.0033
	38	MAX_0019	Sago leaves	Sago trunks	0.0475	0.0475	0.0475	**0.8750**
	39	MAX_0020	Sago leaves	Sago trunks	0.1088	0.1088	0.1088	**0.6735**
	40	MAX_0021	Non-sago	Non-sago	**0.9995**	0.0002	0.0002	0.0002
	41	MAX_0022	Sago leaves	Sago trunks	0.1166	0.0950	0.0950	**0.6934**
	42	MAX_0023	Sago leaves	Non-sago	**0.2500**	0.2500	0.2500	0.2500
	43	MAX_0024	Sago leaves	Non-sago	**0.2756**	0.2415	0.2415	0.2415
	44	MAX_0025	Sago leaves	Sago trunks	0.1381	0.0112	0.0112	**0.8394**
	45	MAX_0026	Non-sago	Sago trunks	0.0321	0.0228	0.0228	**0.9224**
	46	MAX_0027	Non-sago	Non-sago	**0.2969**	0.2344	0.2344	0.2344
	47	MAX_0028	Sago leaves	Non-sago	**0.2500**	0.2500	0.2500	0.2500
	48	MAX_0029	Sago leaves	Sago trunks	0.2445	0.2371	0.2371	**0.2814**
	49	MAX_0030	Sago leaves	Sago trunks	0.2080	0.2080	0.2080	**0.3760**
	50	MAX_0031	Non-sago	Non-sago	**0.9541**	0.0153	0.0153	0.0153
	51	MAX_0032	Sago leaves	Sago trunks	0.2582	0.2381	0.2381	**0.2657**
	52	MAX_0033	Sago leaves	Sago trunks	0.2206	0.2206	0.2206	**0.3381**
	53	MAX_0034	Sago leaves	Non-sago	**0.2500**	0.2500	0.2500	0.2500
	54	MAX_0035	Sago leaves	Non-sago	**0.2500**	0.2500	0.2500	0.2500

	55	MAX_0036	Non-sago	Non-sago	**1.0000**	0.0000	0.0000	0.0000
	56	MAX_0037	Sago leaves	Non-sago	**0.3130**	0.2290	0.2290	0.2290
	57	MAX_0038	Non-sago	Non-sago	**1.0000**	0.0000	0.0000	0.0000
	58	MAX_0039	Non-sago	Non-sago	**0.9937**	0.0021	0.0021	0.0021
	59	MAX_0040	Sago leaves	Sago trunks	0.2001	0.2001	0.2001	**0.3998**
	60	MAX_0041	Sago leaves	Sago trunks	0.2340	0.2308	0.2308	**0.3045**
	61	MAX_0042	Sago leaves	Non-sago	**0.3778**	0.2074	0.2074	0.2074
	62	MAX_0043	Non-sago	Non-sago	**1.0000**	0.0000	0.0000	0.0000
	63	MAX_0044	Sago leaves	Non-sago	**0.2500**	0.2500	0.2500	0.2500
	64	MAX_0045	Sago flowers	Sago flowers	0.0001	**0.9994**	0.0001	0.0005
	65	MAX_0046	Sago flowers	Sago flowers	0.0012	**0.9835**	0.0012	0.0142
	66	MAX_0047	Sago flowers	Non-sago	**0.4129**	0.1969	0.1825	0.2077
	67	MAX_0048	Sago flowers	Non-sago	**0.3195**	0.2272	0.2099	0.2435
	68	MAX_0468	Sago leaves	Non-sago	**0.2500**	0.2500	0.2500	0.2500
	69	MAX_0469	Sago leaves	Non-sago	**0.2500**	0.2500	0.2500	0.2500
	70	MAX_0470	Sago leaves	Sago trunks	0.2468	0.2468	0.2468	**0.2595**
	71	MAX_0471	Sago leaves	Non-sago	**0.9930**	0.0023	0.0024	0.0023
	72	MAX_0536	Sago leaves	Non-sago	**0.3015**	0.2413	0.2282	0.2289
	73	MAX_0537	Sago leaves	Non-sago	**0.7756**	0.0748	0.0748	0.0748
	74	MAX_0538	Non-sago	Non-sago	**0.9999**	0.0000	0.0000	0.0000
	75	MAX_0539	Sago leaves	Sago trunks	0.0000	0.0000	0.0000	**1.0000**
	76	MAX_0540	Sago leaves	Non-sago	**0.4744**	0.1752	0.1752	0.1752
	77	MAX_0541	Sago leaves	Sago trunks	0.1840	0.1840	0.1840	**0.4481**
	78	MAX_0542	Sago leaves	Non-sago	**0.5290**	0.1462	0.1462	0.1786
	79	MAX_0543	Sago leaves	Non-sago	**0.8921**	0.0360	0.0360	0.0360
	80	MAX_0544	Sago leaves	Non-sago	**0.4830**	0.1723	0.1723	0.1723
	81	MAX_0546	Non-sago	Non-sago	**0.9058**	0.0311	0.0311	0.0320
	82	MAX_0547	Sago leaves	Sago trunks	0.2580	0.2267	0.2265	**0.2888**
	83	MAX_0549	Sago leaves	Non-sago	**0.2841**	0.2386	0.2386	0.2386
	84	no	Non-sago	Non-sago	**1.0000**	0.0000	0.0000	0.0000
	85	non	Non-sago	Non-sago	**0.2500**	0.2500	0.2500	0.2500
	86	nonsa	Non-sago	Sago flowers	0.0754	**0.9016**	0.0115	0.0115
	87	nonsag	Non-sago	Non-sago	**0.3587**	0.2138	0.2138	0.2138
	88	sf	Sago flowers	Non-sago	**0.2530**	0.2489	0.2489	0.2491
	89	sf1	Sago flowers	Non-sago	**0.2500**	0.2500	0.2500	0.2500
	90	sff	Sago flowers	Sago flowers	0.2563	**0.4569**	0.1434	0.1434
	91	sl	Sago leaves	Non-sago	**0.2500**	0.2500	0.2500	0.2500
	92	sl1	Sago leaves	Non-sago	**0.2500**	0.2500	0.2500	0.2500
	93	sl2	Sago leaves	Non-sago	**0.2500**	0.2500	0.2500	0.2500
	94	testnon	Non-sago	Non-sago	**1.0000**	0.0000	0.0000	0.0000

	95	testnons	Non-sago	Non-sago	**0.8132**	0.0623	0.0623	0.0623
	96	testnonss	Non-sago	Non-sago	**0.9999**	0.0000	0.0000	0.0000
	97	testrunk	Sago trunks	Sago trunks	0.0000	0.0000	0.0000	**1.0000**
	98	testsag	Sago leaves	Sago trunks	0.2492	0.2472	0.2472	**0.2565**
	99	testsl	Sago leaves	Non-sago	**0.2500**	0.2500	0.2500	0.2500
	100	testtr	Sago trunks	Sago trunks	0.0001	0.0001	0.0001	**0.9998**
	101	trunk	Sago trunks	Sago trunks	0.0000	0.0000	0.0000	**1.0000**
	102	trunks	Sago trunks	Sago trunks	0.0000	0.0000	0.0000	**1.0000**
	103	trunkss	Sago trunks	Sago trunks	0.0000	0.0000	0.0000	**1.0000**

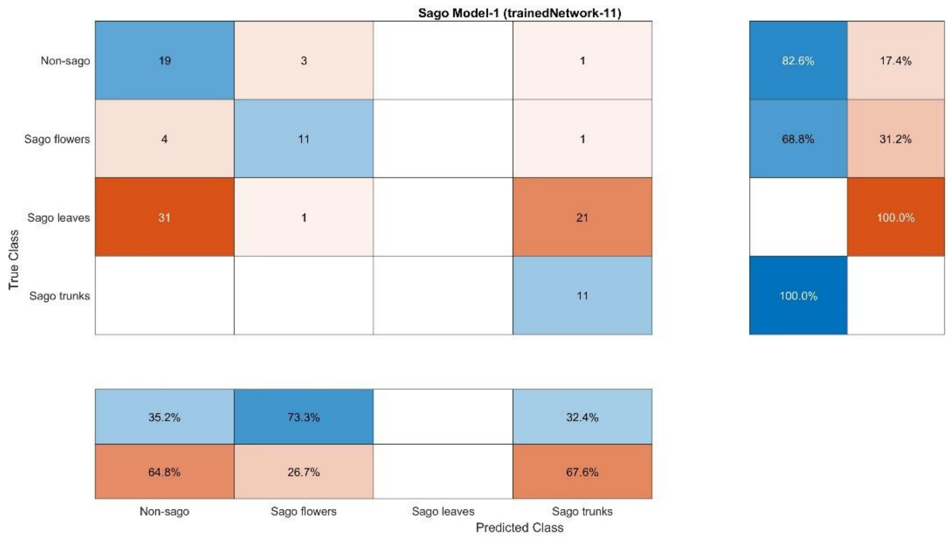

Figure D.3. Confusion matrix of trained Network-11.

Table D.6. The prediction result of trained Network-15.

Parameter training setup		**No**	**Test Image**	**Target15**	**Predict15**	**Non-sago**	**Sago flowers**	**Sago leaves**	**Sago trunks**
Parameter name	**Value**	1	10-rev	Sago trunks	Sago leaves	0.0004	0.0004	**0.9960**	0.0032
Epoch	10	2	11-rev	Sago trunks	Sago trunks	0.0047	0.0002	0.0008	**0.9943**
Initial Learning rate	0.0001	3	12	Sago flowers	Sago leaves	0.0015	0.0292	**0.9654**	0.0039
Validation freq	4	4	12-rev	Sago flowers	Sago leaves	0.0016	0.0358	**0.9596**	0.0030
Learning rate weight coeff	10	5	14	Sago leaves	Sago leaves	0.0006	0.0006	**0.9982**	0.0006
Learning rate bias coeff	10	6	15	Sago leaves	Sago leaves	0.0002	0.0002	**0.9994**	0.0002
Momentum	0.9	7	15-rev	Sago leaves	Sago leaves	0.0002	0.0002	**0.9995**	0.0002
L2 Regulation	0.0001	8	19-rev	Sago leaves	Sago trunks	0.0000	0.0000	0.0000	**1.0000**
Min Batch size	10	9	20-rev	Sago leaves	Sago trunks	0.0000	0.0000	0.0000	**1.0000**

	10	DJI_0081	Sago leaves	Sago leaves	0.0002	0.0003	**0.9993**	0.0002
	11	DJI_0100	Sago trunks	Sago trunks	0.0014	0.0011	0.0020	**0.9956**
trainedNetwork_15	12	DJI_0101	Sago trunks	Sago trunks	0.0000	0.0000	0.0000	**1.0000**
	13	DJI_0103	Sago trunks	Non-sago	**0.9660**	0.0069	0.0080	0.0191
Accuracy	14	DJI_0106	Sago flowers	Sago flowers	0.0321	**0.6643**	0.2886	0.0151
validation accuracy=91.67%	15	DJI_0107	Sago flowers	Sago flowers	0.0228	**0.8468**	0.1237	0.0066
elapsed time=33 min 30 sec	16	DJI_0108	Sago flowers	Sago flowers	0.0000	**1.0000**	0.0000	0.0000
	17	DJI_0121	Sago flowers	Sago flowers	0.0002	**0.9948**	0.0049	0.0002
	18	DJI_0122	Sago flowers	Sago flowers	0.0047	**0.7688**	0.2222	0.0040
	19	DJI_0123	Sago flowers	Sago leaves	0.0067	0.4739	**0.5157**	0.0038
	20	img1	Sago trunks	Sago trunks	0.0005	0.0006	0.0145	**0.9844**
	21	MAX_0001	Sago leaves	Sago leaves	0.0000	0.0000	**0.9999**	0.0001
	22	MAX_0002	Non-sago	Non-sago	**1.0000**	0.0000	0.0000	0.0000
	23	MAX_0003	Sago leaves	Sago leaves	0.0000	0.0000	**1.0000**	0.0000
	24	MAX_0004	Sago leaves	Sago leaves	0.0000	0.0000	**1.0000**	0.0000
	25	MAX_0006	Sago leaves	Sago leaves	0.0002	0.0003	**0.9993**	0.0002
	26	MAX_0007	Sago leaves	Sago leaves	0.0000	0.0000	**1.0000**	0.0000
	27	MAX_0008	Non-sago	Sago flowers	0.0794	**0.4176**	0.1502	0.3527
	28	MAX_0009	Non-sago	Sago leaves	0.0138	0.1147	**0.8595**	0.0120
	29	MAX_0010	Sago leaves	Sago leaves	0.0135	0.0338	**0.9159**	0.0367
	30	MAX_0011	Sago flowers	Sago leaves	0.0000	0.0001	**0.9996**	0.0003
	31	MAX_0012	Sago leaves	Sago leaves	0.0001	0.0001	**0.9996**	0.0002
	32	MAX_0013	Non-sago	Non-sago	**0.9999**	0.0000	0.0001	0.0000
	33	MAX_0014	Sago leaves	Sago leaves	0.0370	0.2976	**0.5787**	0.0861
	34	MAX_0015	Non-sago	Non-sago	**1.0000**	0.0000	0.0000	0.0000
	35	MAX_0016	Sago leaves	Sago leaves	0.0001	0.0001	**0.9997**	0.0002
	36	MAX_0017	Sago leaves	Sago leaves	0.0005	0.0006	**0.9983**	0.0006
	37	MAX_0018	Non-sago	Non-sago	**0.9999**	0.0000	0.0001	0.0000
	38	MAX_0019	Sago leaves	Sago leaves	0.0014	0.0018	**0.7902**	0.2066
	39	MAX_0020	Sago leaves	Sago leaves	0.0000	0.0000	**0.9995**	0.0005
	40	MAX_0021	Non-sago	Non-sago	**1.0000**	0.0000	0.0000	0.0000
	41	MAX_0022	Sago leaves	Sago leaves	0.0000	0.0000	**0.9998**	0.0002
	42	MAX_0023	Sago leaves	Sago leaves	0.0000	0.0000	**1.0000**	0.0000
	43	MAX_0024	Sago leaves	Sago leaves	0.0001	0.0001	**0.9998**	0.0001
	44	MAX_0025	Sago leaves	Sago leaves	0.2811	0.0113	**0.4908**	0.2168
	45	MAX_0026	Non-sago	Sago leaves	0.1766	0.2046	**0.3178**	0.3010
	46	MAX_0027	Non-sago	Non-sago	**0.9853**	0.0024	0.0117	0.0007

	47	MAX_0028	Sago leaves	Sago leaves	0.0000	0.0000	**1.0000**	0.0000
	48	MAX_0029	Sago leaves	Sago leaves	0.0006	0.0003	**0.9953**	0.0038
	49	MAX_0030	Sago leaves	Sago leaves	0.0000	0.0000	**1.0000**	0.0000
	50	MAX_0031	Non-sago	Sago leaves	0.0290	0.0455	**0.8992**	0.0262
	51	MAX_0032	Sago leaves	Sago leaves	0.0001	0.0001	**0.9997**	0.0002
	52	MAX_0033	Sago leaves	Sago leaves	0.0000	0.0000	**1.0000**	0.0000
	53	MAX_0034	Sago leaves	Sago leaves	0.0000	0.0000	**1.0000**	0.0000
	54	MAX_0035	Sago leaves	Sago leaves	0.0000	0.0000	**1.0000**	0.0000
	55	MAX_0036	Non-sago	Non-sago	**0.9999**	0.0000	0.0000	0.0000
	56	MAX_0037	Sago leaves	Sago leaves	0.0000	0.0000	**0.9999**	0.0000
	57	MAX_0038	Non-sago	Non-sago	**0.9941**	0.0001	0.0058	0.0001
	58	MAX_0039	Non-sago	Non-sago	**0.9980**	0.0004	0.0016	0.0001
	59	MAX_0040	Sago leaves	Sago leaves	0.0001	0.0001	**0.9992**	0.0006
	60	MAX_0041	Sago leaves	Sago leaves	0.0001	0.0001	**0.9996**	0.0002
	61	MAX_0042	Sago leaves	Sago leaves	0.0000	0.0000	**0.9999**	0.0001
	62	MAX_0043	Non-sago	Non-sago	**0.9994**	0.0000	0.0006	0.0000
	63	MAX_0044	Sago leaves	Sago leaves	0.0001	0.0001	**0.9997**	0.0001
	64	MAX_0045	Sago flowers	Sago flowers	0.0142	**0.8291**	0.0650	0.0916
	65	MAX_0046	Sago flowers	Sago flowers	0.0013	**0.9044**	0.0835	0.0108
	66	MAX_0047	Sago flowers	Sago leaves	0.0004	0.0005	**0.9975**	0.0015
	67	MAX_0048	Sago flowers	Sago leaves	0.0009	0.0287	**0.9652**	0.0051
	68	MAX_0468	Sago leaves	Sago leaves	0.0013	0.0012	**0.9964**	0.0011
	69	MAX_0469	Sago leaves	Sago leaves	0.0148	0.0128	**0.9606**	0.0117
	70	MAX_0470	Sago leaves	Sago leaves	0.0000	0.0000	**1.0000**	0.0000
	71	MAX_0471	Sago leaves	Non-sago	**0.9716**	0.0007	0.0271	0.0006
	72	MAX_0536	Sago leaves	Sago leaves	0.0025	0.0587	**0.9315**	0.0073
	73	MAX_0537	Sago leaves	Non-sago	**0.5302**	0.0049	0.4613	0.0036
	74	MAX_0538	Non-sago	Non-sago	**0.9855**	0.0080	0.0132	0.0005
	75	MAX_0539	Sago leaves	Sago trunks	0.0102	0.0121	0.0719	**0.9059**
	76	MAX_0540	Sago leaves	Sago leaves	0.0081	0.0111	**0.9726**	0.0081
	77	MAX_0541	Sago leaves	Sago leaves	0.0001	0.0001	**0.9995**	0.0004
	78	MAX_0542	Sago leaves	Sago leaves	0.2298	0.0557	**0.6912**	0.0232
	79	MAX_0543	Sago leaves	Non-sago	**0.5013**	0.0085	0.4831	0.0071
	80	MAX_0544	Sago leaves	Sago leaves	0.0012	0.0005	**0.9978**	0.0005
	81	MAX_0546	Non-sago	Sago leaves	0.1768	0.0091	**0.8113**	0.0027
	82	MAX_0547	Sago leaves	Sago leaves	0.0002	0.0003	**0.9989**	0.0007
	83	MAX_0549	Sago leaves	Sago leaves	0.0002	0.0002	**0.9993**	0.0002

	84	no	Non-sago	Non-sago	**1.0000**	0.0000	0.0000	0.0000
	85	non	Non-sago	Sago leaves	0.0840	0.0562	**0.8588**	0.0076
	86	nonsa	Non-sago	Non-sago	**0.8402**	0.0584	0.0817	0.0197
	87	nonsag	Non-sago	Sago leaves	0.0155	0.0067	**0.9760**	0.0017
	88	sf	Sago flowers	Sago leaves	0.0000	0.0000	**0.9999**	0.0000
	89	sf1	Sago flowers	Sago flowers	0.0272	**0.5073**	0.1514	0.3140
	90	sff	Sago flowers	Sago flowers	0.0038	**0.9204**	0.0669	0.0090
	91	sl	Sago leaves	Sago leaves	0.0001	0.0030	**0.9993**	0.0002
	92	sl1	Sago leaves	Sago leaves	0.0061	0.0067	**0.9526**	0.0347
	93	sl2	Sago leaves	Sago leaves	0.0000	0.0000	**1.0000**	0.0000
	94	testnon	Non-sago	Non-sago	**0.9886**	0.0001	0.0113	0.0001
	95	testnons	Non-sago	Non-sago	**0.9107**	0.0096	0.0751	0.0045
	96	testnonss	Non-sago	Non-sago	**1.0000**	0.0000	0.0000	0.0000
	97	testrunk	Sago trunks	Sago trunks	0.0000	0.0000	0.0000	**1.0000**
	98	testsag	Sago leaves	Sago leaves	0.0094	0.0149	**0.9379**	0.0378
	99	testsl	Sago leaves	Sago leaves	0.0002	0.0003	**0.9993**	0.0002
	100	testtr	Sago trunks	Sago trunks	0.0000	0.0000	0.0000	**1.0000**
	101	trunk	Sago trunks	Sago trunks	0.0000	0.0000	0.0000	**1.0000**
	102	trunks	Sago trunks	Sago trunks	0.0000	0.0000	0.0000	**1.0000**
	103	trunkss	Sago trunks	Sago trunks	0.0000	0.0000	0.0000	**1.0000**

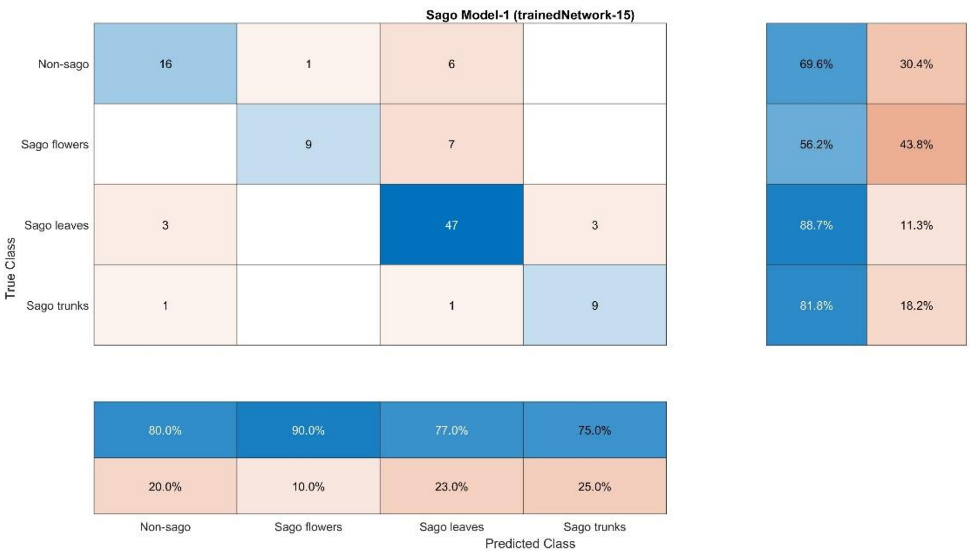

Figure D.4. Confusion matrix trained Network-15.

Table D.7. The prediction result of trained Network-16.

Parameter training setup		No	Test Image	Target16	Predict16	Non-sago	Sago flowers	Sago leaves	Sago trunks
Parameter name	**Value**	1	10-rev	Sago trunks	Sago leaves	0.0001	0.0001	**0.9994**	0.0004
Epoch	8	2	11-rev	Sago trunks	Sago trunks	0.0179	0.0015	0.0003	**0.9803**
Initial Learning rate	0.0001	3	12	Sago flowers	Sago flowers	0.0002	**0.5083**	0.4913	0.0002
Validation freq	4	4	12-rev	Sago flowers	Sago flowers	0.0002	**0.5784**	0.4212	0.0002
Learning rate weight coeff	10	5	14	Sago leaves	Sago leaves	0.0000	0.0000	**1.0000**	0.0000
Learning rate bias coeff	10	6	15	Sago leaves	Sago leaves	0.0000	0.0000	**1.0000**	0.0000
Momentum	0.9	7	15-rev	Sago leaves	Sago leaves	0.0000	0.0000	**1.0000**	0.0000
L2 Regulation	0.0001	8	19-rev	Sago leaves	Sago trunks	0.0000	0.0072	0.0000	**0.9928**
Min Batch size	10	9	20-rev	Sago leaves	Sago trunks	0.0000	0.0000	0.0000	**1.0000**
		10	DJI_0081	Sago leaves	Sago leaves	0.0000	0.0000	**0.9998**	0.0000
		11	DJI_0100	Sago trunks	Sago leaves	0.1757	0.0244	**0.6549**	0.1450
trainedNetwork_16		12	DJI_0101	Sago trunks	Sago trunks	0.0000	0.0000	0.0000	**1.0000**
		13	DJI_0103	Sago trunks	Non-sago	**0.9263**	0.0178	0.0016	0.0003
Accuracy		14	DJI_0106	Sago flowers	Sago leaves	0.0013	0.0031	**0.9953**	0.0003
validation accuracy=90.91%		15	DJI_0107	Sago flowers	Sago leaves	0.0032	0.0304	**0.9659**	0.0005
elapsed time=59 mins 39 sec		16	DJI_0108	Sago flowers	Sago leaves	0.0000	0.1224	**0.8775**	0.0000
		17	DJI_0121	Sago flowers	Sago flowers	0.0000	**0.9990**	0.0010	0.0000
		18	DJI_0122	Sago flowers	Sago flowers	0.0000	**0.9952**	0.0048	0.0000
		19	DJI_0123	Sago flowers	Sago flowers	0.0001	**0.8430**	0.1569	0.0000
		20	img1	Sago trunks	Sago trunks	0.0000	0.1060	0.0062	**0.9832**
		21	MAX_0001	Sago leaves	Sago leaves	0.0000	0.0000	**1.0000**	0.0000
		22	MAX_0002	Non-sago	Non-sago	**1.0000**	0.0000	0.0000	0.0000
		23	MAX_0003	Sago leaves	Sago leaves	0.0000	0.0000	**1.0000**	0.0000
		24	MAX_0004	Sago leaves	Sago leaves	0.0000	0.0000	**1.0000**	0.0000
		25	MAX_0006	Sago leaves	Sago leaves	0.0000	0.0000	**1.0000**	0.0000
		26	MAX_0007	Sago leaves	Sago leaves	0.0000	0.0000	**1.0000**	0.0000
		27	MAX_0008	Non-sago	Sago flowers	0.0002	**0.9981**	0.0015	0.0002
		28	MAX_0009	Non-sago	Sago leaves	0.0002	0.0011	**0.9985**	0.0001
		29	MAX_0010	Sago leaves	Sago leaves	0.0008	0.0027	**0.9934**	0.0032
		30	MAX_0011	Sago flowers	Sago leaves	0.0000	0.0000	**0.9999**	0.0000
		31	MAX_0012	Sago leaves	Sago leaves	0.0011	0.0048	**0.9907**	0.0034
		32	MAX_0013	Non-sago	Non-sago	**1.0000**	0.0000	0.0000	0.0000

	33	MAX_0014	Sago leaves	Sago flowers	0.0651	**0.6163**	0.2975	0.0210
	34	MAX_0015	Non-sago	Non-sago	**1.0000**	0.0000	0.0000	0.0000
	35	MAX_0016	Sago leaves	Sago leaves	0.0045	0.0057	**0.9821**	0.0077
	36	MAX_0017	Sago leaves	Sago leaves	0.0850	0.0206	**0.8852**	0.0091
	37	MAX_0018	Non-sago	Non-sago	**1.0000**	0.0000	0.0000	0.0000
	38	MAX_0019	Sago leaves	Sago trunks	0.0108	0.2176	0.2892	**0.4824**
	39	MAX_0020	Sago leaves	Sago leaves	0.0108	0.0199	**0.8216**	0.1477
	40	MAX_0021	Non-sago	Non-sago	**1.0000**	0.0000	0.0000	0.0000
	41	MAX_0022	Sago leaves	Sago leaves	0.2669	0.0230	**0.5798**	0.1304
	42	MAX_0023	Sago leaves	Sago leaves	0.0000	0.0000	**1.0000**	0.0000
	43	MAX_0024	Sago leaves	Sago leaves	0.0001	0.0000	**0.9998**	0.0000
	44	MAX_0025	Sago leaves	Non-sago	**0.9889**	0.0007	0.0050	0.0055
	45	MAX_0026	Non-sago	Sago flowers	0.0820	**0.5024**	0.1886	0.2270
	46	MAX_0027	Non-sago	Non-sago	**0.9701**	0.0018	0.0280	0.0002
	47	MAX_0028	Sago leaves	Sago leaves	0.0000	0.0000	**1.0000**	0.0000
	48	MAX_0029	Sago leaves	Sago leaves	0.0545	0.0108	**0.8958**	0.0390
	49	MAX_0030	Sago leaves	Sago leaves	0.0000	0.0000	**1.0000**	0.0000
	50	MAX_0031	Non-sago	Sago leaves	0.1864	0.2064	**0.4996**	0.1076
	51	MAX_0032	Sago leaves	Sago leaves	0.0002	0.0001	**0.9997**	0.0001
	52	MAX_0033	Sago leaves	Sago leaves	0.0000	0.0000	**1.0000**	0.0000
	53	MAX_0034	Sago leaves	Sago leaves	0.0000	0.0000	**1.0000**	0.0000
	54	MAX_0035	Sago leaves	Sago leaves	0.0000	0.0000	**1.0000**	0.0000
	55	MAX_0036	Non-sago	Non-sago	**1.0000**	0.0000	0.0000	0.0000
	56	MAX_0037	Sago leaves	Sago leaves	0.0000	0.0000	**1.0000**	0.0000
	57	MAX_0038	Non-sago	Non-sago	**1.0000**	0.0000	0.0000	0.0000
	58	MAX_0039	Non-sago	Non-sago	**0.9983**	0.0012	0.0002	0.0003
	59	MAX_0040	Sago leaves	Sago leaves	0.0000	0.0000	**0.9996**	0.0003
	60	MAX_0041	Sago leaves	Sago leaves	0.0005	0.0002	**0.9991**	0.0002
	61	MAX_0042	Sago leaves	Sago leaves	0.0003	0.0002	**0.9992**	0.0003
	62	MAX_0043	Non-sago	Non-sago	**1.0000**	0.0000	0.0000	0.0000
	63	MAX_0044	Sago leaves	Sago leaves	0.0000	0.0000	**1.0000**	0.0000
	64	MAX_0045	Sago flowers	Sago flowers	0.0000	**1.0000**	0.0000	0.0000
	65	MAX_0046	Sago flowers	Sago flowers	0.0000	**1.0000**	0.0000	0.0000
	66	MAX_0047	Sago flowers	Sago leaves	0.0078	0.0777	**0.9103**	0.0042
	67	MAX_0048	Sago flowers	Sago leaves	0.0009	0.1938	**0.8035**	0.0019
	68	MAX_0468	Sago leaves	Sago leaves	0.0000	0.0000	**0.9999**	0.0000
	69	MAX_0469	Sago leaves	Sago leaves	0.0000	0.0000	**1.0000**	0.0000

	70	MAX_0470	Sago leaves	Sago leaves	0.0000	0.0000	**1.0000**	0.0000
	71	MAX_0471	Sago leaves	Non-sago	**0.8981**	0.0002	0.1016	0.0001
	72	MAX_0536	Sago leaves	Sago leaves	0.0001	0.0002	**0.9996**	0.0001
	73	MAX_0537	Sago leaves	Sago leaves	0.0701	0.0000	**0.9298**	0.0000
	74	MAX_0538	Non-sago	Non-sago	**0.7498**	0.0059	0.2405	0.0038
	75	MAX_0539	Sago leaves	Sago trunks	0.0030	0.0007	0.0033	**0.9957**
	76	MAX_0540	Sago leaves	Sago leaves	0.0001	0.0001	**0.9997**	0.0001
	77	MAX_0541	Sago leaves	Sago leaves	0.0000	0.0000	**1.0000**	0.0000
	78	MAX_0542	Sago leaves	Sago leaves	0.0018	0.0001	**0.9981**	0.0000
	79	MAX_0543	Sago leaves	Sago leaves	0.1273	0.0001	**0.8725**	0.0001
	80	MAX_0544	Sago leaves	Sago leaves	0.0007	0.0001	**0.9990**	0.0001
	81	MAX_0546	Non-sago	Sago leaves	0.2898	0.0030	**0.7067**	0.0005
	82	MAX_0547	Sago leaves	Sago leaves	0.0001	0.0001	**0.9997**	0.0001
	83	MAX_0549	Sago leaves	Sago leaves	0.0002	0.0002	**0.9995**	0.0002
	84	no	Non-sago	Non-sago	**1.0000**	0.0000	0.0000	0.0000
	85	non	Non-sago	Sago leaves	0.0141	0.0602	**0.9191**	0.0066
	86	nonsa	Non-sago	Non-sago	**0.9793**	0.0151	0.0042	0.0013
	87	nonsag	Non-sago	Sago leaves	0.0190	0.2230	**0.7519**	0.0062
	88	sf	Sago flowers	Sago leaves	0.0000	0.0000	**1.0000**	0.0000
	89	sf1	Sago flowers	Sago flowers	0.0013	**0.6239**	0.3665	0.0082
	90	sff	Sago flowers	Sago flowers	0.0008	**0.7746**	0.2235	0.0011
	91	sl	Sago leaves	Sago leaves	0.0000	0.0000	**1.0000**	0.0000
	92	sl1	Sago leaves	Sago leaves	0.0001	0.0002	**0.9996**	0.0002
	93	sl2	Sago leaves	Sago leaves	0.0000	0.0000	**1.0000**	0.0000
	94	testnon	Non-sago	Non-sago	**0.9993**	0.0002	0.0003	0.0002
	95	testnons	Non-sago	Non-sago	**0.9970**	0.0006	0.0024	0.0001
	96	testnonss	Non-sago	Non-sago	**1.0000**	0.0000	0.0000	0.0000
	97	testrunk	Sago trunks	Sago trunks	0.0000	0.0000	0.0000	**1.0000**
	98	testsag	Sago leaves	Sago leaves	0.0034	0.0051	**0.9881**	0.0034
	99	testsl	Sago leaves	Sago leaves	0.0000	0.0001	**0.9998**	0.0000
	100	testtr	Sago trunks	Sago trunks	0.0000	0.0000	0.0001	**0.9999**
	101	trunk	Sago trunks	Sago trunks	0.0000	0.0000	0.0000	**1.0000**
	102	trunks	Sago trunks	Sago trunks	0.0000	0.0000	0.0001	**0.9999**
	103	trunkss	Sago trunks	Sago trunks	0.0000	0.0000	0.0000	**1.0000**

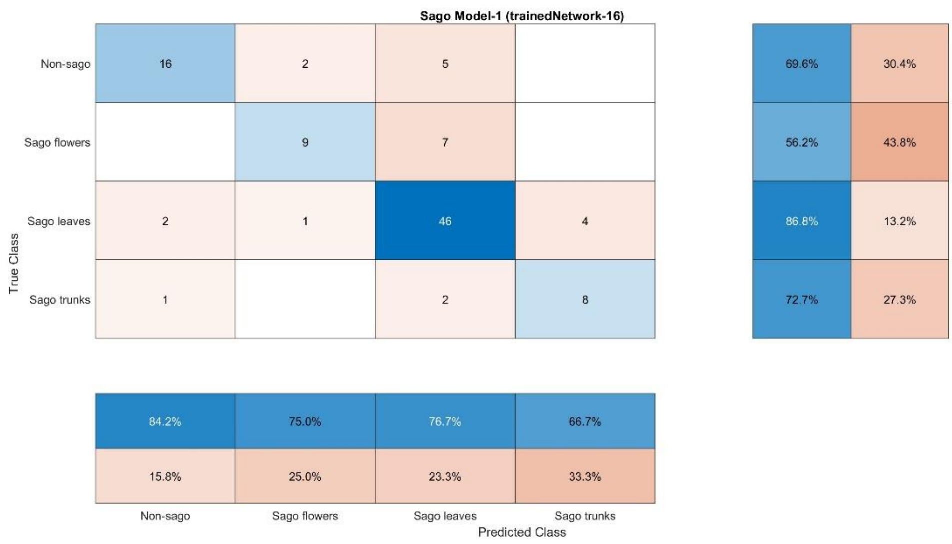

Figure D.5. Confusion matrix trained Network-16.

Table D.8. The prediction result of trained Network-17.

Parameter training setup		**No**	**Test Image**	**Target17**	**Predict17**	**Non-sago**	**Sago flowers**	**Sago leaves**	**Sago trunks**
Parameter name	**Value**	1	10-rev	Sago trunks	Sago leaves	0.0000	0.0052	**0.7989**	0.1958
Epoch	10	2	11-rev	Sago trunks	Sago trunks	0.0001	0.0005	0.0000	**0.9994**
Initial Learning rate	0.0001	3	12	Sago flowers	Sago flowers	0.0000	**0.8677**	0.1322	0.0001
Validation freq	4	4	12-rev	Sago flowers	Sago flowers	0.0000	**0.8897**	0.1102	0.0000
Learning rate weight coeff	10	5	14	Sago leaves	Sago leaves	0.0000	0.0023	**0.9977**	0.0000
Learning rate bias coeff	10	6	15	Sago leaves	Sago flowers	0.0000	**0.5658**	0.4335	0.0007
Momentum	0.9	7	15-rev	Sago leaves	Sago flowers	0.0000	**0.5939**	0.4054	0.0007
L2 Regulation	0.0001	8	19-rev	Sago leaves	Sago trunks	0.0000	0.0090	0.0000	**0.9910**
Min Batch size	64	9	20-rev	Sago leaves	Sago trunks	0.0000	0.0008	0.0000	**0.9991**
		10	DJI_0081	Sago leaves	Sago trunks	0.0014	0.0708	**0.9272**	0.0007
		11	DJI_0100	Sago trunks	Sago trunks	0.0010	0.0046	0.3171	**0.6772**
		12	DJI_0101	Sago trunks	Sago trunks	0.0000	0.0000	0.0000	**1.0000**
trainedNetwork_17		13	DJI_0103	Sago trunks	Sago flowers	0.3009	**0.3055**	0.2969	0.0967
		14	DJI_0106	Sago flowers	Sago flowers	0.0003	**0.9643**	0.0353	0.0001
		15	DJI_0107	Sago flowers	Sago flowers	0.0004	**0.9510**	0.0485	0.0010
Accuracy		16	DJI_0108	Sago flowers	Sago flowers	0.0000	**0.9961**	0.0039	0.0000
validation accuracy= 88.64%		17	DJI_0121	Sago flowers	Sago flowers	0.0000	**0.9503**	0.0497	0.0000
elapsed time=8 min 9 sec		18	DJI_0122	Sago flowers	Sago flowers	0.0000	**0.9604**	0.0396	0.0000
		19	DJI_0123	Sago flowers	Sago flowers	0.0000	**0.9645**	0.0354	0.0000

	20	img1	Sago trunks	Sago trunks	0.0000	0.0111	0.0000	**0.9889**
	21	MAX_0001	Sago leaves	Sago leaves	0.0000	0.0014	**0.9984**	0.0002
	22	MAX_0002	Non-sago	Non-sago	**1.0000**	0.0000	0.0000	0.0000
	23	MAX_0003	Sago leaves	Sago leaves	0.0002	0.0049	**0.9950**	0.0000
	24	MAX_0004	Sago leaves	Sago leaves	0.0000	0.0028	**0.9972**	0.0000
	25	MAX_0006	Sago leaves	Sago leaves	0.0000	0.0008	**0.9992**	0.0000
	26	MAX_0007	Sago leaves	Sago leaves	0.0000	0.0001	**0.9999**	0.0000
	27	MAX_0008	Non-sago	Sago flowers	0.0037	**0.5895**	0.2649	0.1419
	28	MAX_0009	Non-sago	Sago flowers	0.0002	**0.5558**	0.4424	0.0016
	29	MAX_0010	Sago leaves	Sago trunks	0.0001	0.4039	0.1638	**0.4323**
	30	MAX_0011	Sago flowers	Sago leaves	0.0000	0.0243	**0.9756**	0.0000
	31	MAX_0012	Sago leaves	Sago leaves	0.0001	0.2126	**0.7587**	0.0286
	32	MAX_0013	Non-sago	Non-sago	**0.9999**	0.0001	0.0000	0.0000
	33	MAX_0014	Sago leaves	Sago leaves	0.0213	0.3126	**0.5135**	0.1527
	34	MAX_0015	Non-sago	Non-sago	**0.9999**	0.0000	0.0001	0.0000
	35	MAX_0016	Sago leaves	Sago leaves	0.0021	0.0187	**0.9398**	0.0394
	36	MAX_0017	Sago leaves	Sago leaves	0.0002	0.0023	**0.9973**	0.0002
	37	MAX_0018	Non-sago	Non-sago	**0.9995**	0.0001	0.0004	0.0000
	38	MAX_0019	Sago leaves	Sago trunks	0.0003	0.0046	0.3788	**0.6163**
	39	MAX_0020	Sago leaves	Sago leaves	0.0023	0.0080	**0.8719**	0.1177
	40	MAX_0021	Non-sago	Non-sago	**0.9997**	0.0002	0.0001	0.0000
	41	MAX_0022	Sago leaves	Sago leaves	0.0725	0.0008	**0.9265**	0.0001
	42	MAX_0023	Sago leaves	Sago leaves	0.0000	0.0030	**0.9968**	0.0020
	43	MAX_0024	Sago leaves	Sago leaves	0.0000	0.0001	**0.9999**	0.0000
	44	MAX_0025	Sago leaves	Sago leaves	0.3523	0.0125	**0.5526**	0.0826
	45	MAX_0026	Non-sago	Sago leaves	0.3578	0.0506	**0.3788**	0.2128
	46	MAX_0027	Non-sago	Non-sago	**0.7897**	0.0236	0.1856	0.0009
	47	MAX_0028	Sago leaves	Sago leaves	0.0000	0.0002	**0.9997**	0.0001
	48	MAX_0029	Sago leaves	Sago leaves	0.3219	0.0059	**0.6438**	0.0285
	49	MAX_0030	Sago leaves	Sago leaves	0.0000	0.0002	**0.9935**	0.0063
	50	MAX_0031	Non-sago	Non-sago	**0.9948**	0.0001	0.0050	0.0001
	51	MAX_0032	Sago leaves	Sago leaves	0.0001	0.0004	**0.9993**	0.0002
	52	MAX_0033	Sago leaves	Sago leaves	0.0000	0.0002	**0.9997**	0.0001
	53	MAX_0034	Sago leaves	Sago leaves	0.0000	0.0001	**0.9999**	0.0000
	54	MAX_0035	Sago leaves	Sago leaves	0.0000	0.0002	**0.9998**	0.0000
	55	MAX_0036	Non-sago	Non-sago	**0.9999**	0.0000	0.0000	0.0001

	56	MAX_0037	Sago leaves	Sago leaves	0.0000	0.0000	**1.0000**	0.0000
	57	MAX_0038	Non-sago	Non-sago	**0.9981**	0.0001	0.0018	0.0000
	58	MAX_0039	Non-sago	Non-sago	**0.9733**	0.0212	0.0051	0.0005
	59	MAX_0040	Sago leaves	Sago leaves	0.0004	0.0012	**0.8608**	0.1376
	60	MAX_0041	Sago leaves	Sago leaves	0.0013	0.0027	**0.9412**	0.0548
	61	MAX_0042	Sago leaves	Sago leaves	0.0018	0.0022	**0.9954**	0.0006
	62	MAX_0043	Non-sago	Non-sago	**0.9999**	0.0000	0.0000	0.0000
	63	MAX_0044	Sago leaves	Sago leaves	0.0000	0.0033	**0.9957**	0.0009
	64	MAX_0045	Sago flowers	Sago trunks	0.0034	0.4206	0.0123	**0.5637**
	65	MAX_0046	Sago flowers	Sago flowers	0.0002	0.0756	**0.5240**	0.4001
	66	MAX_0047	Sago flowers	Non-sago	**0.5618**	0.0633	0.3641	0.0108
	67	MAX_0048	Sago flowers	Sago flowers	0.0030	0.1685	**0.8272**	0.0040
	68	MAX_0468	Sago leaves	Sago leaves	0.2348	0.0076	**0.7576**	0.0000
	69	MAX_0469	Sago leaves	Sago leaves	0.0031	0.0055	**0.9914**	0.0000
	70	MAX_0470	Sago leaves	Sago leaves	0.0000	0.0001	**0.9999**	0.0000
	71	MAX_0471	Sago leaves	Non-sago	**0.9944**	0.0017	0.0038	0.0000
	72	MAX_0536	Sago leaves	Sago flowers	0.0000	0.4341	**0.5655**	0.0003
	73	MAX_0537	Sago leaves	Non-sago	**0.8571**	0.0356	0.1072	0.0001
	74	MAX_0538	Non-sago	Non-sago	**0.9980**	0.0001	0.0018	0.0000
	75	MAX_0539	Sago leaves	Sago leaves	0.0000	0.0072	**0.5058**	0.4870
	76	MAX_0540	Sago leaves	Sago leaves	0.0264	0.0662	**0.9073**	0.0001
	77	MAX_0541	Sago leaves	Sago leaves	0.0000	0.0052	**0.9905**	0.0043
	78	MAX_0542	Sago leaves	Sago leaves	0.2631	0.0536	**0.6531**	0.0002
	79	MAX_0543	Sago leaves	Non-sago	**0.9211**	0.0023	0.0766	0.0000
	80	MAX_0544	Sago leaves	Sago leaves	0.0000	0.0035	**0.9965**	0.0000
	81	MAX_0546	Non-sago	Sago flowers	0.0035	**0.6432**	0.3268	0.0264
	82	MAX_0547	Sago leaves	Sago leaves	0.0000	0.0424	**0.9575**	0.0001
	83	MAX_0549	Sago leaves	Sago leaves	0.0000	0.0006	**0.9994**	0.0000
	84	no	Non-sago	Non-sago	**0.9999**	0.0000	0.0001	0.0000
	85	non	Non-sago	Non-sago	**0.9964**	0.0058	0.0276	0.0002
	86	nonsa	Non-sago	Non-sago	**0.7125**	0.0054	0.2812	0.0008
	87	nonsag	Non-sago	Non-sago	**0.4703**	0.1369	0.3929	0.0002
	88	sf	Sago flowers	Sago leaves	0.0000	0.0064	**0.9936**	0.0000
	89	sf1	Sago flowers	Sago flowers	0.0000	**0.9949**	0.0051	0.0001
	90	sff	Sago flowers	Sago flowers	0.0000	**0.9940**	0.0059	0.0001
	91	sl	Sago leaves	Sago leaves	0.0000	0.0074	**0.9920**	0.0005

	92	sl1	Sago leaves	Sago leaves	0.0000	0.2090	**0.7884**	0.0027
	93	sl2	Sago leaves	Sago leaves	0.0000	0.0000	**1.0000**	0.0000
	94	testnon	Non-sago	Non-sago	**0.9936**	0.0003	0.0003	0.0000
	95	testnons	Non-sago	Non-sago	**0.6932**	0.0011	0.3054	0.0002
	96	testnonss	Non-sago	Non-sago	**0.9999**	0.0001	0.0000	0.0000
	97	testrunk	Sago trunks	Sago trunks	0.0000	0.0006	0.0001	**0.9992**
	98	testsag	Sago leaves	Sago leaves	0.0000	0.0196	**0.9793**	0.0011
	99	testsl	Sago leaves	Sago leaves	0.0014	0.0708	**0.9272**	0.0007
	100	testtr	Sago trunks	Sago trunks	0.0000	0.0019	0.0000	**0.9980**
	101	trunk	Sago trunks	Sago trunks	0.0000	0.0000	0.0000	**1.0000**
	102	trunks	Sago trunks	Sago trunks	0.0000	0.0000	0.0000	**1.0000**
	103	trunkss	Sago trunks	Sago trunks	0.0000	0.0000	0.0000	**1.0000**

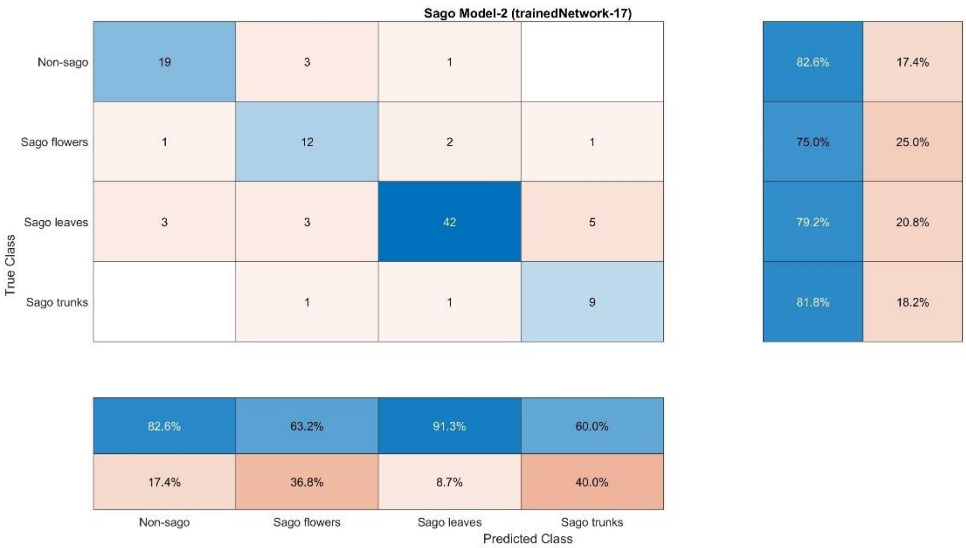

Figure D.6. Confusion matrix trained Network-17.

Table D.9. The prediction result of trained Network-18.

Parameter training setup		**No**	**Test Image**	**Target18**	**Predict18**	**Non-sago**	**Sago flowers**	**Sago leaves**	**Sago trunks**
Parameter name	**Value**	1	10-rev	Sago trunks	Sago leaves	0.0000	0.0001	**0.9525**	0.0474
Epoch	8	2	11-rev	Sago trunks	Sago trunks	0.0003	0.0001	0.0011	**0.9985**
Initial Learning rate	0.0001	3	12	Sago flowers	Sago leaves	0.0000	0.2397	**0.7602**	0.0000
Validation freq	4	4	12-rev	Sago flowers	Sago leaves	0.0000	0.2767	**0.7232**	0.0000
Learning rate weight coeff	10	5	14	Sago leaves	Sago leaves	0.0000	0.0011	**0.9989**	0.0000
Learning rate bias coeff	10	6	15	Sago leaves	Sago leaves	0.0000	0.0057	**0.9942**	0.0000

Momentum 0.9	7	15-rev	Sago leaves	Sago leaves	0.0000	0.0072	**0.9928**	0.0000
L2 Regulation 0.0001	8	19-rev	Sago leaves	Sago trunks	0.0000	0.0095	0.0004	**0.9901**
Min Batch size 32	9	20-rev	Sago leaves	Sago trunks	0.0000	0.0000	0.0009	**0.9990**
	10	DJI_0081	Sago leaves	Sago leaves	0.0001	0.0050	**0.9948**	0.0000
	11	DJI_0100	Sago trunks	Sago trunks	0.0032	0.0002	0.0173	**0.9793**
	12	DJI_0101	Sago trunks	Sago trunks	0.0000	0.0000	0.0000	**1.0000**
trainedNetwork_18	13	DJI_0103	Sago trunks	Non-sago	**0.8184**	0.0128	0.1639	0.0048
	14	DJI_0106	Sago flowers	Sago flowers	0.0012	**0.7866**	0.2121	0.0000
	15	DJI_0107	Sago flowers	Sago flowers	0.0012	**0.7380**	0.2608	0.0000
Accuracy	16	DJI_0108	Sago flowers	Sago flowers	0.0000	**0.9822**	0.0178	0.0000
validation accuracy=89.39	17	DJI_0121	Sago flowers	Sago flowers	0.0000	**0.9957**	0.0043	0.0000
elapsed time= 6 min 37 sec	18	DJI_0122	Sago flowers	Sago flowers	0.0000	**0.9811**	0.0189	0.0000
	19	DJI_0123	Sago flowers	Sago flowers	0.0000	**0.9800**	0.0199	0.0000
	20	img1	Sago trunks	Sago trunks	0.0000	0.0000	0.0000	**1.0000**
	21	MAX_0001	Sago leaves	Sago leaves	0.0000	0.0001	**0.9999**	0.0000
	22	MAX_0002	Non-sago	Non-sago	**1.0000**	0.0000	0.0000	0.0000
	23	MAX_0003	Sago leaves	Sago leaves	0.0000	0.0063	**0.9936**	0.0000
	24	MAX_0004	Sago leaves	Sago leaves	0.0000	0.0003	**0.9997**	0.0000
	25	MAX_0006	Sago leaves	Sago leaves	0.0000	0.0233	**0.9769**	0.0000
	26	MAX_0007	Sago leaves	Sago leaves	0.0000	0.0002	**0.9998**	0.0000
	27	MAX_0008	Non-sago	Sago flowers	0.0073	**0.5903**	0.3826	0.0199
	28	MAX_0009	Non-sago	Sago leaves	0.0002	0.4426	**0.5572**	0.0000
	29	MAX_0010	Sago leaves	Sago leaves	0.0000	0.1695	**0.7961**	0.0344
	30	MAX_0011	Sago flowers	Sago leaves	0.0000	0.0613	**0.9387**	0.0000
	31	MAX_0012	Sago leaves	Sago leaves	0.0000	0.0013	**0.9101**	0.0886
	32	MAX_0013	Non-sago	Non-sago	**0.9999**	0.0000	0.0000	0.0000
	33	MAX_0014	Sago leaves	Sago leaves	0.3874	0.0087	**0.6020**	0.0020
	34	MAX_0015	Non-sago	Non-sago	**0.9999**	0.0000	0.0001	0.0000
	35	MAX_0016	Sago leaves	Sago leaves	0.0071	0.0288	**0.9087**	0.0553
	36	MAX_0017	Sago leaves	Sago leaves	0.0000	0.0020	**0.9979**	0.0001
	37	MAX_0018	Non-sago	Non-sago	**0.9999**	0.0001	0.0001	0.0000
	38	MAX_0019	Sago leaves	Sago trunks	0.0000	0.0005	0.3513	**0.6482**
	39	MAX_0020	Sago leaves	Sago leaves	0.0000	0.0120	**0.5317**	0.4563
	40	MAX_0021	Non-sago	Non-sago	**0.9999**	0.0000	0.0001	0.0000
	41	MAX_0022	Sago leaves	Sago leaves	0.3448	0.0017	**0.6530**	0.0005
	42	MAX_0023	Sago leaves	Sago leaves	0.0000	0.0033	**0.9965**	0.0002
	43	MAX_0024	Sago leaves	Sago leaves	0.0000	0.0065	**0.9935**	0.0000

	44	MAX_0025	Sago leaves	Non-sago	**0.8959**	0.0058	0.0717	0.0266
	45	MAX_0026	Non-sago	Sago leaves	0.1219	0.0916	**0.6918**	0.0947
	46	MAX_0027	Non-sago	Non-sago	**0.7950**	0.0121	0.1928	0.0002
	47	MAX_0028	Sago leaves	Sago leaves	0.0000	0.0023	**0.9977**	0.0000
	48	MAX_0029	Sago leaves	Sago leaves	0.3741	0.0023	**0.5010**	0.1225
	49	MAX_0030	Sago leaves	Sago leaves	0.0000	0.0015	**0.9982**	0.0002
	50	MAX_0031	Non-sago	Non-sago	**0.9419**	0.0041	0.0530	0.0011
	51	MAX_0032	Sago leaves	Sago leaves	0.0000	0.0005	**0.9995**	0.0000
	52	MAX_0033	Sago leaves	Sago leaves	0.0000	0.0000	**0.9999**	0.0001
	53	MAX_0034	Sago leaves	Sago leaves	0.0000	0.0000	**1.0000**	0.0000
	54	MAX_0035	Sago leaves	Sago leaves	0.0000	0.0001	**0.9999**	0.0000
	55	MAX_0036	Non-sago	Non-sago	**1.0000**	0.0000	0.0000	0.0000
	56	MAX_0037	Sago leaves	Sago leaves	0.0000	0.0000	**1.0000**	0.0000
	57	MAX_0038	Non-sago	Non-sago	**0.9995**	0.0001	0.0004	0.0000
	58	MAX_0039	Non-sago	Non-sago	**0.9805**	0.0056	0.0139	0.0000
	59	MAX_0040	Sago leaves	Sago leaves	0.0000	0.0002	**0.8447**	0.1551
	60	MAX_0041	Sago leaves	Sago leaves	0.0001	0.0001	**0.9798**	0.0201
	61	MAX_0042	Sago leaves	Sago leaves	0.0001	0.0007	**0.9992**	0.0000
	62	MAX_0043	Non-sago	Non-sago	**0.9999**	0.0000	0.0000	0.0000
	63	MAX_0044	Sago leaves	Sago leaves	0.0000	0.0001	**0.9999**	0.0000
	64	MAX_0045	Sago flowers	Sago flowers	0.0008	**0.9721**	0.0194	0.0076
	65	MAX_0046	Sago flowers	Sago flowers	0.0001	**0.5442**	0.4383	0.0174
	66	MAX_0047	Sago flowers	Sago leaves	0.0785	0.0529	**0.8592**	0.0094
	67	MAX_0048	Sago flowers	Sago flowers	0.0001	**0.7187**	0.2808	0.0004
	68	MAX_0468	Sago leaves	Sago leaves	0.0172	0.0022	**0.9806**	0.0000
	69	MAX_0469	Sago leaves	Sago leaves	0.0004	0.0011	**0.9985**	0.0000
	70	MAX_0470	Sago leaves	Sago leaves	0.0000	0.0001	**0.9999**	0.0000
	71	MAX_0471	Sago leaves	Non-sago	**0.9936**	0.0017	0.0047	0.0000
	72	MAX_0536	Sago leaves	Sago leaves	0.0000	0.0538	**0.9462**	0.0000
	73	MAX_0537	Sago leaves	Non-sago	**0.5830**	0.0306	0.3864	0.0000
	74	MAX_0538	Non-sago	Non-sago	**0.9986**	0.0001	0.0013	0.0000
	75	MAX_0539	Sago leaves	Sago leaves	0.0000	0.0261	**0.9650**	0.0090
	76	MAX_0540	Sago leaves	Sago leaves	0.0076	0.0623	**0.9300**	0.0000
	77	MAX_0541	Sago leaves	Sago leaves	0.0000	0.0000	**1.0000**	0.0000
	78	MAX_0542	Sago leaves	Sago leaves	0.0252	0.0320	**0.9427**	0.0000
	79	MAX_0543	Sago leaves	Non-sago	**0.9023**	0.0026	0.0951	0.0000
	80	MAX_0544	Sago leaves	Sago leaves	0.0000	0.0004	**0.9996**	0.0000

	81	MAX_0546	Non-sago	Sago leaves	0.0003	0.0136	**0.9860**	0.0001
	82	MAX_0547	Sago leaves	Sago leaves	0.0000	0.0069	**0.9931**	0.0000
	83	MAX_0549	Sago leaves	Sago leaves	0.0000	0.0014	**0.9986**	0.0000
	84	no	Non-sago	Non-sago	**0.9998**	0.0000	0.0002	0.0000
	85	non	Non-sago	Non-sago	**0.9653**	0.0017	0.0330	0.0000
	86	nonsa	Non-sago	Non-sago	**0.8277**	0.0042	0.1680	0.0000
	87	nonsag	Non-sago	Sago leaves	0.0940	0.2248	**0.6812**	0.0000
	88	sf	Sago flowers	Sago leaves	0.0000	0.0436	**0.9564**	0.0000
	89	sf1	Sago flowers	Sago flowers	0.0000	**0.9665**	0.0335	0.0000
	90	sff	Sago flowers	Sago leaves	0.0000	0.1658	**0.8342**	0.0000
	91	sl	Sago leaves	Sago leaves	0.0000	0.0119	**0.9881**	0.0000
	92	sl1	Sago leaves	Sago leaves	0.0000	0.0038	**0.9962**	0.0000
	93	sl2	Sago leaves	Sago leaves	0.0000	0.0018	**0.9982**	0.0000
	94	testnon	Non-sago	Non-sago	**0.9740**	0.0089	0.0171	0.0000
	95	testnons	Non-sago	Non-sago	**0.9098**	0.0081	0.0821	0.0000
	96	testnonss	Non-sago	Non-sago	**1.0000**	0.0000	0.0000	0.0000
	97	testrunk	Sago trunks	Sago trunks	0.0000	0.0001	0.0001	**0.9998**
	98	testsag	Sago leaves	Sago leaves	0.0000	0.0029	**0.9970**	0.0001
	99	testsl	Sago leaves	Sago leaves	0.0001	0.0050	**0.9948**	0.0000
	100	testtr	Sago trunks	Sago trunks	0.0000	0.0001	0.0000	**0.9999**
	101	trunk	Sago trunks	Sago trunks	0.0000	0.0000	0.0000	**1.0000**
	102	trunks	Sago trunks	Sago trunks	0.0000	0.0000	0.0000	**1.0000**
	103	trunkss	Sago trunks	Sago trunks	0.0000	0.0000	0.0000	**1.0000**

Figure D.7. Confusion matrix trained Network-18.

Table D.10. The prediction result of trained Network-19.

Parameter training setup		**No**	**Test Image**	**Target19**	**Predict19**	**Non-sago**	**Sago flowers**	**Sago leaves**	**Sago trunks**
Parameter name	**Value**	1	10-rev	Sago trunks	Sago trunks	0.0000	0.0055	0.1126	**0.8819**
Epoch	15	2	11-rev	Sago trunks	Sago trunks	0.0004	0.0000	0.0000	**0.9995**
Initial Learning rate	0.0001	3	12	Sago flowers	Sago leaves	0.0000	0.3764	**0.6236**	0.0000
Validation freq	4	4	12-rev	Sago flowers	Sago leaves	0.0000	0.3925	**0.6075**	0.0000
Learning rate weight coeff	10	5	14	Sago leaves	Sago leaves	0.0000	0.0010	**0.9990**	0.0000
Learning rate bias coeff	10	6	15	Sago leaves	Sago leaves	0.0000	0.3155	**0.6842**	0.0001
Learning rate schedule		7	15-rev	Sago leaves	Sago leaves	0.0000	0.3295	**0.6704**	0.0001
Momentum	0.9	8	19-rev	Sago leaves	Sago trunks	0.0000	0.0093	0.0001	**0.9906**
L2 Regulation	0.0001	9	20-rev	Sago leaves	Sago trunks	0.0000	0.0001	0.0000	**0.9998**
Min Batch size	64	10	DJI_0081	Sago leaves	Sago leaves	0.0029	0.0380	**0.9589**	0.0002
		11	DJI_0100	Sago trunks	Sago trunks	0.0240	0.0040	0.1428	**0.8292**
		12	DJI_0101	Sago trunks	Sago trunks	0.0000	0.0000	0.0000	**1.0000**
trainedNetwork_19		13	DJI_0103	Sago trunks	Non-sago	**0.8995**	0.0059	0.0836	0.0111
		14	DJI_0106	Sago flowers	Sago flowers	0.0006	**0.7653**	0.2340	0.0000
Accuracy		15	DJI_0107	Sago flowers	Sago flowers	0.0003	**0.6410**	0.3586	0.0000
Validation accuracy=87.12		16	DJI_0108	Sago flowers	Sago flowers	0.0000	**0.9966**	0.0034	0.0000
elapsed time: 10 min 11 sec		17	DJI_0121	Sago flowers	Sago flowers	0.0000	**0.9871**	0.0129	0.0000
		18	DJI_0122	Sago flowers	Sago flowers	0.0000	**0.9834**	0.0166	0.0000
		19	DJI_0123	Sago flowers	Sago flowers	0.0006	**0.6929**	0.3065	0.0000
		20	img1	Sago trunks	Sago trunks	0.0000	0.0008	0.0000	**0.9992**
		21	MAX_0001	Sago leaves	Sago leaves	0.0000	0.0020	**0.9964**	0.0016
		22	MAX_0002	Non-sago	Non-sago	**1.0000**	0.0000	0.0000	0.0000
		23	MAX_0003	Sago leaves	Sago leaves	0.0001	0.0044	**0.9956**	0.0000
		24	MAX_0004	Sago leaves	Sago leaves	0.0000	0.0018	**0.9982**	0.0000
		25	MAX_0006	Sago leaves	Sago leaves	0.0000	0.0808	**0.9191**	0.0001
		26	MAX_0007	Sago leaves	Sago leaves	0.0000	0.0062	**0.9938**	0.0000
		27	MAX_0008	Non-sago	Sago flowers	0.1474	**0.6833**	0.0856	0.0837
		28	MAX_0009	Non-sago	Sago flowers	0.0027	**0.5077**	0.4893	0.0003
		29	MAX_0010	Sago leaves	Sago trunks	0.0027	0.2672	0.2542	**0.4759**
		30	MAX_0011	Sago flowers	Sago leaves	0.0000	0.1200	**0.8789**	0.0002
		31	MAX_0012	Sago leaves	Sago leaves	0.0003	0.0174	**0.9404**	0.0420
		32	MAX_0013	Non-sago	Non-sago	**1.0000**	0.0000	0.0000	0.0000
		33	MAX_0014	Sago leaves	Non-sago	**0.8949**	0.0237	0.0778	0.0036

	34	MAX_0015	Non-sago	Non-sago	**1.0000**	0.0000	0.0000	0.0000
	35	MAX_0016	Sago leaves	Sago leaves	0.0429	0.0176	**0.8283**	0.1111
	36	MAX_0017	Sago leaves	Sago leaves	0.0006	0.0021	**0.9973**	0.0001
	37	MAX_0018	Non-sago	Non-sago	**1.0000**	0.0000	0.0000	0.0000
	38	MAX_0019	Sago leaves	Sago leaves	0.0007	0.0044	**0.9249**	0.0700
	39	MAX_0020	Sago leaves	Sago leaves	0.0012	0.0039	**0.9869**	0.0080
	40	MAX_0021	Non-sago	Non-sago	**1.0000**	0.0000	0.0000	0.0000
	41	MAX_0022	Sago leaves	Sago leaves	0.4603	0.0010	**0.5386**	0.0002
	42	MAX_0023	Sago leaves	Sago leaves	0.0000	0.0210	**0.9784**	0.0007
	43	MAX_0024	Sago leaves	Sago leaves	0.0000	0.0010	**0.9990**	0.0000
	44	MAX_0025	Sago leaves	Non-sago	**0.9387**	0.1010	0.0470	0.0042
	45	MAX_0026	Non-sago	Non-sago	**0.4411**	0.2879	0.0597	0.2113
	46	MAX_0027	Non-sago	Non-sago	**0.9697**	0.0072	0.0228	0.0002
	47	MAX_0028	Sago leaves	Sago leaves	0.0000	0.0016	**0.9983**	0.0001
	48	MAX_0029	Sago leaves	Sago leaves	0.0857	0.0021	**0.8991**	0.0131
	49	MAX_0030	Sago leaves	Sago leaves	0.0000	0.0014	**0.9969**	0.0017
	50	MAX_0031	Non-sago	Non-sago	**0.9957**	0.0004	0.0037	0.0002
	51	MAX_0032	Sago leaves	Sago leaves	0.0003	0.0016	**0.9980**	0.0002
	52	MAX_0033	Sago leaves	Sago leaves	0.0000	0.0010	**0.9976**	0.0014
	53	MAX_0034	Sago leaves	Sago leaves	0.0000	0.0002	**0.9998**	0.0001
	54	MAX_0035	Sago leaves	Sago leaves	0.0000	0.0000	**1.0000**	0.0000
	55	MAX_0036	Non-sago	Non-sago	**1.0000**	0.0000	0.0000	0.0000
	56	MAX_0037	Sago leaves	Sago leaves	0.0000	0.0001	**0.9999**	0.0000
	57	MAX_0038	Non-sago	Non-sago	**0.9998**	0.0000	0.0001	0.0000
	58	MAX_0039	Non-sago	Non-sago	**0.9929**	0.0053	0.0017	0.0001
	59	MAX_0040	Sago leaves	Sago trunks	0.0022	0.0041	0.0808	**0.9129**
	60	MAX_0041	Sago leaves	Sago leaves	0.0013	0.0044	**0.9306**	0.0637
	61	MAX_0042	Sago leaves	Sago leaves	0.0089	0.0146	**0.9731**	0.0033
	62	MAX_0043	Non-sago	Non-sago	**1.0000**	0.0000	0.0000	0.0000
	63	MAX_0044	Sago leaves	Sago leaves	0.0000	0.0018	**0.9956**	0.0026
	64	MAX_0045	Sago flowers	Sago flowers	0.0011	**0.8897**	0.0095	0.0997
	65	MAX_0046	Sago flowers	Sago flowers	0.0030	**0.8419**	0.1350	0.0228
	66	MAX_0047	Sago flowers	Sago leaves	0.1696	0.0625	**0.7517**	0.0161
	67	MAX_0048	Sago flowers	Sago leaves	0.0040	0.2456	**0.7447**	0.0056
	68	MAX_0468	Sago leaves	Sago leaves	0.0089	0.0266	**0.9645**	0.0000
	69	MAX_0469	Sago leaves	Sago leaves	0.0017	0.0353	**0.9630**	0.0000
	70	MAX_0470	Sago leaves	Sago leaves	0.0000	0.0006	**0.9994**	0.0000
	71	MAX_0471	Sago leaves	Non-sago	**0.9965**	0.0009	0.0026	0.0000

	72	MAX_0536	Sago leaves	Sago flowers	0.0000	**0.7254**	0.2745	0.0001
	73	MAX_0537	Sago leaves	Non-sago	**0.8266**	0.0045	0.1688	0.0001
	74	MAX_0538	Non-sago	Non-sago	**0.9998**	0.0001	0.0001	0.0000
	75	MAX_0539	Sago leaves	Sago leaves	0.0005	0.0895	**0.7136**	0.1964
	76	MAX_0540	Sago leaves	Sago flowers	0.0575	**0.4767**	0.4656	0.0001
	77	MAX_0541	Sago leaves	Sago leaves	0.0000	0.0275	**0.9707**	0.0018
	78	MAX_0542	Sago leaves	Non-sago	**0.8789**	0.0137	0.1074	0.0000
	79	MAX_0543	Sago leaves	Non-sago	**0.9837**	0.0200	0.0143	0.0000
	80	MAX_0544	Sago leaves	Sago leaves	0.0000	0.0403	**0.9597**	0.0000
	81	MAX_0546	Non-sago	Non-sago	**0.4020**	0.2196	0.3775	0.0010
	82	MAX_0547	Sago leaves	Sago leaves	0.0000	0.1980	**0.8018**	0.0001
	83	MAX_0549	Sago leaves	Sago leaves	0.0000	0.0060	**0.9940**	0.0000
	84	no	Non-sago	Non-sago	**1.0000**	0.0000	0.0000	0.0000
	85	non	Non-sago	Non-sago	**0.9708**	0.0072	0.0219	0.0001
	86	nonsa	Non-sago	Non-sago	**0.9727**	0.0108	0.0160	0.0004
	87	nonsag	Non-sago	Non-sago	**0.6460**	0.1186	0.2352	0.0002
	88	sf	Sago flowers	Sago leaves	0.0000	0.0417	**0.9581**	0.0002
	89	sf1	Sago flowers	Sago flowers	0.0000	**0.9901**	0.0099	0.0000
	90	sff	Sago flowers	Sago flowers	0.0001	**0.9842**	0.0157	0.0000
	91	sl	Sago leaves	Sago leaves	0.0000	0.0118	**0.9876**	0.0006
	92	sl1	Sago leaves	Sago leaves	0.0000	0.1664	**0.8315**	0.0022
	93	sl2	Sago leaves	Sago leaves	0.0000	0.0006	**0.9994**	0.0000
	94	testnon	Non-sago	Non-sago	**0.9980**	0.0016	0.0003	0.0000
	95	testnons	Non-sago	Non-sago	**0.9938**	0.0008	0.0052	0.0002
	96	testnonss	Non-sago	Non-sago	**1.0000**	0.0000	0.0000	0.0000
	97	testrunk	Sago trunks	Sago trunks	0.0000	0.0026	0.0000	**0.9974**
	98	testsag	Sago leaves	Sago leaves	0.0000	0.0133	**0.9844**	0.0023
	99	testsl	Sago leaves	Sago leaves	0.0029	0.0380	**0.9589**	0.0002
	100	testtr	Sago trunks	Sago trunks	0.0000	0.0018	0.0000	**0.9982**
	101	trunk	Sago trunks	Sago trunks	0.0000	0.0000	0.0000	**1.0000**
	102	trunks	Sago trunks	Sago trunks	0.0000	0.0000	0.0000	**1.0000**
	103	trunkss	Sago trunks	Sago trunks	0.0000	0.0001	0.0000	**0.9999**

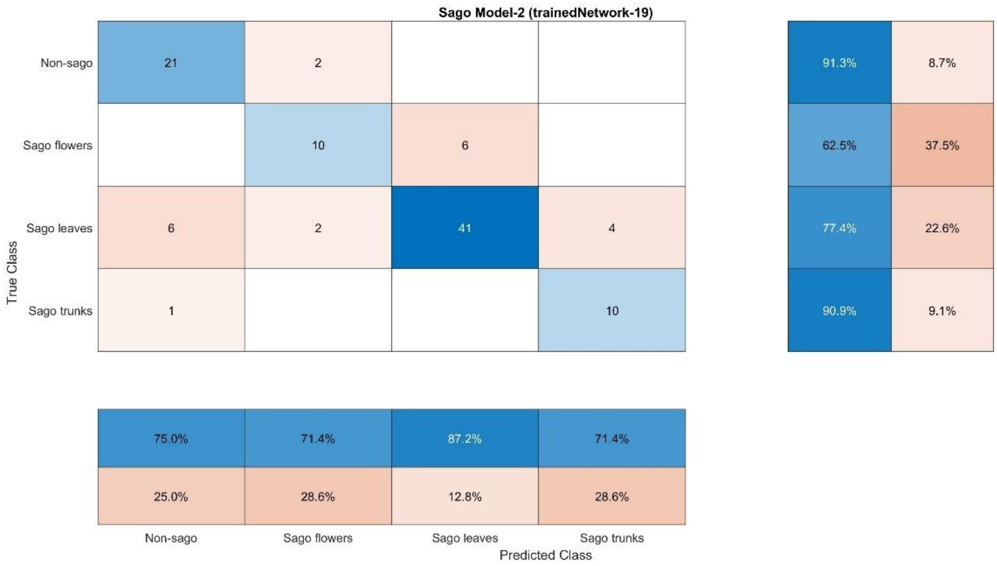

Figure D.8. Confusion matrix of trained Network-19.

Table D.11. The prediction result of trained Network-21.

Parameter training setup		**No**	**Test Image**	**Target21**	**Predict21**	**Non-sago**	**Sago flowers**	**Sago leaves**	**Sago trunks**
Parameter name	**Value**	1	10-rev	Sago trunks	Sago trunks	0.0000	0.0002	0.0436	**0.9562**
Epoch	10	2	11-rev	Sago trunks	Sago trunks	0.0047	0.0003	0.0017	**0.9933**
Initial Learning rate	0.0001	3	12	Sago flowers	Sago flowers	0.0002	**0.9867**	0.0117	0.0014
Validation freq	4	4	12-rev	Sago flowers	Sago flowers	0.0002	**0.9867**	0.0117	0.0014
Learning rate weight coeff	10	5	14	Sago leaves	Sago leaves	0.0000	0.0012	**0.9987**	0.0000
Learning rate bias coeff	10	6	15	Sago leaves	Sago leaves	0.0002	0.4760	**0.5232**	0.0070
Momentum	0.9	7	15-rev	Sago leaves	Sago flowers	0.0002	**0.5742**	0.4249	0.0006
L2 Regulation	0.0001	8	19-rev	Sago leaves	Sago trunks	0.0000	0.0000	0.0000	**1.0000**
Min Batch size	10	9	20-rev	Sago leaves	Sago trunks	0.0000	0.0000	0.0000	**1.0000**
		10	DJI_0081	Sago leaves	Sago flowers	0.0020	**0.7101**	0.2868	0.0010
		11	DJI_0100	Sago trunks	Sago trunks	0.0018	0.0010	0.0076	**0.9896**
Accuracy		12	DJI_0101	Sago trunks	Sago trunks	0.0000	0.0000	0.0000	**1.0000**
validation accuracy= 91.69%		13	DJI_0103	Sago trunks	Sago flowers	0.3678	**0.3830**	0.0134	0.2358
elapsed time= 33 mins 30 sec		14	DJI_0106	Sago flowers	Sago flowers	0.0002	**0.9998**	0.0000	0.0000
		15	DJI_0107	Sago flowers	Sago flowers	0.0001	**0.9998**	0.0001	0.0000
		16	DJI_0108	Sago flowers	Sago flowers	0.0000	**1.0000**	0.0000	0.0000
		17	DJI_0121	Sago flowers	Sago flowers	0.0000	**0.9997**	0.0002	0.0000
		18	DJI_0122	Sago flowers	Sago flowers	0.0001	**0.9998**	0.0001	0.0000

	19	DJI_0123	Sago flowers	Sago flowers	0.0004	**0.9995**	0.0001	0.0000
trainedNetwork_21 Validation accuracy: 87.88% elapsed time=43 min 48 sec	20	img1	Sago trunks	Sago trunks	0.0000	0.0000	0.0000	**1.0000**
	21	MAX_0001	Sago leaves	Sago leaves	0.0001	0.0001	**0.9996**	0.0002
	22	MAX_0002	Non-sago	Non-sago	**1.0000**	0.0000	0.0000	0.0000
	23	MAX_0003	Sago leaves	Sago leaves	0.0001	0.0005	**0.9994**	0.0000
	24	MAX_0004	Sago leaves	Sago leaves	0.0000	0.0000	**1.0000**	0.0000
	25	MAX_0006	Sago leaves	Sago leaves	0.0004	0.0286	**0.9705**	0.0006
	26	MAX_0007	Sago leaves	Sago leaves	0.0000	0.0015	**0.9981**	0.0003
	27	MAX_0008	Non-sago	Sago trunks	0.0104	0.0162	0.0008	**0.9726**
	28	MAX_0009	Non-sago	Sago leaves	0.0031	0.2791	**0.7178**	0.0000
	29	MAX_0010	Sago leaves	Sago trunks	0.0100	0.0158	0.0178	**0.9563**
	30	MAX_0011	Sago flowers	Sago leaves	0.0000	0.0007	**0.9993**	0.0000
	31	MAX_0012	Sago leaves	Sago trunks	0.0014	0.0035	0.0375	**0.9576**
	32	MAX_0013	Non-sago	Non-sago	**0.9999**	0.0000	0.0000	0.0001
	33	MAX_0014	Sago leaves	Sago trunks	0.0488	0.0723	0.1715	**0.7074**
	34	MAX_0015	Non-sago	Non-sago	**1.0000**	0.0000	0.0000	0.0000
	35	MAX_0016	Sago leaves	Sago leaves	0.0077	0.0018	**0.8121**	0.1783
	36	MAX_0017	Sago leaves	Sago leaves	0.0057	0.0101	**0.8185**	0.1658
	37	MAX_0018	Non-sago	Non-sago	**0.9999**	0.0000	0.0001	0.0000
	38	MAX_0019	Sago leaves	Sago trunks	0.0001	0.0004	0.0903	**0.9092**
	39	MAX_0020	Sago leaves	Sago trunks	0.0002	0.0004	0.0237	**0.9756**
	40	MAX_0021	Non-sago	Non-sago	**0.9999**	0.0001	0.0000	0.0000
	41	MAX_0022	Sago leaves	Sago leaves	0.1798	0.0096	**0.6446**	0.1661
	42	MAX_0023	Sago leaves	Sago leaves	0.0002	0.0085	**0.9889**	0.0024
	43	MAX_0024	Sago leaves	Sago leaves	0.0000	0.0011	**0.9988**	0.0000
	44	MAX_0025	Sago leaves	Sago trunks	0.2999	0.0063	0.1332	**0.5607**
	45	MAX_0026	Non-sago	Sago trunks	0.4757	0.0131	0.0174	**0.4938**
	46	MAX_0027	Non-sago	Non-sago	**0.9866**	0.0016	0.0118	0.0000
	47	MAX_0028	Sago leaves	Sago leaves	0.0000	0.0000	**1.0000**	0.0000
	48	MAX_0029	Sago leaves	Sago trunks	0.0050	0.0005	0.0700	**0.9245**
	49	MAX_0030	Sago leaves	Sago leaves	0.0000	0.0011	**0.9905**	0.0084
	50	MAX_0031	Non-sago	Non-sago	**0.9665**	0.0005	0.0280	0.0051
	51	MAX_0032	Sago leaves	Sago leaves	0.0004	0.0036	**0.9959**	0.0002
	52	MAX_0033	Sago leaves	Sago leaves	0.0000	0.0000	**0.9992**	0.0007
	53	MAX_0034	Sago leaves	Sago leaves	0.0000	0.0000	**0.9992**	0.0008
	54	MAX_0035	Sago leaves	Sago leaves	0.0000	0.0000	**0.9999**	0.0001
	55	MAX_0036	Non-sago	Non-sago	**0.9991**	0.0000	0.0003	0.0006

	56	MAX_0037	Sago leaves	Sago leaves	0.0000	0.0000	**0.9999**	0.0000
	57	MAX_0038	Non-sago	Non-sago	**0.9998**	0.0000	0.0002	0.0000
	58	MAX_0039	Non-sago	Non-sago	**0.9976**	0.0007	0.0010	0.0007
	59	MAX_0040	Sago leaves	Sago trunks	0.0005	0.0004	0.3373	**0.6619**
	60	MAX_0041	Sago leaves	Sago trunks	0.0042	0.0230	0.4834	**0.4894**
	61	MAX_0042	Sago leaves	Sago leaves	0.0102	0.0079	**0.9817**	0.0002
	62	MAX_0043	Non-sago	Non-sago	**0.9998**	0.0000	0.0002	0.0000
	63	MAX_0044	Sago leaves	Sago leaves	0.0001	0.0007	**0.9991**	0.0001
	64	MAX_0045	Sago flowers	Sago trunks	0.0007	0.0536	0.0001	**0.9455**
	65	MAX_0046	Sago flowers	Sago trunks	0.0003	0.0048	0.0005	**0.9945**
	66	MAX_0047	Sago flowers	Sago leaves	0.1045	0.0388	**0.8358**	0.0209
	67	MAX_0048	Sago flowers	Sago leaves	0.0306	0.0708	**0.8934**	0.0043
	68	MAX_0468	Sago leaves	Sago leaves	0.1064	0.1614	**0.7322**	0.0000
	69	MAX_0469	Sago leaves	Sago leaves	0.0052	0.0140	**0.9808**	0.0000
	70	MAX_0470	Sago leaves	Sago leaves	0.0000	0.0000	**1.0000**	0.0000
	71	MAX_0471	Sago leaves	Non-sago	**0.9981**	0.0016	0.0003	0.0000
	72	MAX_0536	Sago leaves	Sago leaves	0.0047	0.2906	**0.7046**	0.0002
	73	MAX_0537	Sago leaves	Non-sago	**0.5932**	0.0049	0.4020	0.0000
	74	MAX_0538	Non-sago	Non-sago	**0.9994**	0.0000	0.0006	0.0000
	75	MAX_0539	Sago leaves	Sago trunks	0.0001	0.0003	0.0202	**0.9794**
	76	MAX_0540	Sago leaves	Sago leaves	0.3878	0.0145	**0.5977**	0.0000
	77	MAX_0541	Sago leaves	Sago trunks	0.0004	0.0026	0.4154	**0.5817**
	78	MAX_0542	Sago leaves	Sago leaves	0.3971	0.0077	**0.5952**	0.0000
	79	MAX_0543	Sago leaves	Non-sago	**0.9727**	0.0010	0.0262	0.0000
	80	MAX_0544	Sago leaves	Sago leaves	0.0099	0.0025	**0.9873**	0.0002
	81	MAX_0546	Non-sago	Sago flowers	0.0057	**0.8037**	0.1773	0.0134
	82	MAX_0547	Sago leaves	Sago leaves	0.0029	0.0107	**0.9842**	0.0022
	83	MAX_0549	Sago leaves	Sago leaves	0.0001	0.0000	**0.9998**	0.0000
	84	no	Non-sago	Non-sago	**1.0000**	0.0000	0.0000	0.0000
	85	non	Non-sago	Non-sago	**0.9987**	0.0004	0.0009	0.0000
	86	nonsa	Non-sago	Non-sago	**0.9998**	0.0001	0.0001	0.0000
	87	nonsag	Non-sago	Sago leaves	0.2387	0.0203	**0.7410**	0.0000
	88	sf	Sago flowers	Sago leaves	0.0000	0.0003	**0.9997**	0.0000
	89	sf1	Sago flowers	Sago flowers	0.0000	**1.0000**	0.0000	0.0000
	90	sff	Sago flowers	Sago flowers	0.0054	**0.9554**	0.0386	0.0006
	91	sl	Sago leaves	Sago leaves	0.0002	0.0235	**0.9723**	0.0041
	92	sl1	Sago leaves	Sago leaves	0.0000	0.0097	**0.9831**	0.0072

	93	sl2	Sago leaves	Sago leaves	0.0000	0.0000	**1.0000**	0.0000
	94	testnon	Non-sago	Non-sago	**0.9985**	0.0002	0.0013	0.0000
	95	testnons	Non-sago	Non-sago	**0.9730**	0.0004	0.0264	0.0000
	96	testnonss	Non-sago	Non-sago	**0.9999**	0.0000	0.0000	0.0000
	97	testrunk	Sago trunks	Sago trunks	0.0000	0.0000	0.0000	**1.0000**
	98	testsag	Sago leaves	Sago leaves	0.0031	0.0018	**0.9596**	0.0355
	99	testsl	Sago leaves	Sago flowers	0.0020	**0.7101**	0.2868	0.0010
	100	testtr	Sago trunks	Sago trunks	0.0000	0.0000	0.0000	**1.0000**
	101	trunk	Sago trunks	Sago trunks	0.0000	0.0000	0.0000	**1.0000**
	102	trunks	Sago trunks	Sago trunks	0.0000	0.0000	0.0000	**1.0000**
	103	trunkss	Sago trunks	Sago trunks	0.0000	0.0000	0.0000	**1.0000**

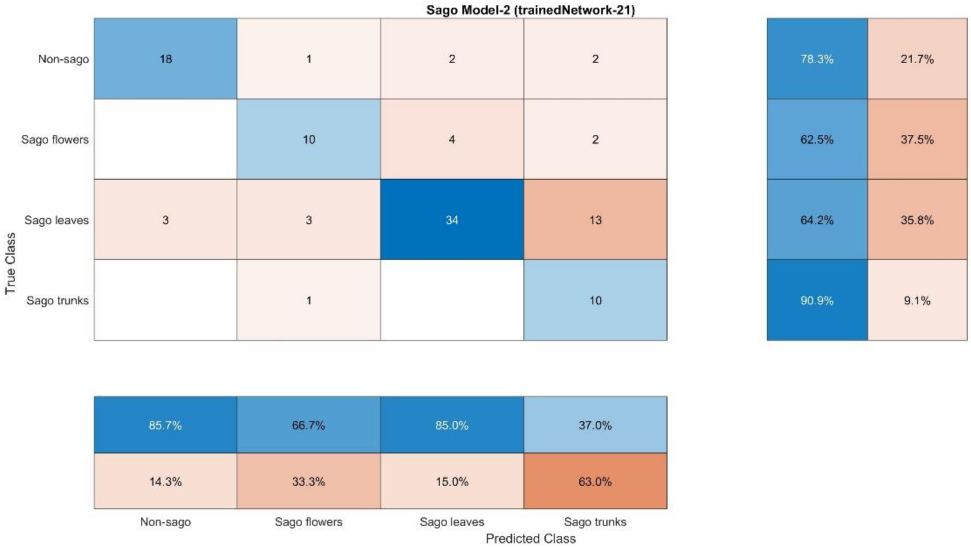

Figure D.9. Confusion matrix trained Network-21.

Table D.12. The prediction result of trained Network-22.

Parameter training setup		No	Test Image	Target22	Predict22	Non-sago	Sago flowers	Sago leaves	Sago trunks
Parameter name	**Value**	1	10-rev	Sago trunks	Sago leaves	0.0000	0.0000	**0.8586**	0.1432
Epoch	8	2	11-rev	Sago trunks	Sago trunks	0.0006	0.0001	0.0053	**0.9940**
Initial Learning rate	0.0001	3	12	Sago flowers	Sago leaves	0.0001	0.0033	**0.9962**	0.0003
Validation freq	4	4	12-rev	Sago flowers	Sago leaves	0.0001	0.0032	**0.9963**	0.0003
Learning rate weight coeff	10	5	14	Sago leaves	Sago leaves	0.0000	0.0000	**1.0000**	0.0000
Learning rate bias coeff	10	6	15	Sago leaves	Sago leaves	0.0004	0.0332	**0.9664**	0.0001
Momentum	0.9	7	15-rev	Sago leaves	Sago leaves	0.0004	0.0407	**0.9588**	0.0001

L2 Regulation 0.0001	8	19-rev	Sago leaves	Sago trunks	0.0000	0.0001	0.0002	**0.9997**
Min Batch size 10	9	20-rev	Sago leaves	Sago trunks	0.0002	0.0001	0.0001	**0.9997**
	10	DJI_0081	Sago leaves	Sago leaves	0.0004	0.0317	**0.9679**	0.0001
	11	DJI_0100	Sago trunks	Sago leaves	0.0089	0.0103	**0.7780**	0.2027
Accuracy	12	DJI_0101	Sago trunks	Sago trunks	0.0000	0.0000	0.0067	**0.9933**
validation accuracy= 90.15%	13	DJI_0103	Sago trunks	Non-sago	**0.8012**	0.0987	0.0805	0.0197
elapsed time= 59 mins 39 sec	14	DJI_0106	Sago flowers	Sago flowers	0.0238	**0.9434**	0.0329	0.0000
	15	DJI_0107	Sago flowers	Sago flowers	0.0589	**0.8624**	0.0786	0.0000
	16	DJI_0108	Sago flowers	Sago flowers	0.0001	**0.9324**	0.0676	0.0000
	17	DJI_0121	Sago flowers	Sago flowers	0.0001	**0.8395**	0.1604	0.0001
	18	DJI_0122	Sago flowers	Sago flowers	0.0001	**0.7165**	0.2827	0.0007
	19	DJI_0123	Sago flowers	Sago flowers	0.0001	**0.9434**	0.0562	0.0003
trainedNetwork_22	20	img1	Sago trunks	Sago trunks	0.0000	0.0004	0.0003	**0.9992**
Validation accuracy: 86.36%	21	MAX_0001	Sago leaves	Sago leaves	0.0000	0.0000	**1.0000**	0.0000
elapsed time: 31 min 40 sec	22	MAX_0002	Non-sago	Non-sago	**1.0000**	0.0000	0.0000	0.0000
	23	MAX_0003	Sago leaves	Sago leaves	0.0000	0.0001	**0.9999**	0.0000
	24	MAX_0004	Sago leaves	Sago leaves	0.0000	0.0000	**1.0000**	0.0000
	25	MAX_0006	Sago leaves	Sago leaves	0.0000	0.0000	**1.0000**	0.0000
	26	MAX_0007	Sago leaves	Sago leaves	0.0000	0.0000	**1.0000**	0.0000
	27	MAX_0008	Non-sago	Sago leaves	0.0271	0.1890	**0.7577**	0.0262
	28	MAX_0009	Non-sago	Sago leaves	0.0012	0.1142	**0.8846**	0.0000
	29	MAX_0010	Sago leaves	Sago leaves	0.0055	0.0202	**0.8433**	0.1309
	30	MAX_0011	Sago flowers	Sago leaves	0.0000	0.0000	**0.9999**	0.0000
	31	MAX_0012	Sago leaves	Sago leaves	0.0004	0.0000	**0.9931**	0.0065
	32	MAX_0013	Non-sago	Non-sago	**1.0000**	0.0000	0.0000	0.0000
	33	MAX_0014	Sago leaves	Sago leaves	0.0275	0.0174	**0.9515**	0.0036
	34	MAX_0015	Non-sago	Non-sago	**0.9999**	0.0000	0.0001	0.0000
	35	MAX_0016	Sago leaves	Sago leaves	0.0012	0.0000	**0.9949**	0.0039
	36	MAX_0017	Sago leaves	Sago leaves	0.0045	0.0002	**0.9943**	0.0010
	37	MAX_0018	Non-sago	Non-sago	**0.9990**	0.0001	0.0009	0.0000
	38	MAX_0019	Sago leaves	Sago leaves	0.0005	0.0001	**0.9924**	0.0071
	39	MAX_0020	Sago leaves	Sago leaves	0.0010	0.0011	**0.9764**	0.0215
	40	MAX_0021	Non-sago	Non-sago	**1.0000**	0.0000	0.0000	0.0000
	41	MAX_0022	Sago leaves	Sago leaves	0.0640	0.0028	**0.8913**	0.0419
	42	MAX_0023	Sago leaves	Sago leaves	0.0000	0.0000	**1.0000**	0.0000
	43	MAX_0024	Sago leaves	Sago leaves	0.0000	0.0005	**0.9994**	0.0000
	44	MAX_0025	Sago leaves	Sago trunks	0.1000	0.0040	0.0961	**0.7999**

	45	MAX_0026	Non-sago	Non-sago	**0.5974**	0.0505	0.2321	0.1200
	46	MAX_0027	Non-sago	Sago leaves	0.3549	0.0049	**0.6404**	0.0000
	47	MAX_0028	Sago leaves	Sago leaves	0.0000	0.0000	**1.0000**	0.0000
	48	MAX_0029	Sago leaves	Sago leaves	0.0966	0.0001	**0.8683**	0.0350
	49	MAX_0030	Sago leaves	Sago leaves	0.0000	0.0000	**0.9999**	0.0001
	50	MAX_0031	Non-sago	Non-sago	**0.8474**	0.0058	0.0900	0.0569
	51	MAX_0032	Sago leaves	Sago leaves	0.0000	0.0001	**0.9998**	0.0000
	52	MAX_0033	Sago leaves	Sago leaves	0.0000	0.0000	**1.0000**	0.0000
	53	MAX_0034	Sago leaves	Sago leaves	0.0000	0.0000	**1.0000**	0.0000
	54	MAX_0035	Sago leaves	Sago leaves	0.0000	0.0000	**1.0000**	0.0000
	55	MAX_0036	Non-sago	Non-sago	**0.9984**	0.0007	0.0006	0.0003
	56	MAX_0037	Sago leaves	Sago leaves	0.0000	0.0000	**1.0000**	0.0000
	57	MAX_0038	Non-sago	Non-sago	**0.9990**	0.0001	0.0008	0.0000
	58	MAX_0039	Non-sago	Non-sago	**0.9990**	0.0007	0.0003	0.0000
	59	MAX_0040	Sago leaves	Sago leaves	0.0001	0.0000	**0.9959**	0.0040
	60	MAX_0041	Sago leaves	Sago leaves	0.0021	0.0022	**0.9882**	0.0075
	61	MAX_0042	Sago leaves	Sago leaves	0.0041	0.0616	**0.9301**	0.0042
	62	MAX_0043	Non-sago	Non-sago	**0.9999**	0.0001	0.0000	0.0000
	63	MAX_0044	Sago leaves	Sago leaves	0.0000	0.0000	**1.0000**	0.0000
	64	MAX_0045	Sago flowers	Sago flowers	0.0015	**0.9741**	0.0011	0.0233
	65	MAX_0046	Sago flowers	Sago trunks	0.0000	0.0130	0.0350	**0.9520**
	66	MAX_0047	Sago flowers	Sago flowers	0.0412	**0.4573**	0.2460	0.2555
	67	MAX_0048	Sago flowers	Sago flowers	0.0200	**0.6568**	0.3144	0.0071
	68	MAX_0468	Sago leaves	Sago leaves	0.0169	0.1769	**0.8062**	0.0000
	69	MAX_0469	Sago leaves	Sago leaves	0.0022	0.0017	**0.9961**	0.0000
	70	MAX_0470	Sago leaves	Sago leaves	0.0000	0.0000	**1.0000**	0.0000
	71	MAX_0471	Sago leaves	Non-sago	**0.9458**	0.0269	0.0273	0.0000
	72	MAX_0536	Sago leaves	Sago leaves	0.0011	0.3413	**0.6569**	0.0008
	73	MAX_0537	Sago leaves	Sago leaves	0.0876	0.0050	**0.9074**	0.0000
	74	MAX_0538	Non-sago	Non-sago	**0.8588**	0.0005	0.1407	0.0000
	75	MAX_0539	Sago leaves	Sago trunks	0.0000	0.0001	0.1790	**0.8209**
	76	MAX_0540	Sago leaves	Sago leaves	0.0210	0.0040	**0.9749**	0.0000
	77	MAX_0541	Sago leaves	Sago leaves	0.0000	0.0015	**0.9964**	0.0021
	78	MAX_0542	Sago leaves	Sago leaves	0.0999	0.0425	**0.8575**	0.0000
	79	MAX_0543	Sago leaves	Non-sago	**0.9439**	0.0086	0.0475	0.0000
	80	MAX_0544	Sago leaves	Sago leaves	0.0003	0.0015	**0.9982**	0.0000
	81	MAX_0546	Non-sago	Sago leaves	0.0044	0.4142	**0.5719**	0.0023

	82	MAX_0547	Sago leaves	Sago leaves	0.0000	0.0000	**0.9998**	0.0001
	83	MAX_0549	Sago leaves	Sago leaves	0.0000	0.0002	**0.9997**	0.0000
	84	no	Non-sago	Non-sago	**0.9997**	0.0001	0.0002	0.0000
	85	non	Non-sago	Sago leaves	0.2956	0.0623	**0.6417**	0.0004
	86	nonsa	Non-sago	Non-sago	**0.9971**	0.0013	0.0015	0.0001
	87	nonsag	Non-sago	Sago leaves	0.0313	0.0165	**0.9522**	0.0000
	88	sf	Sago flowers	Sago leaves	0.0000	0.0000	**1.0000**	0.0000
	89	sf1	Sago flowers	Sago flowers	0.0000	**0.9718**	0.0282	0.0000
	90	sff	Sago flowers	Sago flowers	0.0056	**0.9075**	0.0811	0.0058
	91	sl	Sago leaves	Sago leaves	0.0000	0.0000	**1.0000**	0.0000
	92	sl1	Sago leaves	Sago leaves	0.0000	0.0001	**0.9998**	0.0001
	93	sl2	Sago leaves	Sago leaves	0.0000	0.0000	**1.0000**	0.0000
	94	testnon	Non-sago	Non-sago	**0.9966**	0.0030	0.0004	0.0000
	95	testnons	Non-sago	Non-sago	**0.7367**	0.0002	0.2630	0.0001
	96	testnonss	Non-sago	Non-sago	**0.9999**	0.0001	0.0000	0.0000
	97	testrunk	Sago trunks	Sago trunks	0.0000	0.0000	0.0000	**1.0000**
	98	testsag	Sago leaves	Sago leaves	0.0011	0.0002	**0.9956**	0.0032
	99	testsl	Sago leaves	Sago leaves	0.0004	0.0317	**0.9679**	0.0001
	100	testtr	Sago trunks	Sago trunks	0.0000	0.0003	0.0000	**0.9997**
	101	trunk	Sago trunks	Sago trunks	0.0000	0.0000	0.0002	**0.9998**
	102	trunks	Sago trunks	Sago trunks	0.0000	0.0000	0.0002	**0.9998**
	103	trunkss	Sago trunks	Sago trunks	0.0000	0.0000	0.0000	**1.0000**

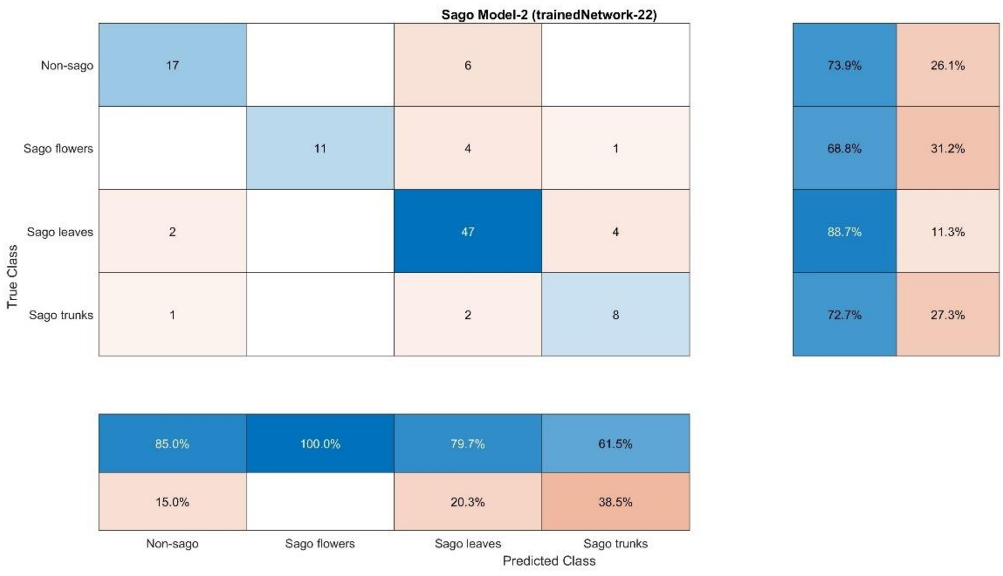

Figure D.10. Confusion matrix trained Network-22.

Table D.13. Recall, precision, and F1-score.

	trainedNetwork-1				**trainedNetwork-2**				**trainedNetwork-3**			
	Non-sago	Sago flowers	Sago leaves	Sago trunks	Non-sago	Sago flowers	Sago leaves	Sago trunks	Non-sago	Sago flowers	Sago leaves	Sago trunks
Recall	65	56	83	82	70	56	81	82	70	56	81	82
Precision	83	50	85	60	73	90	75	64	73	90	75	64
F-1 Score	73	53	84	69	71	69	78	72	71	69	78	72

	trainedNetwork-4				**trainedNetwork-5**				**trainedNetwork-6**			
	Non-sago	Sago flowers	Sago leaves	Sago trunks	Non-sago	Sago flowers	Sago leaves	Sago trunks	Non-sago	Sago flowers	Sago leaves	Sago trunks
Recall	65	75	70	82	74	75	72	91	57	63	83	82
Precision	71	46	86	69	77	75	85	50	72	77	75	69
F-1 Score	68	57	77	75	76	75	78	65	63	69	79	75

	trainedNetwork-7				**trainedNetwork-8**				**trainedNetwork-9**			
	Non-sago	Sago flowers	Sago leaves	Sago trunks	Non-sago	Sago flowers	Sago leaves	Sago trunks	Non-sago	Sago flowers	Sago leaves	Sago trunks
Recall	57	56	89	82	No results/Error				No results/Error			
Precision	81	75	76	69								
F-1 Score	67	64	82	75								

	trainedNetwork-10				**trainedNetwork-11**				**trainedNetwork-12**			
	Non-sago	Sago flowers	Sago leaves	Sago trunks	Non-sago	Sago flowers	Sago leaves	Sago trunks	Non-sago	Sago flowers	Sago leaves	Sago trunks
Recall	74	56	57	100	83	69	-	100	78	75	-	91
Precision	74	64	77	37	35	73	-	32	34	67	-	31
F-1 Score	74	60	66	53	49	71	-	49	47	71	-	46

	trainedNetwork-13				**trainedNetwork-14**				**trainedNetwork-15**			
	Non-sago	Sago flowers	Sago leaves	Sago trunks	Non-sago	Sago flowers	Sago leaves	Sago trunks	Non-sago	Sago flowers	Sago leaves	Sago trunks
Recall	61	63	79	82	70	81	76	82	70	56	89	82
Precision	74	83	74	60	73	68	89	53	80	90	77	75
F-1 Score	67	71	76	69	71	74	82	64	74	69	82	78

	trainedNetwork-16				**trainedNetwork-17**				**trainedNetwork-18**			
	Non-sago	Sago flowers	Sago leaves	Sago trunks	Non-sago	Sago flowers	Sago leaves	Sago trunks	Non-sago	Sago flowers	Sago leaves	Sago trunks
Recall	70	56	87	73	83	75	79	82	78	63	87	82
Precision	84	75	77	67	83	63	91	60	78	91	81	75
F-1 Score	76	64	81	70	83	68	85	69	78	74	84	78

	trainedNetwork-19				trainedNetwork-20			
	Non-sago	Sago flowers	Sago leaves	Sago trunks	Non-sago	Sago flowers	Sago leaves	Sago trunks
Recall	91	63	77	91	96	44	76	90
Precision	75	71	87	71	69	78	85	67
F-1 Score	82	67	82	80	80	56	80	77

	trainedNetwork-21				trainedNetwork-22			
	Non-sago	Sago flowers	Sago leaves	Sago trunks	Non-sago	Sago flowers	Sago leaves	Sago trunks
Recall	78	63	64	91	74	69	89	73
Precision	86	67	85	34	85	100	80	62
F-1 Score	82	65	73	49	78	82	84	67

APPENDIX E

List of publications:

1. Publication-1:
   Type: Article
   Title: Land cover changes from 1990 to 2019 in Papua, Indonesia: Results of the remote sensing imagery.
   Authors: Letsoin, S.M.A., Herak, D., Rahmawan, F., Purwestri, R.C.
   Year: 2020.
   Published in: Sustainability, 2020, 12(16), 6623.
   Indexed by: Web of Science JIF 3.889; Scopus cite score 5.0.
   Link: https://www.mdpi.com/2071-1050/12/16/6623.
2. Publication-2:
   Type: Conference paper
   Title: Evaluation Land Use Cover Changes over 29 Years in Papua Province of Indonesia Using Remote Sensing Data.
   Authors: Letsoin, S.M.A., Herak, D., Purwestri, R.C.
   Year: 2022.
   Published in: IOP Conference Series: Earth and Environmental Science 2022, 1034(1), 012013.
   Indexed by: Scopus, SJR 2022: 0.2.
   Link: https://iopscience.iop.org/article/10.1088/1755-1315/1034/1/012013.
3. Publication-3:
   Type: Article.
   Title: Recognition of Sago Palm Trees Based on Transfer Learning.
   Authors: Letsoin, S.M.A., Purwestri, R.C., Rahmawan, F., Herak, D.
   Year: 2022.
   Published in: Remote Sensing, 2022, 14(19), 4932.
   Indexed by: Web of Science JIF 5.349; Scopus cite score 7.4.
   Link: https://www.mdpi.com/2072-4292/14/19/4932.
4. Publication-4:
   Type: Conference paper (TAE2022 conference).
   Title: Combining Surveillance of Unmanned Aerial Vehicle and Deep Learning Methods in Sago Palm Detection.
   Authors: Letsoin, S.M.A., Herak, D., Purwestri, R.C.
   Year: 2022.
   Published in: tae-conference.cz.
   Indexed by: Google Scholar.
   Link: https://2022.tae-conference.cz/proceeding/TAE2022-41-Sri-Murniani-Angelina-LETSOIN.pdf.

5. Publication-5:
   Type: Review article.
   Title: A Sago Positive Character: A Literature Review.
   Authors: Setiawan, B., Fetriyuna, F., Letsoin, S. M. A., Purwestri, R. C., & Jati, I. R. A. (2022).
   Year: 2022.
   Published in: Jurnal Ilmiah Kedokteran Wijaya Kusuma.
   Indexed by: SINTA S3 IF 1.71 (Accredited by Indonesia Ministry of Education, Culture, Research and Technology)-GARUDA-Google scholar, DOAJ, Crossref.
   Link: https://journal.uwks.ac.id/index.php/jikw/article/view/2443/pdf.
6. Publication-6:
   Type: Review article.
   Title: Potential uses of underutilized sago to support the sustainability of food suppy and bioeconomy.
   Authors: Fetriyuna, F, Letsoin S.M.A, Jati, I. R. A, Purwestri, R. C, Setiawan, B, Wirawan, N.N, Herak, D, Hajek, M., Nurhasanah, Yuliana, T.
   Year: 2022.
   Published in: Res Militaris.
   Indexed by: google scholar.
   Link: https://resmilitaris.net/menu-script/index.php/resmilitaris/article/view/1130.
7. Publication-7:
   Type: Conference paper (ICBB)
   Title: Analysing Maize Plant Height Using Unmanned Aerial Vehicle (UAV) RGB based on Digital Surface Models (DSM).
   Authors: Letsoin, S. M. A., Guth, D., Herak, D., & Purwestri, R. C. (2023, May)
   Year: 2023.
   Published in: IOP Conference Series: Earth and Environmental Science (Vol. 1187, No. 1, p. 012028). IOP Publishing.
   Indexed by: Scopus, SJR 2022: 0.2.
   Link: https://iopscience.iop.org/article/10.1088/1755-1315/1187/1/012028/meta.
8. Publication-8:
   Type: Article.
   Title: Monitoring of Paddy and Maize Fields Using Sentinel-1 SAR Data and NGB Images: A Case Study in Papua, Indonesia.
   Authors: Letsoin, S. M. A., Purwestri, R. C., Perdana, M. C., Hnizdil, P., & Herak, D. (2023).
   Year: 2023.
   Published in: Processes, 11(3), 647.
   Indexed by: Web of Science JIF 3.352; Scopus cite score 3.5.
   Link: https://www.mdpi.com/2227-9717/11/3/647.

APPENDIX F

Ground photographs and in-situ measurement during fieldwork in Mappi Regency and Merauke Regency of Papua Province, Indonesia. The ground photographs, observation and situ measurement, were conducted in July-August 2019, February 2022, and July 2022.

(a)

(b)

Figure E.1. Traditional sago processing in harvest time (local farmer in Mappi Regency of Papua Province).

(a)

(b)

(c)

Figure E.2. Sago field in Tambat village (Tanah Miring district), Merauke Regency, (a) wild stand sago in swampy area, (b) sago live with other vegetation, (c) non-sago. (other vegetation).

Figure E.3. Dataset in Experiment-3. All data test were captured by a UAV in sago fieldwork.

The mission flight planner was arranged as presented in chapter 4, section 4.1 in particular Figure 11.

(a)

(b)

Figure E.4. In-situ measurement in Merauke Regency. (a) in sago field with local farmer, (b) consolidation with stakeholders (Food rops and Horticulture Department).